HELMHOLTZ
CENTRE FOR
ENVIRONMENTAL
RESEARCH – UFZ

PhD Dissertation 10/2009

Impact of substrate bioavailability on microbially induced stable isotope fractionation

Makeba Kampara

ISSN 1860-0387

Impact of substrate bioavailability on microbially induced stable isotope fractionation

Der Fakultät für Biowissenschaften, Pharmazie und Psychologie

der Universität Leipzig

eingereichte

D I S S E R T A T I O N

zur Erlangung des akademischen Grades

doctor rerum naturalium

Dr. rer. nat.

vorgelegt von

Master of Science Makeba Kampara

geboren am 20.05.1978 in Helsinki, Finnland

Leipzig, den 05.12.2008

BIBLIOGRAPHISCHE DARSTELLUNG

Makeba Kampara

Impact of substrate bioavailability on microbially induced stable isotope fractionation

Fakultät für Biowissenschaften, Pharmazie und Psychologie

Universität Leipzig

Dissertation

99 Seiten, 91 Literaturangaben, 17 Abbildungen, 1 Tabelle

Konstante Isotopenfraktionierungsfaktoren sind eine Voraussetzung für die Charakterisierung und Quantifizierung des biologischen Schadstoffabbaus in kontaminierten Böden und Grundwasserleiter. Jedoch ist der konstante Isotopeneffekt einer biochemischen Reaktion nur dann vollständig ausgeprägt, wenn der isotopenfraktionierende Schritt ratenlimitierend für den gesamten Transformationsprozess ist. Wenn Massentransfer-Prozesse vor der fraktionierenden Reaktion ratenlimitierend sind, dann wird eine reduzierte Isotopenfraktionierung im Vergleich zu dem biochemischen Effekt beobachtet. Im Grundwasserleiter ist die Abbaurate von hydrophoben organischen Schadstoffen oft durch deren Bioverfügbarkeit kontrolliert. Die Bioverfügbarkeit für den Abbau von organischen Schadstoffen ist ein Prozess, der vom Massenstransfer relativ zur potentiellen Abbaurate bestimmt wird. Bei einer limitierten Bioverfügbarkeit ist der Substratfluss langsamer als die Abbaukapazität der Mikroorganismen. Dies sollte theoretisch zu einer reduzierten Isotopenfraktionierung führen.

In dieser Promotionsarbeit wurde der Einfluss der Substratbioverfügbarkeit auf die beobachtete Isotopenfraktionierung in einem Laborsystem gezeigt und anhand eines mathematischen Modells beschrieben. Unsere Versuche zeigten, dass die beobachtete Isotopenfraktionierung bei niedriger Bioverfügbarkeit deutlich tiefer war als in Systemen ohne Massentransferlimitierung. Dieser Effekt wurde durch ein mathematisches Modell eingehend untersucht, um die Variabilität in Abhängigkeit der Konzentration und Bioverfügbarkeit des Substrats für verschiedene umweltrelevante Massentransferverhältnisse aufzuzeigen. Es wurde beobachtet, dass die Verwendung von Isotopenfraktionierungsfaktoren, die normalerweise bei unbegrenzter Substratverfügbarkeit bestimmt wurden, für die Quantifizierung des Schadstoffabbaus bei Massentransferlimitierungen zu einen signifikanten Fehler führen kann.

Die Möglichkeit Isotopenfraktionierung als flussbasierter Indikator für eine eingeschränkte Bioverfügbarkeit zu verwenden wurde in verscshiedenen Laborsystemen untersucht. Es konnte gezeigt werden, dass das Ausmaß der Bioverfügbarkeit gut durch die Erfassung der Isotopenfraktionierung abgeschätzt werden kann. Diese Dissertation ist die theoretische Basis für die Beschreibung des Zusammenhanges zwischen Isotopenfraktionierung und Bioverfügbarkeit. Aufbauend auf die gewonnenen Erkenntnisse kann diese Korrelation für ein breites Spektrum an Mikroorganismen und Substraten untersucht werden.

Of strawberries and isotopes – a popular analogy

Let us observe a large strawberry field in northern Europe in late May. The spring has been warm and sunny, and strawberries are growing fast. We can see strawberry lovers gathering to pick and eat the berries, 5 kg per hour in total. Fortunately, all the time new strawberries are appearing from the green plants, corresponding to 10 kg per hour, so the ***availability is high***. If we look carefully, we can see that the deep red, nicely formed "perfect strawberries" get picked faster than slightly deformed "imperfect strawberries". In fact, we can observe a ***strong enrichment of "imperfect strawberries"*** on the field, as the "perfect strawberries" rapidly disappear to decorate summer desserts.

Same time the following year, after a long winter, prolonged by a cold rainy spring, the same people return to the field eager to eat fresh strawberries again. They methodically start picking at their rate of 5 kg per hour total, but they soon notice they need to slow down. Alas, this year the weather conditions do not allow fast strawberry growth, barely 5 kg per hour, ***availability is low***. "Perfect strawberries" still get picked faster, but before new strawberries appear, most of the "imperfect strawberries" also end up to the mouths or baskets. ***Little enrichment of "imperfect strawberries"*** can thus be observed.

Similarly, bacteria degrade molecules containing light isotopes only at a faster rate than the ones containing a heavier isotope. This isotope fractionation leads to an ***enrichment of heavy isotope*** in the residual substrate pool, which can be used to assess in situ biodegradation. However, when ***availability is low***, substrate molecules will be consumed independent of their isotopic nature, and ***less enrichment of heavy isotope*** can be observed.

ABSTRACT

The analysis of the stable isotope composition of organic compounds is increasingly used for a variety of applications, such as in situ assessment of contaminant biodegradation, elucidation of biochemical pathways, food web studies and identification of sources and sinks of green house gases. These applications rely on robust fractionation factors that do not significantly vary in function of environmental conditions. The biochemical kinetic isotope effect is indeed constant for a given reaction and leads to constant enzymatic fractionation factors. However, isotope fractionation is generally analyzed by determining the isotope composition of the residual substrate in the bulk liquid, where the full isotope effect can only be observed if the isotope sensitive bond cleavage is the rate limiting step of the overall transformation process. If slow mass transfer processes precede the fractionating reaction step, samples taken in the bulk do not reflect the isotope composition at the enzyme, and a reduced isotope fractionation is observed.

The use of stable isotope fractionation analysis of organic contaminants, in order to determine their behavior in soil and groundwater, has notably increased in the last years. For reliable characterization and quantification of biodegradation, constant fractionation factors are necessary. However, the isotope sensitive transformation is not always the rate limiting step for degradation. In the subsurface the degradation rate of hydrophobic organic pollutants is often limited by their bioavailability. Bioavailability for degradation of organic contaminants is an interactive process that is determined by the rate of physical mass transfer to microbial cells relative to their intrinsic catabolic activity. At bioavailability limited conditions, a situation often encountered in the subsurface, the pollutant supply does not meet the intrinsic degradation capacity of the microorganisms and theoretically thus can lead to a significantly reduced observed isotope fractionation.

In this thesis, the influence of substrate bioavailability on the observed stable isotope fractionation was unambiguously demonstrated in a well defined laboratory system and theoretically described using mathematical modeling, and the possible use of the effect for the assessment of bioavailability was investigated. The effect was first demonstrated in a batch laboratory system, where mass transfer conditions were varied by applying different substrate concentrations. Bioavailability as defined here refers to the mass transfer of the contaminant to a cell relative to the cell's specific affinity. The effective bioavailability experienced by a cell, however, also depends on the absolute contaminant concentration in the bulk liquid. In order to link substrate concentration to bioavailability, the new concept of "effective bioavailability" was derived. "Effective bioavailability" was here defined as the ratio of the actual degradation rate, possibly affected by mass transfer limitations, to the maximal degradation rate at a given concentration without mass transfer limitations. "Effective bioavailability" is thus a function of contaminant concentration. Isotope fractionation was shown to be significantly reduced at low substrate concentrations and low effective bioavailability. This effect was also described by mathematical modeling. An expression for the observed fractionation factor in function of substrate concentration and bioavailability was derived, which allowed simulations of various bioavailability conditions possibly found in the environment. Using a fractionation factor determined at high substrate concentrations for the quantification of biodegradation at low bioavailability conditions was shown to result in a significant error.

The variability of the fractionation factor can also provide information about physical mass transfer processes limiting biodegradation. Our results indicate that the observed isotope fractionation is determined by the substrate flux to a single cell relative to its intrinsic degradation capacity. Biases of stable isotope fractionation could thus be used as a flux based indicator for bioavailability restrictions in a system. The possibility of applying stable isotope

fractionation for the assessment of bioavailability was explored by means of different laboratory setups, in which mass transfer conditions could be varied. In a simple batch system, cell density was shown to influence both single cell bioavailability and isotope fractionation. A mathematical explanation for this effect was derived based on the overlap between the substrate depleted areas surrounding each degrading cell. An even more pronounced effect of cell density on isotope fractionation was seen in a two-liquid-phase system, in which the substrate, toluene, had to dissolve from a NAPL phase to the aqueous phase where degradation took place. Such situations are common in contaminated aquifers, where NAPLs are often present and serve as a reservoir for hydrophobic contaminants. The increase in bioavailability, due to larger mass transfer surface area, did not have a significant effect on the isotope fractionation at low cell densities, possibly because the difference in mass transfer was not large enough. However, at the highest density tested, fractionation was slightly higher with the larger area.

Since bacteria in aquifers are most often not suspended in pore water, but attached on solid surfaces, experiments were also performed in a model laboratory column system with immobilized bacteria. Bioavailability in the columns was varied by applying different flow rates. Some increase in degradation rates was observed with increasing flow rates, accompanied by an increasing trend in isotope fractionation. Curiously, the isotope fractionation observed in the columns was generally higher than in the batch systems, despite lower degradation rates. An improved method for the determination of fractionation factors in the column system would be needed for the confirmation of the results and to explain the discrepancy between isotope fractionation in column and batch systems.

This fundamental study clearly demonstrates the effect of substrate bioavailability on the observed stable isotope fractionation. Possible bioavailability limitations should be taken into

account when interpreting isotope fractionation data from contaminated field sites, and the practical impact of this phenomenon on the quantification of biodegradation under field conditions should be further investigated. Our results also support the possible use of stable isotope fractionation for the assessment of bioavailability. Low bioavailability resulted in decreased isotope fractionation in all systems investigated here, although there were unexplained discrepancies when columns were compared with other systems. Due to its analytical simplicity and its high sensitivity, isotope fractionation could become a valuable diagnostic tool for the quantification of bioavailability in well defined systems. This thesis lays the theoretical basis for further studies needed for the validation of this novel application of stable isotope fractionation and its expansion to other organisms and substrates.

ZUSAMMENFASSUNG

Die Bestimmung der Verhältnisse stabiler Isotope organischer Verbindungen wird immer häufiger für die Erklärung von umweltrelevanten Fragestellungen genutzt, wie z.B. zur Erfassung des biologischen Schadstoffabbaus, der Aufklärung biochemischer Abbauwege, für Untersuchungen von Nahrungsketten und der Identifizierung von Quellen und Senken für Treibhausgase. Für die Beschreibung von Umweltsysteme und. -prozesse auf Grundlage stabiler Isotopendaten, werden robuste, unveränderliche Isotopenfraktionierungsfaktore vorausgesetzt. Es wird erwartet, dass der kinetische Isotopeneffekt einer biochemischen Reaktion konstant ist. Jedoch ist der Isotopeneffekt einer biochemischen Reaktion nur dann vollständig ausgeprägt, wenn der isotopenfraktionierende Schritt ratenlimitierend für den gesamten Transformationsprozess ist. Wenn Massentransfer-Prozesse vor der fraktionierenden Reaktion ratenlimitierend sind, dann wird eine reduzierte Isotopenfraktionierung im Vergleich zu dem biochemischen Effekt beobachtet.

Konstante Isotopenfraktionierungsfaktoren sind eine Voraussetzung für die Charakterisierung und Quantifizierung des biologischen Schadstoffabbaus in kontaminierten Böden und Grundwasserleiter. Im Grundwasserleiter ist die Abbaurate von hydrophoben organischen Schadstoffen aber oft durch deren Bioverfügbarkeit kontrolliert. Die Bioverfügbarkeit für den Abbau von organischen Schadstoffen ist ein Prozess, der vom Massenstransfer relativ zur potentiellen Abbaurate bestimmt wird. Bei einer limitierten Bioverfügbarkeit ist der Substratfluss langsamer als die Abbaukapazität der Mikroorganismen. Dies sollte theoretisch zu einer reduzierten Isotopenfraktionierung führen.

In dieser Promotionsarbeit wurde der Einfluss der Substratbioverfügbarkeit auf die beobachtete Isotopenfraktionierung in einem Laborsystem gezeigt und anhand eines mathematischen Modells beschrieben. Ferner wurde die Beeinflussung der

Isotopenfraktionierung genutzt, um das Ausmaß der Bioverfügbarkeit zu erfassen. Die Variabilität der Isotopenfraktionierung wurde erst in einem Laborbatchsystem demonstriert, bei dem die Bioverfügbarkeit durch die Einstellung von verschiedenen Substratkonzertrationen verändert wurde. Bioverfügbarkeit wurde hier als Verhältnis zwischen dem Substratmassentransfer und der spezifischen Substrataffinität der Mikroorganism definiert. Um die Abhängigkeit der Bioverfügbarkeit von Substratkonzentration zu beschreiben, wurde das Konzept der „effektiven Bioverfügbarkeit“ (EB) entwickelt. Damit kann für eine bestimmte Substratkonzentration EB als Verhältnis zwischen der durch Massentransferlimitierung beeinflussten Abbaurate und der maximalen Abbaurate beschrieben werden. EB ist also konzentrationsabhängig. Unsere Versuche zeigten, dass die beobachtete Isotopenfraktionierung bei niedrigen Konzentrationen und niedriger EB deutlich tiefer war als in Systemen ohne Massentransferlimitierung. Dieser Effekt wurde durch ein mathematisches Modell eingehend untersucht, um die Variabilität in Abhängigkeit der Konzentration und Bioverfügbarkeit des Substrats für verschiedene umweltrelevante Massentransferverhältnisse aufzuzeigen. Es wurde beobachtet, dass die Verwendung von Isotopenfraktionierungsfaktoren, die bei unbegrenzter Substratverfügbarkeit bestimmt wurden, für die Quantifizierung des Schadstoffabbaus bei Massentransferlimitierungen zu einen signifikanten Fehler führen kann.

Aufgrund des Zusammenhanges von Massentransfer und Isotopenfraktionierung scheint es möglich zu sein, die Bioverfügbarkeit durch die Variabilität der beobachteten Isotopenfraktionierung zu erfassen. Es konnte gezeigt werden, dass die beobachtete Isotopenfraktionierung durch die Substratflussrate im Verhältnis zu der potentiellen biochemischen Abbaurate reguliert wird. Somit könnte die verminderte Isotopenfraktionierung als flussbasierter Indikator für eine eingeschränkte Bioverfügbarkeit verwendet werden. Diese Möglichkeit wurde in Batch-, Säulen- und

Zweiflüssigphasensystemen im Labor untersucht. In dem Batchsystem wurde der Einfluss der Zelldichte auf die Bioverfügbarkeit und der Isotopenfraktionierung gezeigt. Der Effekt der Zelldichte war noch stärker in einem Zweiflüssigphasensystem, in dem das Substrat (Toluen) von einer Ölphase sich ins Wasser löste. Solche Situationen treten häufig in kontaminierten Grundwasserleitern auf, wo nichtwässrige flüssige Phasen (NAPL) anwesend sind und als Quelle für hydrophobe Schadstoffe dienen. Bei mit Erhöhung der Kontaktoberfläche zwischen Öl und Wasser wurde die Bioverfügbarkeit erhöht, aber bei niedrigen Zelldichten konnte keine Erhöhung der Isotopenfraktionierung beobachtet werden. Erst ab einer Zelldichte von 10^8 mL^{-1} konnte eine Erhöhung der Isotopenfraktionierung bei großen Kontaktoberflächen festgestellt werden.

Im Grundwasserleiter sind Bakterien überwiegend an Sedimentoberflächen gebunden. Um diese Verhältnisse zu simulieren, wurden Abbauversuche mit immobilisierten Bakterien in kleinen Laborsäulen durchgeführt. Eine Substratlösung wurde durch die Säulen gepumpt und die Isotopenfraktionierung aus den Zufluss- und Ablaufkonzentrationen berechnet. Die Bioverfügbarkeit wurde durch die Einstellung von verschiedenen Flussraten variiert. Mit zunehmender Flussrate wurde eine Erhöhung der Abbaurate und Isotopenfraktionerung beobachtet. Trotz niedrigeren Abbauraten war die Isotopenfraktionierung in den Säulen im Vergleich zu den Batchsystemen relativ hoch. Eine geeignetere Methode für die Bestimmung von Isotopenfraktionierungsfaktoren in den Säulensystemen wäre nötig, um die Ergebnisse zu bestätigen und um die Unstimmigkeit zwischen Batch- und Säulensysteme aufzuklären.

Diese grundlegende Arbeit zeigt deutlich dass die Bioverfügbarkeit einen Einfluss auf die beobachtete Isotopenfraktionierung hat. Dieser Effekt ist bei der Erfassung des Schadstoffabbaus anhand von Isotopenuntersuchungen vom kontaminierten Flächen zu berücksichtigen. In weiterführenden Studien sollte die Auswirkung der Bioverfügbarkeit auf

die Isotopenfraktionierung direkt im Bereich von kontaminierten Grundwasserleitern und Böden untersucht werden. Im Rahmen dieser Arbeit konnte auch gezeigt werden, dass durch die Erfassung der Isotopenfraktionierung das Ausmaß der Bioverfügbarkeit gut abgeschätzt werden kann. In allen untersuchten Systemen führte eine niedrige Bioverfügbarkeit zu einer Abnahme der beobachteten Isotopenfraktionierung. Durch die relativ einfache Bestimmung und hohe Sensitivität stellt die Isotopenfraktionierung ein wertvolles diagnostisches Werkzeug für die Erfassung der Bioverfügbarkeit dar. Diese Dissertation ist die theoretische Basis für die Beschreibung des Zusammenhanges zwischen Isotopenfraktionierung und Bioverfügbarkeit. Aufbauend auf die gewonnenen Erkenntnisse kann diese Korrelation für ein breites Spektrum an Mikroorganismen und Substraten untersucht werden.

Table of contents

Chapter 1

Introduction

1.1 Outline of the thesis

1.2 Significance of bioavailability in contaminant biodegradation

1.3 Stable isotope fractionation analysis (SIFA)

1.4 Isotope fractionation and bioavailability

1.1 Outline of the thesis

Many applications of stable isotopes, such as quantification of biodegradation, depend on reliable, constant fractionation factors, expressing the magnitude of isotope fractionation caused by biochemical transformation processes [1]. Even though the fractionation caused by a chemical reaction is constant, the measured observed fractionation may be influenced by physical processes in the environment [1-4]. One important factor often controlling contaminant biodegradation in the field is bioavailability. In this thesis, the effect of substrate bioavailability on microbial stable isotope fractionation was investigated. **Chapter 1** introduces the concepts of bioavailability and stable isotope fractionation. The influence of bioavailability on stable isotope fractionation is discussed based on a conceptual framework, combining the findings of this thesis with a review of the related literature.

In **Chapter 2**, a study demonstrating the effect of bioavailability on stable isotope fractionation, during contaminant biodegradation is presented. In the first part the theoretical basis for the effect is established. An expression for the apparent fractionation factor, depending on the substrate mass transfer and the microbial specific affinity, is developed and used to model possible implications for the quantification of biodegradation. The theory is supported by experimental results from a laboratory model system, presented in the second part of **Chapter 2**. The observed isotope fractionation is expressed in function of the "effective bioavailability", a novel bioavailability concept relating the actual mass transfer limited degradation flux to the maximal degradation potential of the cell.

The potential use of the demonstrated correlation between bioavailability and isotope fractionation for the assessment of bioavailability is addressed in **Chapter 3**. The presented experiments, performed with different laboratory setups, support the use of stable isotope

fractionation as a flux based indicator for bioavailability at the single cell level. Finally in **Chapter 4**, the practical impact of our findings both on the assessment of biodegradation in the field and on the measurement of bioavailability by stable isotope fractionation analysis is critically evaluated, and an outlook on further research needs is given.

1.2 Significance of bioavailability in contaminant biodegradation

Bioavailability refers to the extent of exposure of a biological receptor to a chemical [5]. The term, long used in pharmacology, toxicology and agricultural sciences, has more recently been adapted to the context of environmental pollution and has even been incorporated in the regulatory guidelines for soil remediation of the European Union [5]. A broad variety of definitions for bioavailability exist, but as a summary, bioavailability can be seen as a combination of physical, chemical and biological processes, controlling the availability of contaminants in soils and sediments [5, 6]. There are two operationally different approaches to dealing with bioavailability in a contaminated environment: 1) increasing bioavailability in order to enhance the microbial degradation of contaminants or 2) decreasing bioavailability to reduce the exposure of organisms to the contaminants. In the first case, anthropogenic contaminants serve as carbon source to microorganisms, and a higher availability facilitates the removal of the contaminant by biodegradation. In this context, biodegradation is controlled by the biochemical activity of microorganisms and the mass transfer of a chemical to the microorganism. Bioavailability as defined by Bosma et al. is the ratio of these two processes, i.e. the substrate mass transfer relative to the intrinsic degradation capacity of a cell [7]. Bioavailability dominates degradation, when mass transfer is slower than the potential degradation capacity. Such a situation can result from slow mass transfer rates or high microbial activity.

Bioavailability plays a crucial role in the bioremediation of polluted field sites. In fact, the bioremediation of field sites contaminated with hydrophobic organic contaminants is in many cases limited by bioavailability restrictions, caused by slow mass transfer of contaminants to the degrading microorganisms [7]. In contaminated soil, pollutants and degrading bacteria have different microscopic distributions, and bacteria are mainly immobilized on solid surfaces [8]. Pollutants thus need to be transported to the bacteria before they can be taken up and degraded. This transport is a combination of processes on macro and microscale level. Pollutants in an aquifer are mainly transported with the advective groundwater flow. Around the cell the macroscopic water flow is, however, dominated by viscous forces that cause a thin water film to stick to the cell surface [9]. Within this diffusive boundary layer (DBL) surrounding the cell, transport is controlled by diffusion. The mass transfer of a contaminant to the cell may be restricted due to various chemical and/or physical processes, such as adsorption on soil particles, partitioning in a NAPL phase, or diffusion to pores too small for bacteria. At the microscale, mass transfer is influenced by the varying local contaminant concentrations, effective diffusivities and cell densities [7, 10].

Since the availability of contaminants has a strong impact on biodegradation, the assessment of bioavailability conditions in contaminated soils is important for the choice of suitable remediation techniques. If biodegradation is limited by the availability of the contaminants, remediation methods such as the physical modification of the contaminated material or the addition of surfactants, need to be used in order to increase the contaminant mass transfer to the degrading cells. The methods available for the quantification of bioavailability can be divided in chemical extraction methods and methods involving biological reporters. Extraction methods, such as solid phase extractants (SPE) [11] and cyclodextrins [12], provide a defined bioavailable concentration [13], which however is not necessarily equal to the amount of substrate entering a cell. Solid phase extractants have in some cases shown to

include the bioaccessible fraction, that is the fraction that would be biodegraded only after a longer period of time [14]. The biological methods monitor the effect of a contaminant using a reporter organism, which reflects the amount to which the cell is exposed. A bacterial biosensor, the green fluorescent protein (GFP) the production of which was influenced by the substrate flux to the cell, was developed by Tecon et al. [15]. In this thesis, the possible use of stable isotope fractionation as an alternative flux based indicator for the assessment of bioavailability was addressed.

1.3 Stable isotope fractionation analysis (SIFA)

1.3.1 Theory and Definitions

Stable isotopes are nonradioactive atoms of the same element that differ from each other only in the number of neutrons in their nucleus and thus in molecular mass [16]. Isotope fractionation is due to the fact that a higher activation energy is needed for the cleavage of a chemical bond containing a heavier isotope. Therefore molecules containing lighter isotopes have higher reaction rates, which leads to an enrichment of heavy isotopes in the residual substrate pool [1, 16-18].

The origin of isotope fractionation is the kinetic isotope effect, which also determines the extent of fractionation. The kinetic isotope effect (KIE) is the variation in the rate of a chemical reaction, when an atom in one of the reactants is replaced by its isotope. The effect is due to the mass difference of the isotopes, which affects the vibrational frequency (v) of the chemical bond (Eq.1) and concomitantly the zero point energy of the system (Eq.2, $n = 0$) and the activation energy needed for bond cleavage (Fig. 1.1).

$$v = \frac{1}{2\pi}\sqrt{\frac{k}{\mu}} \tag{1}$$

$$E_n = hv\left(n + \tfrac{1}{2}\right) \tag{2}$$

μ is the reduced mass of the two atoms A and B forming the chemical bond, $\mu = m_A m_B/(m_A+m_B)$. k is the spring constant for the bond and h is the Planck constant. The substitution of an atom by its heavier isotope thus leads to a lower zero point energy, and a higher activation energy is needed for the cleavage of the bond [16]. The KIE is defined as the ratio of the rate constants k, for the reaction rates of the heavier and the lighter atom of the element E [1]:

$$KIE = {}^{l}k \Big/ {}_{h}k \qquad (3)$$

This **intrinsic fractionation** determined by the kinetic isotope effect can only be observed if the fractionating bond cleavage (k_3) represents the rate-determining step in the overall process, as in most chemical (nonenzymatic) reactions. For enzymatic reactions, however, other processes, such as the transport or the binding of the substrate (S) to the enzyme (E), preceding the bond cleavage may be rate limiting.

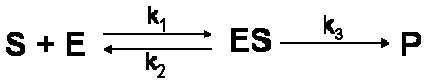

If one of the steps preceding the fractionating bond cleavage is slow, the full intrinsic fractionation will not be observed, i.e. fractionation is masked. In the extreme case, each substrate molecule will be converted and no isotopic discrimination will be observed, although there may be significant KIE for the bond conversion. Northrop introduced the expression "commitment to catalysis" and derived the following equation for the **apparent kinetic isotope effect (AKIE)** [2]:

$$AKIE = \frac{C + KIE}{C + 1} \qquad (4)$$

where $C = k_3/k_2$ is the commitment to catalysis and represents the tendency of the enzyme substrate complex (ES) to react (k_3) as opposed to its tendency to dissociate (k_2).

In this thesis we focused on mass transfer processes outside the cell, bringing the substrate to the cell surface. If these processes are slow they may decrease the observed fractionation as well. For this purpose, the apparent fractionation, defined above is here referred to as "**enzymatic fractionation"**. This term is used for the fractionation caused by a cell at non mass transfer-limited conditions, whereas the "**observed fractionation"** may be influenced by mass transfer limitations (Fig. 1.2).

The magnitude of isotope fractionation between a reactant and its product can be expressed either with the **fractionation factor α**

$$\alpha = \frac{R_{reactant}}{R_{product}} \tag{5}$$

or the **enrichment factor ε**

$$\varepsilon = (\alpha - 1) \times 1000[‰] \tag{6}$$

where $R_{reactant}$ and $R_{product}$ are the ratios of the heavy to light isotope in the reactant and in the product, respectively. For molecules in which all isotopes are located in the same reactive position, α can also be interpreted as the ratio of the rate constants [17]

$$\alpha = \frac{^{h}k}{^{l}k} \tag{7}$$

i.e. α is the reciprocal of KIE. According to the findings of this thesis, a more accurate definition for α would include the concentrations of the respective isotopologues [3, 4]:

$$\alpha = \frac{^{h}k / {}_{h}c}{^{l}k / {}_{l}c} \tag{8}$$

α can be graphically determined from the relationship between concentration change and the shift in the isotope ratio. For closed systems, this relation is given by the **Rayleigh equation** (here in its logarithmic form) [19, 20]

$$\ln\left(\frac{R_t}{R_0}\right) = (\alpha - 1) \times \ln\left(\frac{c_t}{c_0}\right)\left(\frac{R_0 + 1}{R_t + 1}\right) \quad (9)$$

where R_t and R_0 are the substrate isotope ratios at times t and zero, respectively, and c_t and c_0 are the total substrate concentrations at these times. α is derived by plotting measured values of $\ln(R_t/R_0)$ vs. $\ln([c_t/c_0]/[(R_t+1)/(R_0+1)])$ in a Rayleigh plot and obtaining the slope of the linear regression.

Isotope ratios (or isotope signatures) of field or laboratory samples are generally reported as difference in per mil with respect to an international standard, e.g. Vienna Standard Mean Ocean Water (VMOW) for hydrogen and Peedee Belemnite (PDB) for carbon [21], respectively:

$$\delta^h E = \left(\frac{R - R_{ref}}{R_{ref}}\right) \times 1000[‰] \quad (10)$$

R stands for the ratio between the heavy ${}^hE$ and light ${}^lE$ isotopes of a given element E in a given compound $R = {}^hE/{}^lE$. R and R_{ref} are the ratios of heavy to light isotope in the sample and in the standard, respectively. These ratios are obtained using compound specific stable isotope fractionation analysis (CSIA) and can nowadays be determined for carbon ($^{13}C/^{12}C$), hydrogen ($^{2}H/^{1}H$), nitrogen ($^{15}N/^{14}N$), oxygen ($^{18}O/^{16}O$) and chlorine ($^{37}Cl/^{35}Cl$). If the fractionation factor is known, the isotope ratio of field samples can be linked to the extent of biodegradation using the Rayleigh model [1, 18].

1.3.2 Stable isotope fractionation analysis for the assessment of microbial transformation reactions

Many enzymatic reactions in microbial transformation pathways are accompanied by a significant isotope effect, i.e. the product becomes depleted in the heavier isotope, whereas the substrate gets enriched in heavy isotope. The analysis of the residual substrate fraction can

thus provide information about microbial transformation processes. Isotope fractionation analysis is in fact used for the elucidation of reaction mechanisms [1, 22-24] and for the assessment of biodegradation during remediation by monitored natural attenuation (MNA) [25-27]. Natural attenuation takes advantage of naturally occurring processes for the remediation of contaminated soil [28]. It is a cost-effective and environmentally sound solution for the remediation of large contaminated sites. However, for MNA to be accepted as a remediation strategy, it is necessary to unambiguously demonstrate the removal of the contamination. The most desirable natural attenuation process is microbial degradation of the contaminants, since it ideally results in complete mineralization or in harmless end products. Physical processes, such as dilution or sorption, may decrease contaminant concentrations in the pore water, but do not eliminate the contaminant from the system. Stable isotope fractionation analysis has proven to be very useful for the confirmation of biodegradation, since the above listed physical, nondestructive processes do not cause a significant isotope fractionation [29-32]. It should be kept in mind that abiotic degradation processes, such as redox processes with iron minerals in soil [33, 34] or photolysis in surface waters [35], may also cause significant isotope fractionation.

The quantification of biodegradation by stable isotope fractionation analysis relies on invariable fractionation factors relating the shift in the isotope ratio to the change in contaminant concentration [18]. Fractionation factors are normally determined in closed laboratory systems where both isotope ratio and concentration can be monitored [36-40]. They are then applied to calculate the extent of biodegradation in highly heterogeneous environmental systems. The procedure is schematically described in Figure 1.3. For this procedure, it is generally assumed that the fractionation factor for a specific reaction is constant and independent of environmental conditions.

1.4 Isotope fractionation and bioavailability

When degradation is controlled by the activity of the isotope sensitive enzyme, the isotope composition at the enzyme is in equilibrium with the composition at the cell surface and in the bulk liquid. Samples taken from the bulk thus directly reflect the isotope fractionation taking place at the enzyme. For microbial transformation in environmental systems, numerous physical and biological processes may, however, precede the fractionating enzymatic reaction. The fractionation by these processes is negligible compared to the fractionation by the enzymatic reaction, but they may indirectly decrease the observed fractionation. During mass transfer limited degradation, the potential microbial conversion rate exceeds the mass transfer flux to the degrading enzyme. The equilibrium between the bulk and the enzyme thus becomes shifted more into the direction of the enzyme. The enzymatic fractionation may still lead to a strong enrichment of heavy isotope at the enzyme, which however, is not fully reflected in the bulk, due to the shifted equilibrium [2]. The observed isotope fractionation derived from the isotope composition in the bulk is thus reduced compared to the enzymatic fractionation (Fig. 1.4). In an extreme case, mass transfer to the enzyme may become unidirectional and no isotope fractionation is observed in the bulk, despite a significant KIE.

Several studies have addressed the influence of substrate availability on stable isotope fractionation during photosynthesis, methane oxidation, methanogenesis and denitrification [41-46]. A conceptual model for the influence of different mass transfer steps on isotope fractionation was developed by O'Leary [41]. Most of the studies summarized in Table 1 were, however, performed in more complex systems, where other physical effects or physiological changes cannot be excluded, and theoretical description was therefore difficult. Also, to our knowledge, no previous studies about the effect of contaminant mass transfer to the degrading cells on isotope fractionation have been reported. However, indications of a mass transfer effect can be found in several studies describing stable isotope fractionation

during contaminant biodegradation [47-49]. Since bioavailability is here defined as the mass transfer flux relative to the degradation rate, it can also be limited by increased microbial activity. The degradation potential of a cell is influenced by a variety of environmental parameters. For instance, iron availability was shown to significantly accelerate toluene degradation by *Pseudomonas putida* mt-2 [50], and a concomitant decrease in isotope fractionation was also observed [51].

Mass transfer processes affecting bioavailability include 1) desorption/dissolution, 2) diffusion to the cell and 3) uptake through the membrane (Fig. 1.5). A rate limitation due to any of these processes leads to isotopic disequilibrium between the medium and the active site of the enzyme and to a concomitant reduction of the observed isotope fractionation. Steps 4 and 5 of Figure 1.5 are not included in bioavailability processes, since they are not influenced by the environmental conditions, and are not discussed in this thesis. In the next paragraphs, the effect of the different mass transfer processes on the observed isotope fractionation is discussed with emphasis on contaminant biodegradation.

Process 1: Desorption and/or dissolution

Since bacteria are believed to exclusively take up molecules dissolved in water, the first step for biodegradation of contaminants is the transfer of a substrate to the aqueous phase. If this first step is very slow it may have an effect on the observed isotope fractionation. Already in 1979 Zyakun et al. suggested that the isotope fractionation factor for biological methane oxidation may partly depend on the rate of dissolution of CH_4 into the media [43]. For organic contaminants this first step may consist of the dissolution of solid or NAPL compounds or the desorption of contaminants sorbed on soil matter into the aqueous phase. In our experiments presented in section 3.2, the mass transfer from NAPL to the aqueous phase was shown to have an effect on the observed isotope fractionation. To our knowledge, no previous studies

on the effect of this first step on stable isotope fractionation have been reported. The water solubility of a contaminant has however been shown to correlate with isotope fractionation [47-49, 52]. Higher water solubility would increase the transfer of a contaminant into the aqueous phase, but since solubility is also connected to diffusivity in water, these studies are discussed in the context of Process 2: Transport to the cell.

Process 2: Transport to the cell

Since microorganisms in soil are mostly immobilized on surfaces, contaminants need to be transported to the degrading cells. The contaminant flux through the diffusive boundary layer (DBL) surrounding a cell depends on the concentration gradient between the bulk liquid and the cell surface. The substrate concentration in the medium therefore influences the bioavailability. The effect of CO_2 availability on isotope fractionation during photosynthesis has been shown in tomato plants [42], cyanobacteria [53, 54] and algae [53]. O'Leary concluded that the CO_2 concentration reflects the substrate availability: at high CO_2 levels cells can discriminate ^{13}C, whereas at CO_2 limited conditions cells use all CO_2 available, independent of its isotopic nature. A theoretical basis for the effect of substrate concentration on bioavailability and subsequently on the observed fractionation factor, is presented in Chapter 2 [3].

The effect of water solubility on the observed isotope fractionation, observed in several studies [47-49, 52], may also be correlated to mass transfer restrictions. Pond et al. analyzed the hydrogen isotope fractionation during biodegradation of $C_{15} - C_{27}$ n-alkanes and observed a decrease in isotope fractionation with increasing length of the carbon chain [49]. This was explained by a dilution of the kinetic isotope effect by the high number of nonreacting hydrogen atoms in long chain alkenes. However, the degradation rates also correlated with chain length and isotope fractionation. Reduced mass transfer flux, due to low solubility may

thus be the factor decreasing the observed fractionation of long chain alkenes. A correlation between alkane chain length and carbon isotope fractionation was observed by Kinnaman et al. for methane, ethane, propane and n-butane and by Bouchard for n-alkenes from propane to decane [48, 55]. Bouchard et al. corrected the obtained fractionation factors for nonreacting carbons [1], but the chain length dependency still persisted [47]. They therefore hypothesized that transport or binding steps before the fractionating reaction become increasingly limiting with poorly soluble long chain alkanes. An approximately linear relationship was observed between the AKIE and the square root of the molecular mass, indicating that diffusion controlled rate limitation could explain the trend. Bouchard et al. tested this hypothesis by comparing their results with those measured during gas phase reactions with OH radicals by Anderson et al. [56]. Since, chemical reactions in a homogeneous system have no slow steps preceding the fractionating bond cleavage, fractionation should be independent of chain length (except for the dilution effect). After the correction for nonreacting positions, the values obtained from the chemical reaction became independent of chain length [56]. A similar effect might explain the large difference in fractionation between tetrachloroethene (PCE) ($\varepsilon = -5.5 \pm 0.8$ ‰) and trichloroethene (TCE) ($\varepsilon = -13.8 \pm 0.7$ ‰) [40, 52]. Slater et al. hypothesized that the low solubility and/or the high K_{ow} of PCE could cause local substrate limitations, leading to reduced observed isotope fractionation.

The mass transfer to a single cell may also be reduced by high cell density. A mathematical description of the effect of cell density on bioavailability and on isotope fractionation is given in section 3.1. The observed effect could be explained by differences in degradation rates, which correlated with shifts in isotope fractionation [57]. An effect of cell density on isotope fractionation factors was also reported by Templeton et al. [58]. They observed a reduced isotope fractionation at later growth stages during methane oxidation. This was theoretically explained by extending the O'Leary two step scheme to include the effect of total enzyme concentration to the partitioning factor (or "commitment to catalysis" factor in Northrop's

model), which increases with cell density. Since the experiments were performed with a growing culture, the possibility of physiological changes cannot be excluded. The effect was, however, shown to be independent of the type of organism or the form of the methane monooxygenase.

Process 3: Uptake from the cell surface into the cell

Most bacterial cells are surrounded by a cell wall and a biological membrane. In gram positive bacteria a single membrane is surrounded by a thick cell wall consisting mostly of peptidoglycan. The cell wall of gram negative cells consists of a thin layer of peptidoglycan located between an inner and an outer membrane. The peptidoglycan does not normally constitute a transport barrier for solutes due to its porous structure. The ca. 8 nm thick cytoplasmic membrane, generally formed by a phospholipid bilayer, acts as a permeability barrier. Transport through the membrane can be active or passive, depending on the compound [59]. Hydrophobic molecules, such as many organic contaminants, pass through the membrane by simple diffusion, following their concentration gradient [60]. The diffusion through the membrane thus constitutes another potential rate limiting transport step.

Experiments by Nijenhuis et al. clearly demonstrate the effect of mass transfer limitation at the cell membrane [40]. They studied isotope fractionation of tetrachloroethene during reductive dechlorination. In a series of degradation experiments with cyanocobalamin (i.e. the cofactor at the reactive centre) only, with purified enzyme, with crude extract and with growing cells, they could show that the observed fractionation decreased with increasing integrity of the microbial system. For *Desulfitobacterium* sp. PCE-S and *Sulfurospirillum multivorans*, fractionation with growing cells was reduced by 56 and 41%, respectively, compared to the crude extract. The findings indicate that the transfer through the cell wall poses a rate limitation reducing the observed fractionation factor [40]. A similar effect was

observed by Morasch et al. during anaerobic toluene degradation by *Desulfobacterium cetonicum*. The enzyme benzylsuccinate synthase exhibited a 30% higher hydrogen isotope fractionation in cell extract than in growing cells [39].

FIGURES

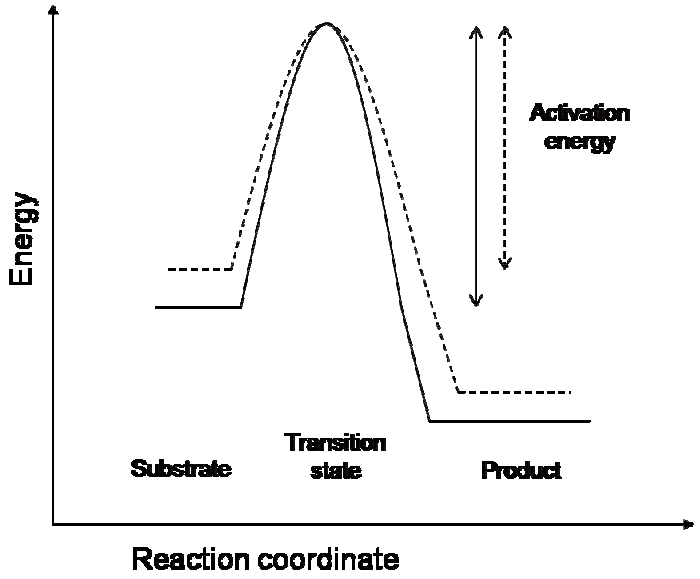

Figure 1.1. The kinetic isotope effect (KIE). Molecules containing heavy isotopes (solid line) have lower zero point energy, and the reaction requires a higher activation energy.

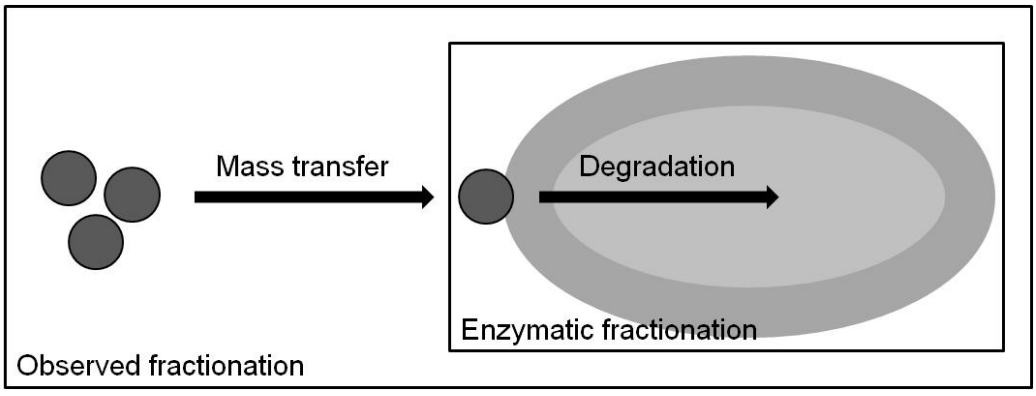

Figure 1.2. Microbial substrate transformation is controlled by the substrate mass transfer flux to the cell and by the biochemical activity of the cell. "Enzymatic fractionation" is determined by the microbial activity only, whereas the "observed fractionation" may also be affected by mass transfer limitations.

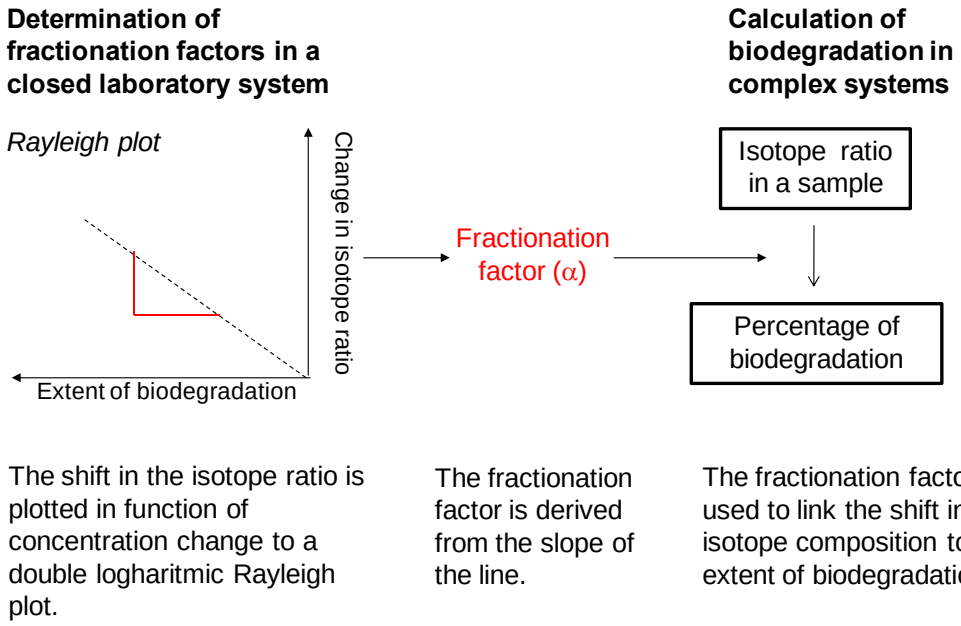

Figure 1.3. Schematic representation of the quantification of biodegradation by stable isotope fractionation.

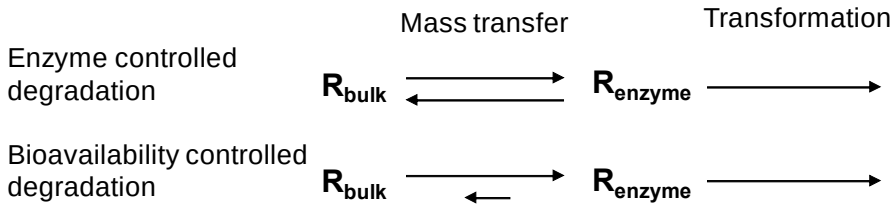

Figure 1.4. The effect of bioavailability limitation on the isotopic equilibrium. Top: The overall degradation rate is controlled by the rate of the isotope sensitive transformation reaction. The isotope composition at the enzyme is in equilibrium with the bulk $R_{bulk} = R_{enzyme}$. Bottom: Mass transfer is rate limiting. There is no equilibrium between the enzyme and the bulk $R_{bulk} \neq R_{enzyme}$, and the observed fractionation measured in the bulk does not reflect the enzymatic fractionation.

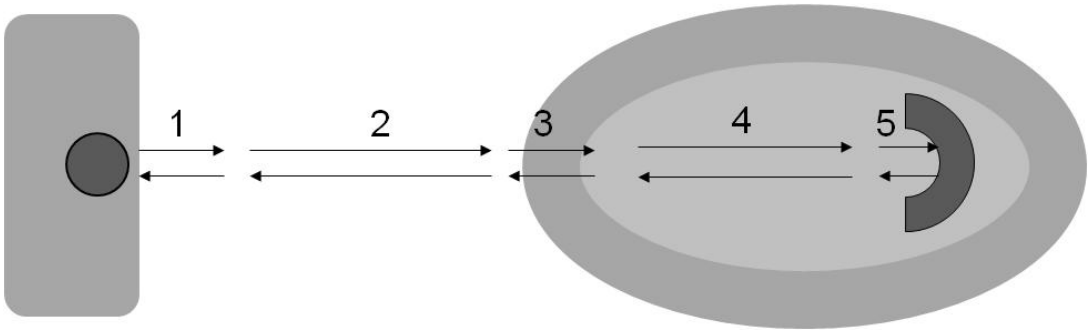

Figure 1.5. The transport of a contaminant to the enzyme consists of several mass transfer processes processes: 1) desorption/dissolution, 2) transport (diffusion), 3) uptake, 4) intracellular transport, 5) binding. Processes 1 – 3 are included in bioavailability processes, since they depend on environmental conditions.

TABLES

Table 1. Literature on the impact of substrate availability on stable isotope fractionation in natural systems.

Process	Observations	Authors' conclusions	References
Photosynthesis	Isotope fractionation is a function of CO_2 concentration	Isotopic disequilibrium between bulk and cell surface	[42],[54]
	Maximal fractionation at high CO_2 concentration and low cell density	Limitation of CO_2 supply leads to reduced fractionation	[53]
	Review summarizing the factors influencing isotope fractionation	Fractionation is determined by CO_2 availability. Theoretical model for the prediction of isotope fractionation, taking into account the partitioning factor (i.e. commitment to catalysis in section 1.3.1)	[41]
	Decrease of fractionation in function of biofilm thickness	$\delta^{13}C$ value depends on the balance between photosynthesis rates and mass transfer limitation controlled by the biofilm thickness	[61]
Methane oxidation	Fractionation depends on CH_4 diffusion from coal crumble	Fractionation depends partly on the rate of CH_4 dissolution	[62, 63]
	Fractionation is a function of cell density in chemostat	Fractionation depends on the CH_4 concentration available per cell	[63, 64]
	Reduced fractionation at later growth stages, high cell density	Fractionation changes in function of total enzyme concentration, which affects the commitment to catalysis term	[58]
	Fractionation is a function of the ambient CH_4 concentration	Fractionation depends on the CH_4 flux into the soil	[46]
Methanogenesis	Higher fractionation at later growth stage, isotope fractionation positively correlated with temperature and/or metabolic rate	Fractionation determined by the Gibbs free energy of catabolism, which controls the reversibility of the reaction	[65], [66]
Denitrification	Low fractionation at high denitrification rates and NO_3^- depletion	Isotope fractionation can give information about denitrification rates in the water column	[44, 67, 68]
	Fractionation higher in the water column than in sediments	Fractionation depends on diffusivity	[44]
Ammonium assimilation	Fractionation depends on NH_4^+ concentration, active transport at low concentrations increases fractionation	Uptake by the cell is the rate limiting step and decreases the fractionation	[69],[70], [71], [72]

Chapter 2

The effect of substrate concentration on stable isotope fractionation

2.1 Impact of bioavailability Restrictions on microbially induced stable isotope fractionation: 1. Theoretical calculations[1]

2.2 Impact of bioavailability Restrictions on microbially induced stable isotope fractionation: 2. Experimental evidence[2]

[1] Environ Sci Technol. 2008, 42, 6544 – 6551
[2] Environ Sci Technol. 2008, 42, 6552 – 6558

An important factor influencing the contaminant mass transfer to a degrading cell is the contaminant concentration in the bulk liquid. In this chapter, the influence of contaminant concentration on the observed isotope fractionation is investigated. The first part of the chapter provides a thorough theoretical background for the effect of concentration and bioavailability on isotope fractionation. A mathematical expression for the observed fractionation factor in function of substrate concentration and bioavailability was derived, which allowed the mathematical simulation of different scenarios in laboratory and field systems and the prediction of the error for the quantification of bioavailability. In the second part of the chapter, experimental results supporting the theory are presented. A standardized laboratory batch system was used to determine isotope fractionation at different substrate concentrations. Isotope fractionation was shown to be reduced in batches with low initial substrate concentration. Isotope fractionation also decreased in a single batch after approximately half of the contaminant had been degraded. In order to link the concentration dependency to bioavailability, the concept of "effective bioavailability" was developed. "Effective bioavailability" was defined as the ratio of the actual degradation flux described by the Best equation to the maximal potential degradation described by the Michaelis-Menten equation. A clear correlation between "effective bioavailability" and the enrichment factor was obtained.

Environ. Sci. Technol. **2008**, *42*, 6544–6551

Impact of Bioavailability Restrictions on Microbially Induced Stable Isotope Fractionation. 1. Theoretical Calculation

MARTIN THULLNER,*,† MAKEBA KAMPARA,† HANS H. RICHNOW,‡ HAUKE HARMS,† AND LUKAS Y. WICK†

Departments of Environmental Microbiology and Isotope Biogeochemistry, UFZ - Helmholtz Centre for Environmental Research, Leipzig, Germany

Received November 6, 2007. Revised manuscript received May 5, 2008. Accepted May 22, 2008.

The microbial degradation of organic substrates often exhibits a fractionation of stable isotopes which leads to an enrichment of the heavier isotope in the remaining substrate. The use of this effect to quantify the amount of biodegraded substrate in contaminated aquifers requires that the isotope fractionation factor is constant in time and space. In many natural and engineered systems the bioavailable concentration at the location of the enzymes differs from the average bulk concentration of the substrate. When enzymatically driven substrate degradation is coupled to a preceding transport step controlling the bioavailability of the substrate, the observed isotope fractionation becomes a function of the bulk substrate concentration. The sensitivity of the observed isotope fractionation factor toward such substrate concentration changes depends on the ratio of bulk substrate concentration and Michaelis–Menten constant and on the ratio between the specific affinity of the microorganisms toward the substrate and the first order rate constant of the bioavailability limiting transport process. Highest sensitivities toward substrate concentration were found for combinations of high substrate concentration with low substrate bioavailability (i.e., high ratios of substrate concentration and Michaelis–Menten constant, and high ratios of specific affinity and transport rate constant). As a consequence, changes in concentration and isotopic composition of a bioavailability limited substrate in batch experiments should not exhibit a linear relation in a Rayleigh plot, and the slope of the Rayleigh plot should show a decreasing trend with concentration decrease. When using isotope fractionation to quantify biodegradation along groundwater flow paths, changes in observed isotope fractionation might occur while contaminant concentration decreases along a flow path.

* Corresponding author. Phone: +49-341-235-1338. Fax: +49-341-235-451338. E-mail: martin.thullner@ufz.de. Corresponding author address: Department of Environmental Microbiology, Helmholtz Centre for Environmental Research - UFZ, Permoserstrasse 15, 04318 Leipzig, Germany.
† Department of Environmental Microbiology.
‡ Department of Isotope Biogeochemistry.

Introduction

Groundwater contamination by organic carbon pollutants is a major environmental problem in many industrialized countries. Especially for contaminated megasites neither pump-and-treat nor any engineered in situ treatments are technically and economically feasible (*1*), and a monitored natural attenuation program is considered as the most reasonable remediation option (*2–4*). The main and most desirable process contributing to the natural attenuation of organic contaminants is their degradation by subsurface microorganisms, but degradation activities are highly variable depending on the specific compound and the environmental conditions (*2*). Therefore, the evaluation of in situ biodegradation is essential for the assessment of natural attenuation strategies (*5*).

In recent years, stable isotope fractionation analysis has gained more and more attention as a tool for characterizing and assessing in situ biodegradation of organic pollutants in contaminated aquifers (*6, 7*). For a closed system, the evolution of the isotopic ratio with advancing degradation is given by the well-known analytical Rayleigh model (*8*), and this approach is typically used for the quantification of in situ biodegradation e.g. refs *9–12*. For environmental systems macroscopic transport processes as well as multiple reactive processes influence contaminant concentrations and isotopic ratios (*13, 14*), which required extensions to the Rayleigh model to address the effects of such additional processes (*15–17*).

All these Rayleigh model-based approaches for the quantification of biodegradation using stable isotope measurements consider the existence of a constant isotope fractionation factor describing the degradation of a specific contaminant at given environmental conditions. Values for fractionation factors are typically determined in laboratory degradation experiments and considered to be applicable for in situ degradation, too (*6*).

However, in natural systems a variety of physical and/or chemical processes take place, which may control the bioavailability of a substrate. Such processes include e.g. sorption, pore size exclusion (in porous media such as aquifers and soil), and microscale transport processes around the microbial cells (*18–20*). As a consequence, the concentration of a dissolved substrate in the immediate vicinity of a metabolically active cell may differ significantly from the average bulk concentration in the system. The consumption rate of the substrate then depends not only on the microbial degradation rate but also on the transfer rate of the substrate from the bulk solution to the microbial cell e.g. refs *21* and *22*. Such rate limiting steps (e.g., microscale transport or substrate uptake) have been shown to reduce kinetic isotope fractionation effects caused by the isotopically sensitive reaction step, which is commonly the cleavage of a chemical bond (*23–25*). In environmental and biological science kinetic isotope fractionation has been used so far to characterize the transition state of chemical reactions, to obtain information on the chemical mechanism, or to identify rate limiting steps in complex biochemical transformation reactions (*26*). Here, it is commonly accepted textbook knowledge that the isotope fractionation in enzyme reactions described by Michaelis–Menten kinetics is not dependent on substrate concentration. In turn, concepts linking isotope fractionation to rate limitations due the bioavailability of the substrate have not been considered adequately although recent fractionation experiments with hydrophobic compounds

10.1021/es702782c CCC: $40.75
Published on Web 07/30/2008

gave indications that bioavailability may affect isotope fractionation (*27*).

In such bioavailability limited systems the "observed" isotope fractionation factor determined from measurement of the bulk liquid might differ from the "enzymatic" isotope fractionation factor determined under ideal conditions. Although a theoretical analysis of Northorp (*26*) implicitly suggests a potential dependency of the apparent isotope fractionation factor on substrate concentration, this relation has not been addressed specifically. As a consequence, it is commonly considered that also in the case of bioavailability limited systems the observed isotope fractionation factor depends only on environmental factors but not on the substrate concentration (*24*).

The aim of the present study is to theoretically evaluate if the above assumption of constant (observed) fractionation factors hold for enzymatic systems with limited bioavailability. By combining and expanding different concepts proposed for enzyme kinetics, stable isotope fractionation, and bioavailability restrictions it is determined if and under which circumstances the observed isotope fractionation may vary with substrate concentration. The experimental verification of these theoretical findings is subject of an accompanying paper (*29*).

Theoretical Background

Quantification of Isotope Fractionation Processes. The isotopic composition of a chemical species can be expressed as the ratio, R, between the concentration of the heavy, ${}^{h}c$, and the light isotope, ${}^{l}c$

$$R = \frac{{}^{h}c}{{}^{l}c} \tag{1}$$

with the total species concentration given by $c = c_{tot} = {}^{h}c + {}^{l}c$.

If the concentration of a species is reduced due to a chemical reaction (e.g., microbial degradation) the specific rate of the reaction might differ between the light and heavy isotope and can be expressed by a fractionation factor α defined as

$$\alpha = \frac{{}^{h}r/{}^{h}c}{{}^{l}r/{}^{l}c} \tag{2}$$

with ${}^{h}r = \partial {}^{h}c/\partial t$ and ${}^{l}r = \partial {}^{l}c/\partial t$ as the utilization rates of the heavy and light isotope, respectively. Usually molecules containing the heavier isotope react slower than those containing the lighter isotope, which results in typical values of α smaller than 1. In case the rates for both isotopes are given by first order rate laws, α is a constant and determined by the ratio of the first order rate constants ${}^{h}k$ and ${}^{l}k$:

$$\alpha = \frac{{}^{h}r/{}^{h}c}{{}^{l}r/{}^{l}c} = \frac{{}^{h}k \cdot {}^{h}c/{}^{h}c}{{}^{l}k \cdot {}^{l}c/{}^{l}c} = \frac{{}^{h}k}{{}^{l}k} \tag{3}$$

As for most reactive processes in nature fractionation effects are rather small ($\alpha \approx 1$), a more convenient enrichment factor ϵ (expressed in ‰) is defined as

$$\varepsilon = (\alpha - 1) \cdot 1000 \tag{4}$$

If α is constant, changes in concentration and changes in the isotopic composition of a species (with initial concentration $c_{tot,0}$ and initial isotope composition R_0) are given by the Rayleigh model (*8, 30*):

$$\left(\frac{c_{tot}/c_{tot,0}}{(R+1)/(R_0+1)}\right)^{\alpha-1} = \left(\frac{R}{R_0}\right) \tag{5}$$

For many elements the natural abundance of the heavy isotope is relatively small ($R \ll 1$). In those cases the Rayleigh model can be simplified to

$$\left(\frac{c_{tot}}{c_{tot,0}}\right)^{\alpha-1} = \left(\frac{R}{R_0}\right) \tag{6}$$

Values for α can be determined experimentally by plotting $\ln(R/R_0)$ against $\ln(c/c_0)$ or $\ln((c/c_0)/((R+1)/(R_0+1)))$, respectively. In such Rayleigh plots all measured values should plot on a straight line exhibiting the constant slope of $(\alpha - 1)$.

Isotope Fractionation in Enzymatic Systems. To describe isotopic effects in enzymatic systems here the simplest mechanistic description of an enzymatic reaction is considered consisting of three steps (Figure 1, top):

1. combination of (bioavailable) substrate, c_{bioav}, and free enzyme, E_{free}, to an activated complex, A, following a bimolecular rate law ($r = k_{MM,1} \cdot c_{bioav} \cdot E_{free}$); 2. decay of the activated complex back to the original enzyme and substrate ($r = k_{MM,-1} \cdot A$); and 3. transformation of the activated complex producing the reaction product, P, and re-releasing the enzyme ($r = k_{MM,2} \cdot A$) with $k_{MM,1}$, $k_{MM,-1}$, and $k_{MM,2}$ as reaction rate parameters and E_{tot} as the total amount of enzymes.

Assuming A and E_{free} in steady state, the overall rate of the reaction is given by the Michaelis–Menten kinetics e.g. ref *31*

$$r_{tot} = \frac{\partial c_{bioav}}{\partial t} = V_{\max} \cdot \frac{c_{bioav}}{c_{bioav} + K_M} \tag{7}$$

with V_{max} as maximum reaction rate and K_M as the Michaelis–Menten constant, both determined by the parameters describing the enzymatic system and its reactive steps

$$V_{\max} = k_{MM,2} \cdot E_{tot} \tag{8}$$

and

$$K_M = \frac{k_{MM,-1} + k_{MM,2}}{k_{MM,1}} \tag{9}$$

Furthermore, the specific affinity, a, of the microorganism promoting the enzymatic reaction is given as (*32*)

$$a = \frac{V_{\max}}{K_M} = \frac{k_{MM,2} \cdot k_{MM,1}}{k_{MM,-1} + k_{MM,2}} \cdot E_{tot} \tag{10}$$

To address isotopic effects caused by such an enzymatic system the above scheme needs to be expanded considering the competition of the light and heavy isotope for the available enzymes (Figure 1, bottom). In analogy to competitive inhibitors it is assumed that molecules containing each type of isotopes are acting as individual species, described by their individual set of parameters (*33*). Solving the resulting system of equations assuming ${}^{h}A$, ${}^{l}A$, and E_{free} in steady state allows for the calculation of the individual consumption rates for each isotope

$$\begin{aligned} {}^{h}r &= \frac{\partial {}^{h}c_{bioav}}{\partial t} = {}^{h}V_{\max} \cdot \frac{{}^{h}c_{bioav}}{{}^{h}c_{bioav} + {}^{h}K_M + {}^{l}c_{bioav}\dfrac{{}^{h}K_M}{{}^{l}K_M}} \\ &= {}^{h}a \cdot \frac{{}^{h}c_{bioav}}{1 + \dfrac{{}^{h}c_{bioav}}{{}^{h}K_M} + \dfrac{{}^{l}c_{bioav}}{{}^{l}K_M}} \end{aligned} \tag{11}$$

and

$$ {}^{l}r = \frac{\partial {}^{l}c_{bioav}}{\partial t} = {}^{l}V_{max} \cdot \frac{{}^{l}c_{bioav}}{{}^{l}c_{bioav} + {}^{l}K_M + {}^{h}c_{bioav}\frac{{}^{l}K_M}{{}^{h}K_M}} $$

$$ = {}^{l}a \cdot \frac{{}^{l}c_{bioav}}{1 + \frac{{}^{h}c_{bioav}}{{}^{h}K_M} + \frac{{}^{l}c_{bioav}}{{}^{l}K_M}} \quad (12) $$

with ${}^{h}V_{max}$, ${}^{l}V_{max}$, ${}^{h}K_M$, ${}^{l}K_M$, ${}^{h}a$, and ${}^{l}a$ defined in analogy to eqs 8–10. The above terms show that differences in the individual reaction rates for each isotope are not necessarily caused by differences in the maximum reaction rate but may also be determined by isotope specific Michaelis–Menten constants. Furthermore, the consumption rate of each isotope is not depending solely on the concentration of the isotope itself but also on the concentration of the other isotope (e.g., the consumption rate of the heavy isotope depends on the concentration of the light isotope, too).

The total consumption rate is then given as

$$ r_{tot} = \frac{\partial c_{bioav,tot}}{\partial t} = {}^{h}r + {}^{l}r = \frac{{}^{h}a \cdot {}^{h}c_{bioav} + {}^{l}a \cdot {}^{l}c_{bioav}}{1 + \frac{{}^{h}c_{bioav}}{{}^{h}K_M} + \frac{{}^{l}c_{bioav}}{{}^{l}K_M}} $$

$$ = \frac{{}^{l}V \cdot {}^{l}c_{bioav} + {}^{h}V \cdot {}^{h}c_{bioav} \cdot \frac{{}^{l}K_M}{{}^{h}K_M}}{{}^{l}c_{bioav} + {}^{l}K_M + {}^{h}c_{bioav} \cdot \frac{{}^{l}K_M}{{}^{h}K_M}} \quad (13) $$

The above equations show that the total consumption rate considering the competing effects between the isotopically heavy and light fraction of the substrate follows Michaelis–Menten kinetics only in the case where V_{max} and K_M are identical for both isotopes (i.e., the absence of any isotope fractionation). If isotope fractionation occurs, neither the total rate nor the rates for the individual isotopes are exactly described by Michaelis–Menten kinetics. However, for the common case of small values of R (${}^{h}c_{bioav} \ll {}^{l}c_{bioav}$) and/or very small isotope fractionation, eq 13 converges to the Michaelis–Menten equation.

Finally, using eqs 11 and 12 the fractionation factor for this enzymatic system is determined by the ratio of the specific affinities of the enzyme system for the heavy and light isotope

$$ \alpha = \frac{{}^{h}r/{}^{h}c_{bioav}}{{}^{l}r/{}^{l}c_{bioav}} = \frac{{}^{h}a}{{}^{l}a} \quad (14) $$

which is a constant determined by the kinetic parameters of the individual reactive steps, only, and being independent of the substrate concentration.

Bioavailability Effects on Observed Isotope Fractionation

Theoretical Relations. The influence of bioavailability restrictions on microbial degradation kinetics can conceptually be described as a nonreactive transport (or mass transfer) step linking the bulk concentration of a substrate, c_{bulk}, to the bioavailable concentration of the substrate, c_{bioav}, e.g. ref *22*. The latter is subject to a reactive consumption with the kinetics of this degradation step controlled by c_{bioav} instead of c_{bulk}. The microscopic transport step might be e.g. the diffusion of the substrate toward a bacterial cell e.g. ref *18* or transport across a cell membrane e.g. refs *32* and *34*. Without resolving the nature of the transport process, it is assumed that it can be described by a capacitive exchange term driven by the difference between bulk and bioavailable concentration and a constant rate parameter, k_{tr} (*35*). For such a system, the observed isotope fractionation factor, α^*, can be defined as the isotope fractionation factor derived from changes in the bulk concentration:

$$ \alpha^* = \frac{\frac{\partial {}^{h}c_{bulk}/\partial t}{{}^{h}c_{bulk}}}{\frac{\partial {}^{l}c_{bulk}/\partial t}{{}^{l}c_{bulk}}} \quad (15) $$

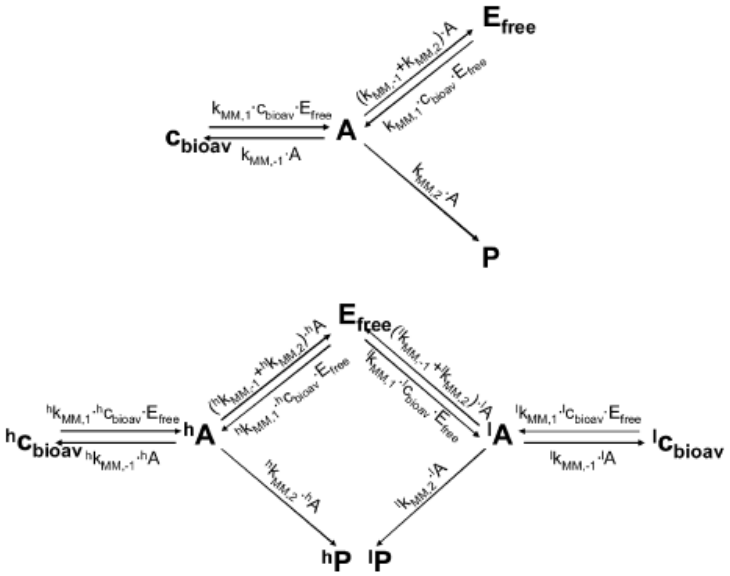

FIGURE 1. Top: Schematic representation of an enzymatic reaction transferring c_{bioav} into *P* following Michaelis–Menten kinetics. Arrows indicate individual transformation steps and the respective transformation rates. Note that the total amount of enzymes, E_{tot}, is assumed to be constant ($A + E_{free} = E_{tot} = const.$). Bottom: Same as above in the case of isotope fractionation taking place. The superscript *h* refers to concentrations and parameters describing the dynamics of the heavy isotope species, whereas the superscript *l* refers to the light isotope.

When combining such a capacitive exchange with a degradation reaction following first order kinetics (Figure 2, top) results from previous studies on the nitrogen uptake of plants (*36*) can be adapted to describe bioavailability effects, which leads to an observed isotope fractionation factor α^* given as

$$\alpha^* = \frac{{}^h k_{reac}}{{}^l k_{reac}} \cdot \frac{{}^h k_{tr}}{{}^l k_{tr}} \cdot \frac{{}^l k_{tr} + {}^l k_{reac}}{{}^h k_{tr} + {}^h k_{reac}} \quad (16)$$

Introducing α_0 as the enzymatic fractionation factor of the degradation step itself (in case no bioavailability restriction occurs) the above expression can be rewritten

$$\alpha^* = \alpha_0 \cdot \frac{1 + {}^l k_{reac}/{}^l k_{tr}}{1 + {}^h k_{reac}/{}^h k_{tr}} \quad (17)$$

with $\alpha_0 = {}^h k_{reac}/{}^l k_{reac}$. A further simplification can be obtained if ${}^h k_{tr} = {}^l k_{tr}$, i.e. when no isotope fractionation is induced by the transport step, which results in

$$\alpha^* = \alpha_0 \cdot \frac{1 + {}^l k_{reac}/{}^l k_{tr}}{1 + \alpha_0 \cdot {}^l k_{reac}/{}^l \lambda_{tr}} \quad (18)$$

This shows that depending on the relative magnitude of the two rate parameters the observed isotope fractionation factor approaches either the value for the enzymatic fractionation factor, α_0, (observable and enzymatic isotope fractionation approximately equal if ${}^l k_{tr} \gg {}^l k_{reac}$) or a value of 1 (diminishing observable isotope fractionation if ${}^l k_{tr} \ll {}^l k_{reac}$), which means that the rate limiting step determines the observed isotope fractionation factor.

Investigating multistep (enzyme catalyzed) biochemical reactions Northrop (*26*) introduced the expression

$$1/\alpha_a = \frac{1/\alpha_i + C}{1 + C} \quad (19)$$

(when written in the nomenclature of the present paper) linking the apparent fractionation factor α_a (describing the isotope fractionation by the entire biochemical reaction) to the intrinsic fractionation factor α_i (describing the single reaction step causing the isotope fractionation) with C as a constant factor representing the 'commitment to catalysis'. Northrop (*26*) could show that in case of very high and very low substrate concentrations C is a function of the rate parameters of the individual reactions steps, only. If the commitment of catalysis concept is formally applied to the two step reaction system of Figure 2 (top), eq 18 can be transformed into eq 19 with α^* corresponding to α_a, α_0 to α_i, and $C = {}^l k_{reac}/{}^l k_{tr}$.

Here we expand the existing theoretical concepts explicitly by combining the above descriptions for the impact of mass transfer or bioavailability limitations on isotope fractionation with equations valid for isotope fractionation in enzymatic systems (see the previous section). To investigate this impact of substrate bioavailability on enzyme kinetics induced isotope fractionation at variable substrate concentrations, reaction schemes in Figures 1 (bottom) and 2 (top) were combined. This leads to a new reaction scheme where the substrate concentration, c_{bioav}, affected by the enzymatic system is linked to the bulk substrate concentration, c_{bulk}, via a capacitive exchange process (Figure 2, bottom). The observed isotope fractionation factor α^* is again given by eq 15.

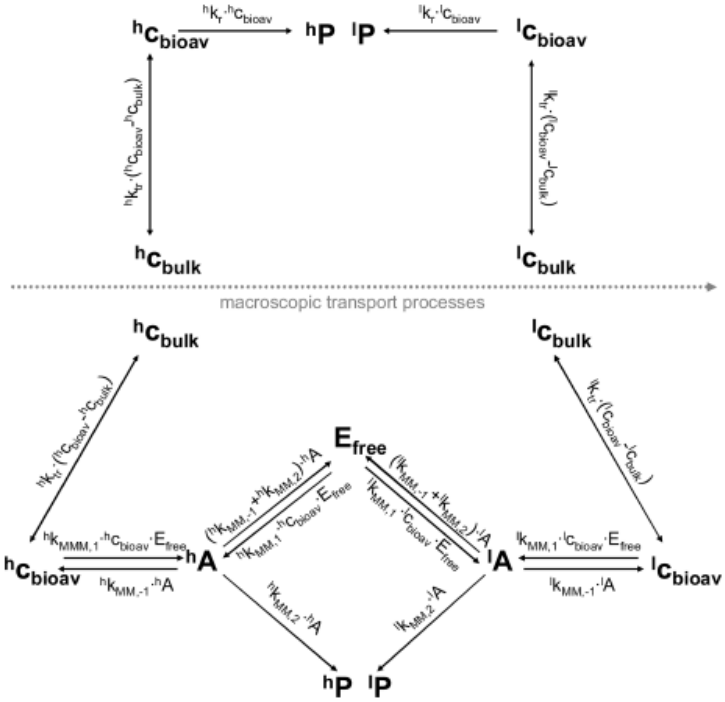

FIGURE 2. Schematic representation of processes contributing to the bioavailability limited degradation rate of a substrate following first order kinetics (top) or Michaelis–Menten kinetics (bottom) for the degradation step. The microscopic transport process controlling substrate bioavailability is considered to be a capacitive exchange process (k_{tr} as rate constant). Macroscopic transport processes are assumed to occur in the bulk liquid only, not affecting concentrations other than ${}^h c_{bulk}$ and ${}^l c_{bulk}$. Released reaction products might be subject to further reactive and/or transport processes, but these further processes are not considered to have any impact on the rate of the displayed processes. Arrows indicate individual transformation steps and the respective transformation rates. Note that (${}^h A + {}^l A + E_{free} = E_{tot} = const$).

Using the equation system describing the entire reaction scheme, this expression can be rewritten as (see the Supporting Information for a detailed derivation)

$$\alpha^* = \frac{{}^h a}{{}^l a} \cdot \frac{{}^h k_{tr}}{{}^l k_{tr}} \cdot \frac{{}^l k_{tr} + {}^l a \cdot \frac{E_{free}}{E_{tot}}}{{}^h k_{tr} + {}^h a \cdot \frac{E_{free}}{E_{tot}}}$$

$$= \alpha_0 \cdot \frac{1 + \frac{{}^l a}{{}^l k_{tr}} \cdot \frac{E_{free}}{E_{tot}}}{1 + \frac{{}^h a}{{}^h k_{tr}} \cdot \frac{E_{free}}{E_{tot}}} \quad (20)$$

which still contains the unknown variable E_{free}. Expressing E_{free} or E_{free}/E_{tot} as a function of known parameters would require the solution of a third-order polynomial equation, the general solution of which cannot be expressed in a meaningful way. However, some general properties of eq 20 can be derived without solving it explicitly: eq 20 has an obvious similarity with eq 18 with E_{free}/E_{tot} representing a weighting factor for the concentration dependent magnitude of the bioavailability impact on isotope fractionation (note that $0 \le E_{free} \le E_{tot}$). For high substrate concentrations the amount of free enzymes is getting small and $\alpha^* \approx \alpha_0$. In the opposite case of low substrate concentrations, $E_{free} \approx E_{tot}$ and $a \approx k_{reac}$ (Michaelis–Menten kinetics reduces to first order kinetics with the specific affinity as first order rate parameter), which brings eqs 18 and 20 in equality (if ${}^h k_{tr} = {}^l k_{tr}$). As a consequence, the observed isotope fractionation factor is not constant but varies with changing bulk substrate concentration. These general observations are supported by solving eq 20 numerically for given sets of parameter values (results not shown).

To allow a more detailed discussion of the dependency of observed isotope fractionation factors on bulk substrate concentration the following simplifications are introduced: for many natural systems the ratio between heavy and light isotopes is relatively small ($R \ll 1$; e.g., $^{13}C/^{12}C \approx 10^{-2}$ or $^2H/^1H \approx 10^{-4}$) and thus the entire substrate turnover is mainly determined by the light isotope. Using this simplification and assuming again that the transport step is not fractionating (${}^h k_{tr} = {}^l k_{tr}$) allows for the expression of E_{free}/E_{tot} in a closed form (omitting the superscript l from all the parameters; see the Supporting Information for a detailed derivation and a discussion of the potential error if $R \ll 1$ is not given):

$$\frac{E}{M} = \frac{k_{tr}}{a} \cdot \left[\frac{1}{2} \cdot \left(\frac{a}{k_{tr}} - \frac{c_{bulk}}{K_M} - 1 \right) + \sqrt{\frac{a}{k_{tr}} + \frac{1}{4} \cdot \left(\frac{a}{k_{tr}} - \frac{c_{bulk}}{K_M} - 1 \right)^2} \right] \quad (21)$$

Inserting this expression into eq 20 yields

$$\alpha^* = \alpha_0 \cdot \frac{1 + \frac{1}{2} \cdot \left(\frac{a}{k_{tr}} - \frac{c_{bulk}}{K_M} - 1 \right) + \sqrt{\frac{a}{k_{tr}} + \frac{1}{4} \cdot \left(\frac{a}{k_{tr}} - \frac{c_{bulk}}{K_M} - 1 \right)^2}}{1 + \alpha_0 \cdot \left[\frac{1}{2} \cdot \left(\frac{a}{k_{tr}} - \frac{c_{bulk}}{K_M} - 1 \right) + \sqrt{\frac{a}{k_{tr}} + \frac{1}{4} \cdot \left(\frac{a}{k_{tr}} - \frac{c_{bulk}}{K_M} - 1 \right)^2} \right]} \quad (22)$$

which allows for the determination of the observed isotope fractionation factor as a function of the enzymatic fractionation factor and only two further terms (Figure 3): the ratio of bulk substrate concentration and the Michaelis–Menten constant, c_{bulk}/K_M, and the ratio of the specific affinity of the organisms toward the substrate and the rate constant of the transport process controlling bioavailability, a/k_{tr}. The latter ratio is the Damköhler number for these processes and the inverse of the bioavailability number introduced by Bosma et al. (*21*) and used there as an indicator for substrate bioavailability. The sensitivity of the observed isotope fractionation toward each of these parameter ratios differs, but changes in both of these ratios can lead to significant changes of the observed isotope fractionation. In particular, changes in the bulk substrate concentration can lead to variations of the observed isotope fractionation factor ranging between the enzymatic fractionation factor and a value set by the relative extent of the bioavailability restriction; the latter approaching 1 in case of severe restrictions. Results also indicate that for a highly bioavailable substrate the dependency of the observed isotope fractionation diminishes and enzymatic and observed isotope fractionation remain approximately equal.

Implication for Individual Batch Experiments. To demonstrate how bioavailability limited biodegradation of a substrate may influence the results of a batch experiment on isotope fractionation, numerical simulations were performed for a series of virtual batch experiments. Simulations were performed using the Biogeochemical Reaction Network Simulator (BRNS) (*37, 38*), an adaptative simulation environment suitable for large, mixed kinetic equilibrium reaction networks (*39, 40*). For the present simulations it was assumed that in the batches the substrate is degraded by microorganisms. Following the scheme shown in Figure 2 (bottom), the substrate is assumed to be transported first to a dispersed microbial cell, where degradation following enzyme kinetics is considered to take place. No macroscopic transport processes were assumed. The rate law controlling each step of the reaction scheme is also following Figure 2 (bottom). The initial isotope ratio was set to $R_0 = 0.01$ and the enzymatic fractionation factor was set to $\alpha_0 = 0.990$; both values are typically encountered in natural systems (*6*). For a base case scenario the rate parameters of each individual step as well as the initial bulk concentration of the substrate were arbitrarily selected to obtain ratios of $a/k_{tr} = 50$ and $c_{bulk}/K_M = 1000$. Four additional scenarios were simulated each increasing or decreasing one ratio of the base case scenario by 1 order of magnitude, whereas the other ratio was kept constant. Transient simulations were performed until $\ln(c/c_0)$ decreased to approximately -10. At given "observation times" simulated bulk concentrations and isotope ratios were recorded and treated as "measured" data points in further analysis. Data points were plotted in a Rayleigh plot to determine the (observed) isotope fractionation factor or as commonly done the (observed) enrichment factor $\varepsilon^* = (\alpha^* - 1) \cdot 1000$. The slopes of these Rayleigh plots were determined for different arbitrarily set intervals showing a decrease of the slope with decreasing substrate concentration (Figure 4). Initial values for ϵ^* were also calculated using eq 22, and for test purposes using eq 20 with a numerical solution of the equation system describing the reaction scheme. Both equations yield identical results (for this and for all further presented examples) showing that for the base scenario the (absolute value of the) initial enrichment factor is already slightly smaller than the enzymatic enrichment factor. Already the slope of the Rayleigh plot for the first interval spanning only half of a ln-unit yields an ϵ^*-value smaller than the initial value. For very small concentrations ϵ^* approaches the value predicted by eq 22 for $c_{bulk} \to 0$. Changes in the slope of the Rayleigh plot are gradual but relatively smooth, which results for most of the selected intervals in a good approximation of the plot by a linear fit. Only around $\ln(c/c_0) \approx -3$ (i.e., approximately 5% of the initial concentration) a strong change in the slope can be observed with most of the changes from the initial to the small concentration value occurring at this

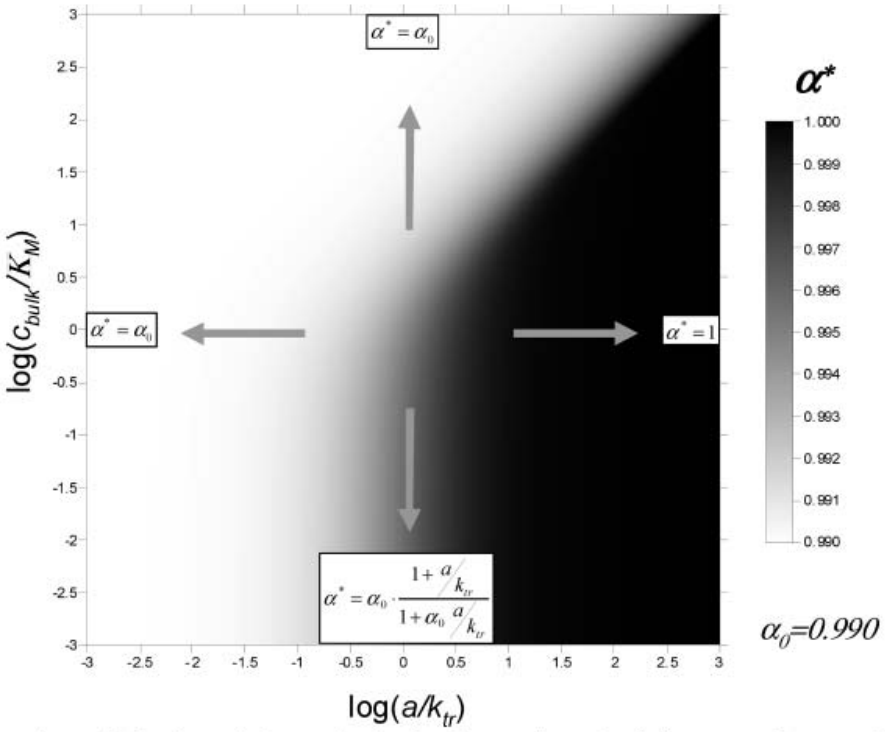

FIGURE 3. Dependency of the observed isotope fractionation factor, α^*, on the bulk concentration c_{bulk} (relative to the Michaelis–Menten constant, K_M), and the ratio between the specific affinity, a, of the microorganisms and the rate parameter, k_{tr}, controlling the bioavailability of the substrate. Arrows and inserted boxes indicate the limits for α^* in case of high and low parameter ratios. The enzymatic isotope fractionation factor was arbitrarily set to $\alpha_0 = 0.990$.

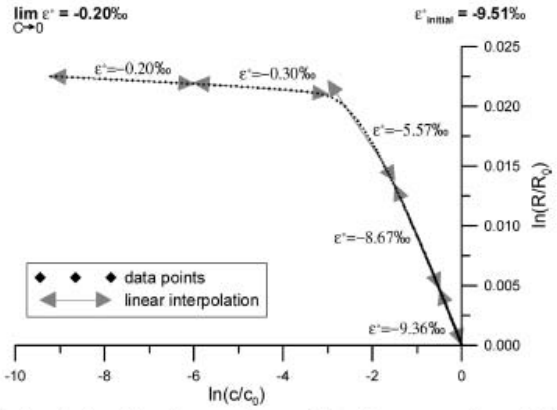

FIGURE 4. Rayleigh plot of a simulated virtual batch experiment with $a/k_{tr} = 50$ and an initial value of $c_{bulk}/K_M = 1000$. The enzymatic enrichment factor is $\epsilon_0 = -10‰$. Arrowheads indicate the size of the interval used to determine the slope of the curve and the observed enrichment factors, ϵ^*. Values for lim ϵ^* and $\epsilon^*_{initial}$ were determined using eq 20.

concentration range. Simulation results of the other scenarios were processed the same way as for the base scenario. For all simulated scenarios a change in the observed enrichment factor can be found throughout the experiment (Figure S3 in the Supporting Information). For high initial concentrations or low a/k_{tr} ratios indicating high substrate bioavailability initial values for ϵ^* were close to the enzymatic value and remain relatively constant for moderate concentration decreases. In contrast, for lower initial concentrations or higher bioavailability restrictions, the initial observed enrichment factors already differ significantly from the enzymatic value. In all simulated scenarios, most of the changes between initial and low concentration values of ϵ^* occur within a relatively small concentration interval. This interval marks the beginning of the region where bioavailability restrictions can no longer be compensated by high bulk substrate concentrations.

A comparison of these simulated values with theoretically derived values using eq 22 shows a good agreement indicating the consistency of the theoretical considerations. Results from the virtual batch experiments (Figure 4 and Figure S3 in the Supporting Information) as well as theoretical predictions (Figure 3) also show that for most concentration ranges changes in the observed isotope fractionation (or enrichment) factor with substrate concentration changes occur monotonously but with relatively low sensitivity toward substrate concentration. For these concentration ranges the obtained Rayleigh plots could be well approximated by linear fits. Thus,

in order to distinguish between experimental uncertainties and underlying shifts in the observed isotope fractionation an experimental verification of these theoretical predictions requires experimental conditions where the observed isotope fractionation is most sensitive toward concentration changes. Applying a rough categorization to the distribution of observed fractionation factors shown in Figure 3, a combination of high a/k_{tr} ratios and high ratios of c_{bulk}/K_M defines the region where a high sensitivity of the observed isotope fractionation factor toward changes of substrate concentration might be found. For other combinations of bioavailability restriction and substrate concentration the observed isotope fractionation factor might differ from the enzymatic fractionation factor but may not show major changes with changing substrate concentrations.

Implications for Quantification of Contaminant Biodegradation in Aquifers. In contaminated aquifers stable isotope fractionation during microbial degradation is used to quantify the amount of contaminants biodegraded along a groundwater flow path using the Rayleigh model (*8*). The applicability of this approach requires among other constrains the knowledge of an isotope enrichment factor, ϵ, valid for the given environmental conditions and this enrichment factor to be constant along the entire flow path. The common approach applying laboratory derived enrichment factors to the field is known to be challenged by a variety of processes masking microbial isotope fractionation in the environment e.g. refs *25* and *41*. However, these masking effects lead to field fractionation factors smaller than those found in the laboratory, which allows the Rayleigh approach to provide a conservative estimate of the biodegradation in the field (*6, 42–44*).

The presented results indicate that substrate bioavailability can be an additional factor masking isotope fractionation in the field and that (in contrast to common assumptions) this masking effect depends on the bulk substrate concentration. The derived equations also allow for a quantitative prediction of the magnitude of this effect for given substrate bioavailability and bulk concentration. Results of this study suggest that if substrate concentrations exhibit major changes along a flow path and if biodegradation is limited by the bioavailabilty of the substrate any isotope enrichment factors assumed to be adequate for a given environment may not be applicable for the entire concentration range. In such a case, enrichment factors obtained for high substrate concentration might be more suitable to provide a conservative estimate of biodegradation in the field using a Rayleigh model-based approach (see the Supporting Information for more details).

In summary, results from this study indicate that concentrations resulting in detectable changes in observed isotope fractionation are to be found in natural and laboratory systems. Values for the Michaelis–Menten constant are typically in the μM-range, and thus substrate concentrations between the μM- and mM-range might be suitable for finding a concentration dependency of the observed isotope fractionation factor if the bioavailability is sufficiently low. For instance, for soil slurry experiments bioavailability numbers corresponding to $a/k_{tr} = 30$ to 60 have been reported in the literature (*21*), which is within the range where changes in the observed fractionation factor with concentration have been found in this study. Reasons why this effect has not been reported yet might be a high substrate bioavailability in the experimental setups, degradation kinetics being influenced by additional parameters (e.g., concentration of nutrients, reaction partners etc.), misinterpretation as statistical effect, or the experimental resolution not allowing for the observation of small gradual changes in the fractionation factor. Many theoretical discussions of isotope fractionation in natural systems consider the biodegradation to be well approximated by first order kinetics e.g. ref *28*, and considering such degradation kinetics would lead to bioavailability influencing observed isotope fractionation but not exhibiting any concentration dependency. In contrast, this means that for systems where observed isotope fractionation is changing with substrate concentration the assumption of first order kinetics might not be appropriate for the description of microbial degradation processes.

An experimental verification of the theoretical results of this study can be found in an accompanying study (*29*).

Acknowledgments

This study was supported by the Helmholtz Association grant VG-NG-338 ("GReaT MoDE") and the European Union grant MEST-CT-2004-8332 ("AXIOM").

Nomenclature

superscript h	heavy isotope
superscript l	light isotope
*	observed values
c_{bulk}	bulk substrate concn [mol/vol]
c_{bioav}	bioavailable substrate concn [mol/vol]
E_{free}, E_{tot}	concn of free and total enzymes [mol/vol]
A	concn of activated enzyme complexes [mol/vol]
R	ratio of heavy to light isotope concn
α (α_0)	isotope fractionation factor (enzymatic)
ϵ (ϵ_0)	isotope enrichment factor (enzymatic) [‰]
r	reaction rate [mol/(vol·time)]
k_{MM1}	bimolecular rate parameter of enzymatic reaction step [vol/(mol·time)]
k_{MM-1}, k_{MM2}	first order rate parameters of enzymatic reaction steps [1/time]
k_{reac}	first order degradation rate parameter [1/time]
k_{tr}	first order rate parameter of microscopic mass transfer of substrate from bulk solution to location of enzymes [1/time]
V_{max}	maximum reaction rate [mol/(vol·time)]
K_M	Michaelis–Menten constant [mol/vol]
a	specific affinity of microorganisms to substrate [1/time]

Supporting Information Available

Detailed derivation of eqs 20–22; applicability limits of eq 22 if $R \ll 1$ is not given; and further simulation results for virtual batch experiment and aquifer flow paths. This material is available free of charge via the Internet at http://pubs.acs.org.

Literature Cited

(1) Travis, C. C.; Doty, C. B. Can contaminated aquifers at Superfund sites be remediated. *Environ. Sci. Technol.* **1990**, *24*, 1464–1466.
(2) Wiedemeier, T. H.; Rifai, H. S.; Newell, C. J.; Wilson, J. T. Natural Attenuation of Fuels and Chlorinated Solvents in the Subsurface; Wiley: New York, NY, U.S.A., 1999.
(3) Chapelle, F. H.; Robertson, J. F.; Landmeyer, J. E.; Bradley, P. M. Methodology for applying monitored natural attenuation to petroleum-contaminated ground-water systems with examples from South Carolina. U.S Geological Survey, Water-Resources Investigation Report 00–4161; Columbia, SC, U.S.A., 2001.
(4) Kaschl, A.; Rügner, H.; Keil, M. Weiss, H. Monitored natural attenuation - applicable to the multi-contaminant situation at megasites? In 8th CONSOIL Conference, Gent Belgium, May 12–16, 2003; S2098-2107.
(5) OSWER. Use of Monitored Natural Attenuation at Superfund, RCRA Corrective Action, and Underground Storage Tank Sites, Office of Solid Waste and Emergency Responses; U.S. Environmental Protection Agency: Washington, DC, 1999.
(6) Meckenstock, R. U.; Morasch, B.; Griebler, C.; Richnow, H. H. Stable isotope fraction analysis as a tool to monitor biodegradation in contaminated aquifers. *J. Contam. Hydrol.* **2004**, *75*, 215–255.

(7) Schmidt, T. C.; Zwank, L.; Elsner, M.; Berg, M.; Meckenstock, R. U.; Haderlein, S. B. Compound-specific stable isotope analysis of organic contaminants in natural environments: a critical review of the state of the art, prospects, and future challenges. *Anal. Bioanal. Chem.* **2004**, *378*, 283–300.
(8) Mariotti, A.; Germon, J. C.; Hubert, P.; Kaiser, P.; Letolle, R.; Tardieux, A.; Tardieux, P. Experimental determination of nitrogen kinetic isotope fractionation: some principles; illustrations for denitrification and nitrification processes. *Plant Soil* **1981**, *62*, 413–430.
(9) Sherwood Lollar, B.; Slater, G. F.; Sleep, B.; Witt, M.; Klecka, G. M.; Harkness, M.; Spivack, J. Stable carbon isotope evidence for intrinsic bioremediation of tetrachloroehene and trichloroethene at area 6, Dover Air Force Base. *Environ. Sci. Technol.* **2001**, *35*, 261–269.
(10) Mancini, S. A.; Lacrampe-Couloume, G.; Jonker, H.; van Breukelen, B. M.; Groen, J.; Volkering, F.; Sherwood Lollar, B. Hydrogen isotopic enrichment: An indicator of biodegradation at a petroleum contaminated field site. *Environ. Sci. Technol.* **2002**, *39*, 1018–1029.
(11) Kuder, T.; Wilson, J. T.; Kaiser, P.; Kolharkar, R.; Philip, P.; Allen, J. Enrichment of stable carbon and hydrogen isotopes during anaerobic biodegradation of MRBE: Microcosms and field evidence. *Environ. Sci. Technol.* **2005**, *39*, 213–220.
(12) Vieth, A.; Kästner, M.; Schirmer, M.; Weiss, H.; Gödecke, S.; Meckenstock, R. U.; Richnow, H. H. Monitoring in situ biodegradation of benzene and toluene by stable carbon isotope fractionation. *Environ. Toxicol. Chem.* **2005**, *24*, 51–60.
(13) Richnow, H. H.; Annweiler, E.; Michaelis, W.; Meckenstock, R. U. Microbial in situ degradation of aromatic hydrocarbons in a contaminated aquifer monitored by carbon isotope fractionation. *J. Contam. Hydrol.* **2003**, *65*, 101–120.
(14) Kopinke, F. D.; Georgi, A.; Voskamp, M.; Richnow, H. H. Carbon isotope fractionation of organic contaminants due to retardation on humic substances: Implications for natural attenuation studies in aquifers. *Environ. Sci. Technol.* **2005**, *39*, 6052–6062.
(15) Mariotti, A.; Landreau, A.; Simon, B. N-15 isotope biogeochemistry and natural denitrification processes in groundwater - Applications to the chalk aquifer of Northern France. *Geochim. Cosmochim. Acta* **1988**, *52*, 1869–1878.
(16) Abe, Y.; Hunkeler, D. Does the Rayleigh equation apply to evaluate field isotope data in contaminant hydrogeology. *Environ. Sci. Technol.* **2006**, *40*, 1588–1596.
(17) Fischer, A.; Theuerkorn, K.; Stelzer, N.; Gehre, M.; Thullner, M.; Richnow, H. H. Applicability of stable isotope fractionation analysis for the characterization of benzene biodegradation in a contaminated aquifer. *Environ. Sci. Technol.* **2007**, *41*, 3689–3696.
(18) Harms, H. Bacterial growth on distant naphthalene diffusing through water, air, and water-saturated and nonsaturated porous media. *Appl. Environ. Microbiol.* **1996**, *62*, 2286–2293.
(19) Semple, K. T.; Morriss, A. W. J.; Paton, G. I. Bioavailability of hydrophobic organic contaminants in soil: fundamental concepts and techniques for analysis. *Eur. J. Soil Sci.* **2003**, *54*, 809–818.
(20) Haws, N. W.; Ball, W. P.; Bouwer, E. J. Modeling and interpreting bioavailability of organic contaminant mixtures in subsurface environments. *J. Contam. Hydrol.* **2006**, *82*, 255–292.
(21) Bosma, T. N. P.; Middeldorp, P. J. M.; Schraa, G.; Zehnder, A. J. B. Mass transfer limitation of biotransformation: quantifying bioavailabilty. *Environ. Sci. Technol.* **1997**, *31*, 248–252.
(22) Simoni, S. F.; Schäfer, A.; Harms, H.; Zehnder, A. J. B. Factors affecting mass transfer limited biodegradation in saturated porous media. *J. Contam. Hydrol.* **2001**, *50*, 99–120.
(23) O'Leary, M. H. Review: Carbon isotope fractionation in plants. *Phytochemistry* **1981**, *20*, 553–567.
(24) Nijenhuis, I.; Andert, J.; Beck, K.; Kästner, M.; Diekert, G.; Richnow, H. H. Stable isotope fractionation of tetrachloroethene during reductive dechlorination by Sulfurospirillum multivorans, Desulfitobacterium sp. strain PCE-S and abiotic reactions with cyanocobalamin. *Appl. Environ. Microbiol.* **2005**, *71*, 3413–3419.
(25) Cichoka, D.; Siegert, M.; Imfeld, G.; Andert, J.; Beck, K.; Diekert, G.; Richnow, H. H.; Nijenhuis, I. Compound specific stable isotope fractionation by Sulfurospirillum spp., Desulfitobacterium sp. strain PCE-S and abiotic reactions with cyanocobalamin during reductive dechlorination of tetra- and trichloroethene. *FEMS Microbiol. Ecol.* **2007**, *62*, 98–107.
(26) Northorp, D. B. The expression of isotope effects on enzyme-catalyzed reactions. *Annu. Rev. Biochem.* **1981**, *50*, 103–131.
(27) Ewald, E. M.; Wagner, A.; Nijenhuis, I.; Richnow, H. H.; Lechner, U. Microbial dehalogenation of trichlorinated dibenzo-p-dioxins by a Dehalococcoides-containing mixed culture is coupled to carbon isotope fractionation. *Environ. Sci. Technol.* **2007**, *41*, 7744–7751.
(28) Elsner, M.; Zwank, L.; Hunkeler, D.; Schwarzenback, R. P. A new concept linking observable stable isotope fractionations to transpormation pathways of organic pollutants. *Environ. Sci. Technol.* **2005**, *39*, 6896–6916.
(29) Kampara, M.; Thullner, M.; Richnow, H. H.; Harms, H.; Wick, L. Y. Impact of bioavailability restrictions on microbially induced apparent stable isotope fractionation: 2. experimental observations. *Environ. Sci. Technol.* **2008**, *42*, 6552–6558.
(30) Rayleigh, J. W. S. Theoretical considerations respecting the separation of gases by diffusion and similar processes. *Philos. Mag.* **1896**, *42*, 493–498.
(31) Lehninger, A.; Nelson, D.; Cox, M. *Principles of Biochemistry*, 4th ed.; Palgrave Macmillan: United Kingdom, 2004.
(32) Button, D. K. Biochemical basis for whole-cell uptake kinetics: specific affinity, oligotrophic capacity, and the meaning of the Michaelis constant. *Appl. Environ. Microbiol.* **1991**, *57*, 2033–2038.
(33) Melander, L.; Saunders, W. H. *Reaction Rates of Isotopic Molecules*; Wiley: New York, NY, U.S.A., 1980.
(34) Button, D. K. Nutrient uptake by microorganisms according to kinetic parameters from theory as related to cytoarchitecture. *Microbiol. Mol. Biol. Rev.* **1998**, *62*, 636–645.
(35) Baveye, P.; Valocchi, A. An evaluation of mathematical models of the transport of biologically reacting solutes in saturated soils and aquifers. *Water Resour. Res.* **1989**, *25*, 1413–1421.
(36) Mariotti, A.; Mariotti, F.; Champigny, M. L.; Amarger, N.; Moyse, A. Nitrogen isotope fractionation associated with nitrate reductase activity and uptake of NO_3^- by Pearl Millet. *Plant Physiol.* **1982**, *69*, 880–884.
(37) Regnier, P.; O'Kane, J. P.; Steefel, C. I.; Vanderborght, J. P. Modeling complex multi-component reactive-transport systems: Towards a simulation environment based on the concept of a Knowledge Base. *Appl. Math. Model.* **2002**, *26*, 913–927.
(38) Aguilera, D. R.; Jourabchi, P.; Spiteri, C.; Regnier, P. A knowledge-based reactive transport approach for the simulation of biogeochemical dynamics in Earth systems. *Geochem. Geophys. Geosyst.* **2005**, *6*, . Q07012, doi:10.1029/2004GC000899.
(39) Thullner, M.; Van Cappellen, P.; Regnier, P. Modeling the impact of microbial activity on redox dynamics in porous media. *Geochim. Cosmochim. Acta* **2005**, *69*, 5005–5019.
(40) Jouranbchi, P.; Van Cappellen, P.; Regnier, P. Quantitative interpretation of pH distributions in aquatic sediments: a reactive transport modeling approach. *Am. J. Sci.* **2005**, *305*, 919–956.
(41) Mancini, S. A.; Hischorn, S. K.; Elsner, M.; Lacrampe-Couloume, G.; Sleep, B. E.; Edwards, E. A.; Sherwood Lollar, B. Effects of trace element concentration on enzyme controlled stable isotope fractionation during aerobic biodegradation of toluene. *Environ. Sci. Technol.* **2006**, *40*, 7675–7681.
(42) Vieth, A.; Kästner, M.; Schirmer, M.; Weiss, H.; Gödeke, S.; Meckenstock, R.; Richnow, H.-H. Monitoring in situ biodegradation of benzene and toluene by stable carbon isotope fractionation. *Environ. Toxicol. Chem.* **2005**, *24*, 51–60.
(43) Elsner, M.; McKelvie, J.; Lacrampe-Couloume, G.; Sherwood Lollar, B. Insight into methyl *tert-butyl* ether (MTBE) stable isotope fractionation from abiotic reference experiments. *Environ. Sci. Technol.* **2007**, *41*, 5693–5700.
(44) Fischer, A.; Herklotz, I.; Herrmann, S.; Thullner, M.; Weelink, S. A. B.; Stams, A. J. M.; Schlömann, M.; Richnow, H.-H.; Vogt, C. Combined carbon and hydrogen isotope fractionation analysis for elucidating benzene biodegradation pathways. *Environ. Sci. Technol* **2008**, *42*, 4356–4362.

ES702782C

Impact of Bioavailability Restrictions on Microbially Induced Stable Isotope Fractionation. 2. Experimental Evidence

MAKEBA KAMPARA,[†] MARTIN THULLNER,[†] HANS H. RICHNOW,[‡] HAUKE HARMS,[†] AND LUKAS Y. WICK*[,†]

Departments of Environmental Microbiology and Isotope Biogeochemistry, UFZ - Helmholtz Centre for Environmental Research, Leipzig, Germany

Received November 6, 2007. Revised manuscript received May 5, 2008. Accepted May 22, 2008.

Stable isotope fractionation analysis (SIFA) of contaminants is an emerging technique to characterize *in situ* microbial activity. The kinetic isotope effect in microbial degradation reactions, or enzyme catalysis, is caused by the preferential cleavage of bonds containing light rather than heavy isotopes. This leads to a relative enrichment of the heavier isotopes in the residual substrate pool. However, a number of nonisotopically sensitive steps preceding the isotopically sensitive bond cleavage may affect the reaction kinetics of a degradation process, thus reducing the observed (i.e., the macroscopically detectable) isotope fractionation. Low bioavailability of contaminants poses kinetic limitations on the biodegradation process and can significantly reduce the observed kinetic isotope fractionation. Here we present experimental evidence for the influence of bioavailability-limited pollutant biodegradation on observed stable isotope fractionation. Batch laboratory experiments were performed to quantify the toluene hydrogen isotope fractionation of *Pseudomonas putida* mt-2(pWWO) subjected to different small concentrations of toluene with and without deuterium label, which corresponded to realistic environmental mass transfer scenarios. Detected isotope fractionations depended significantly on the toluene concentration, hence confirming the influence of substrate mass transfer limitation on observed isotope fractionation, hypothesized by Thullner et al. (*Environ. Sci. Technol.* **2008**, *42*, 6544−6551). Our results indicate that the bioavailability of a substrate should be considered during quantitative analysis of microbial degradation based on SIFA.

Introduction

Stable isotope fractionation analysis (SIFA) is an increasingly important methodology in biology, geology, chemistry, forensics, and environmental sciences. In contaminant hydrology, SIFA has proven to be a valuable tool for the assessment of biodegradation in polluted aquifers (*2*–*4*). Most physical processes of compound attenuation, such as sorption, diffusion, and volatilization do not exhibit significant fractionation (*5*–*8*), whereas many degradation processes do. Observed isotope fractionation is also an indicator of biodegradation, the most desirable attenuation process of anthropogenic pollutants, and of great importance for the acceptance of natural attenuation as a remediation strategy. In addition, it should be kept in mind that any degradation processes involving the cleavage of a chemical bond may cause isotope fractionation. In the past few years, several studies developed SIFA from a qualitative to a quantitative method of biodegradation assessment (*9*–*12*). Several publications and environmental guidelines recommend SIFA for the monitoring of natural attenuation (*4*, *13*, *14*). SIFA is based on the Rayleigh equation (eq 2) which was developed for the fractionation during gas diffusion (*15*) nearly a century before it was shown to apply to fractionation during biodegradation processes (*16*). The Rayleigh equation relates the shift in the isotope ratio to the concentration change, in terms of a fractionation factor (α) or the corresponding enrichment factor (ϵ). Enrichment factors are normally determined in closed homogeneous laboratory systems where both isotope ratio and concentration can be monitored at controlled conditions (*4*, *17*–*20*). Fractionation factors are then applied to calculate the extent of biodegradation in highly heterogeneous environmental systems.

Although SIFA has been successfully used in several field studies to characterize *in situ* biodegradation, unexplained deviations from theoretical predictions have been observed (*21*–*23*).

In contaminant biodegradation, isotope fractionation is often tacitly assumed to be independent of bioavailability restrictions in the aquifer, as a factor influencing the contaminant transfer to catabolically active cells (*24*). Theoretical considerations by Thullner et al. (*1*) demonstrate the influence of different contaminant concentrations and mass transfer processes on the observed (i.e., the macroscopically detectable) stable isotope fractionation. In contrast to isotopically sensitive chemical reactions that are kinetically controlled solely by the bond cleavage, after which the reaction becomes irreversible, microbiologically induced stable isotope fractionation can also be affected by rate limiting steps prior to the fractionating bond cleavage. Rate limiting steps may include substrate mass transfer toward the cell, uptake of substrate by the cell, transport of substrate within the cell, or binding of substrate to the enzyme complex (*19*, *25*, *26*). Although these processes do not directly alter the isotope composition of the substrate, they can reduce the observed isotope fractionation as compared to the enzymatic isotope fractionation associated with the biochemical bond cleavage, only. Studies of CO_2 uptake by plants (*25*, *27*) and cyanobacteria (*28*–*30*), for instance, have shown that the CO_2 concentration has an effect on measured isotope fractionation. Similarly, an effect of both, substrate concentration and cell density, on the stable carbon isotope fractionation were observed during methane oxidation (*31*). Increased iron availability has also been shown to cause a reduction in the observed fractionation (*32*) during aerobic toluene degradation by strain mt-2. This was explained by higher substrate conversion rates relative to preceding physical steps. In a contaminated aquifer, different physical and/or chemical processes may lead to largely variable substrate bioavailability that differs from the controlled laboratory situation used to determine isotope enrichment factors. At the microscale, bioavailability may vary due to

* Corresponding author. Phone: +49-341-235-1316. Fax: +49-341-235-1351. E-mail: lukas.wick@ufz.de. Corresponding author address: Department of Environmental Microbiology, UFZ, Helmholtz Centre for Environmental Research, Permoserstrasse 15, 04318 Leipzig, Germany.

† Department of Environmental Microbiology.

‡ Department of Isotope Biogeochemistry.

10.1021/es702781x CCC: $40.75
Published on Web 07/30/2008

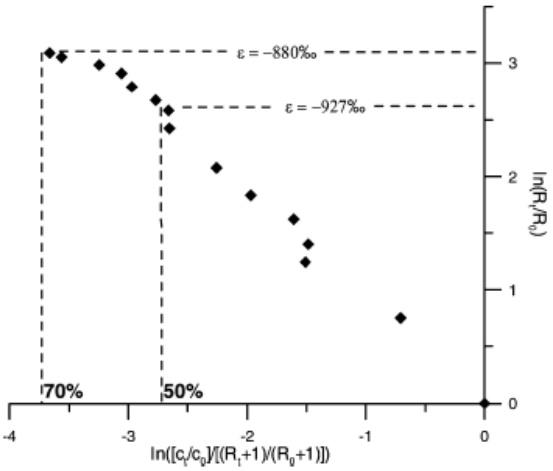

FIGURE 1. Rayleigh plot derived from a typical batch degradation experiment using toluene degrading *Pseudomonas putida* mt-2 (OD_{578} = 0.5) in the presence of an initial toluene concentration of 94 μM. Due to divergence from linearity of the Rayleigh plot, isotope enrichment factors are derived after a 50% and 70% degradation of the initial amount of toluene.

the variability of local contaminant concentrations, effective diffusivities, and cell densities (*33*, *34*). Here we focus on bioavailability variations caused by microscale transport processes. The aim of the present study is to demonstrate the effect of bioavailability (i.e., the combination of mass transfer to and uptake by the cell) on the observed stable isotope fractionation, using a well-defined laboratory setup. The rate of mass transfer was varied by exposing toluene-degrading *Pseudomonas putida* mt-2(pWW0) to different toluene concentrations at nongrowth conditions. Our experimental data show that during batch biodegradation processes observed isotope fractionation factors can depend on the bulk substrate concentration and on the corresponding mass transfer. A theoretical derivation of mass transfer effects on observed isotope fractionation and an assessment of situations under which these effects need to be accounted for are given in the accompanying paper (*1*).

Material and Methods

Organism and Culture Conditions. *Pseudomonas putida* mt-2 carries the TOL plasmid pWW0, containing the genetic information for toluene biodegradation through the TOL pathway. The TOL pathway is initiated by the oxidation of the methyl group of toluene by a monooxygenase reaction (*35*) known to cause substantial hydrogen isotope fractionation (*17*). Strain mt-2 was grown at 30 °C in mineral medium (*36*) with toluene (2.8 mM) as the only carbon and energy source on a rotary shaker at 140 rpm. In the mid exponential growth phase, the cells were harvested by centrifugation (13000×g, 10 min), washed four times with 0.1 M phosphate-buffered saline (PBS) to remove toluene traces, and suspended in 0.1 M PBS. This suspension was used as inoculum for the experiments.

Batch Toluene Biodegradation Experiments. Toluene biodegradation experiments were performed at room temperature (20 °C) in tightly closed, three-neck 1 L-glass bottles with 250 mL of PBS containing a 1:1 mixture (v/v) of toluene-h8 (99.9%, Merck KGaA (Germany)) and per-deuterated toluene-d8 (99.6 atom % D; Sigma-Aldrich Chemie (Germany)) at either 1, 10, or 100 μM total toluene concentration. Toluene degradation and isotope fractionation by strain mt-2 has been shown to be influenced by iron availability (*32*). Iron was not added in the PBS but may have been present at trace amounts. Fifteen h after the addition of the toluene, *P. putida* mt2 was added to give a cell density of ca. 5×10^8 cells mL^{-1}. Cells densities were followed by measuring the optical density at 578 nm using a UV−visible spectrophotometer (Cary 400 Scan, Varian). Shortly before inoculation, immediately after the inoculation, and at regular intervals, samples of 2 mL liquid were taken through airtight Teflon septa using airtight syringes (Gastight #1002, Hamilton Co. Reno, Nevada). The sampling did not cause any observed

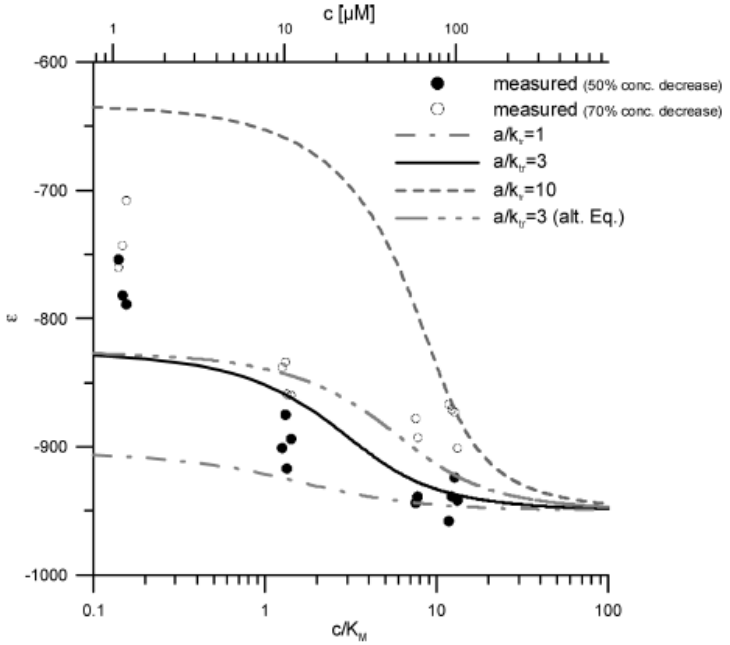

FIGURE 2. Measured observed enrichment factors and theoretical predictions based on eq 5. Solid line represents a conservative estimation of the enrichment factors for 50% degradation (ϵ_0 = −950; a/k_{tr} = 3), dashed lines are indicating sensitivity toward variations of a/k_{tr} (ϵ_0 unchanged) and the relative fraction of deuterated toluene in the bulk (indicated as alt. Eq.), respectively.

change in pressure. The samples were transferred to 10-mL autosampler vials, containing 20 μL of concentrated H_2SO_4 to inhibit further biodegradation. The vials were closed immediately airtight with Teflon-coated butyl rubber septa. The duration of the experiments ranged from 20 min to 5 h, depending on the initial toluene concentrations. The experiments were performed on a magnetic stirrer (300 rpm) to allow for efficient and continuous mixing even during sampling procedures. In order to exclude bacterial growth and physiological changes during the experiments, some flasks were amended with 100 mg L^{-1} of chloramphenicol (Karl Roth GmbH, Germany), an antibiotic inhibiting protein synthesis. As observed fractionation factors remained uninfluenced by the presence of chloramphenicol, the antibiotic was not added in all experiments.

Analytical Procedures. The analysis of D/H isotope fractionation was based on the method described by Morasch et al. (*17*). The concentrations of toluene and toluene-d8 were analyzed by headspace gas chromatography with a flame ionization detector (GC-FID) (Hewlett-Packard 6890 Series). The injection was automated using a headspace autosampler (Hewlett-Packard 7694) with an oven temperature of 95 °C and an injection volume of 1 mL. A fused silica capillary column (Optima δ−3, length 60 m, inside diameter 0.32 mm, film thickness 0.35 μm; Macherey-Nagel, Düren, Germany) was used to separate the D/H toluene isotopologues applying the following temperature sequence: 35 °C for 2 min, heat to 94 °C at a rate of 6 °C min^{-1}, cool down to 35 °C. Separation of the two toluene species was achieved at 105.7 kPa with a N_2 flowrate of 15.0 mL min^{-1} and with a split of 5:1. The FID was operated at 280 °C, and helium was used as carrier gas.

Calculations. *Determination of Isotope Fractionation Factors.* The isotope fractionation factor (α) for microbial degradation reactions is defined as

$$\alpha = \frac{{}^{h}r/{}^{h}c}{{}^{l}r/{}^{l}c} \tag{1}$$

where ${}^{h}r$ and ${}^{l}r$ are the degradation rates of substrate containing the heavy and the light isotope, respectively, and ${}^{h}c$ and ${}^{l}c$ are the respective substrate concentrations (eq 1). For closed systems such as the batches used in the present study, the relation between changes of total substrate concentration ($c = {}^{h}c + {}^{l}c$) and substrate isotope ratio ($R = {}^{h}c/{}^{l}c$) is given by the Rayleigh equation (*15, 16, 37*) (here expressed in its logarithmic form)

$$\ln\left(\frac{R_t}{R_0}\right) = (\alpha - 1) \times \ln\left(\frac{c_t}{c_0}\right)\left(\frac{R_0+1}{R_t+1}\right) \tag{2}$$

where R_t and R_0 are the substrate isotope ratios at times t and zero, respectively, and c_t and c_0 are the total substrate concentrations at these times.

Eq 2 was used for the experimental determination of hydrogen isotope fractionation factors in the batch toluene biodegradation experiments. α was derived by plotting measured values of $\ln(R_t/R_0)$ vs $\ln([c_t/c_0]/[(R_t+1)/(R_0+1)])$ in a Rayleigh plot and obtaining the slope of the linear regression using eq 2. Results are expressed as the enrichment of the heavier isotope using the enrichment factor (ϵ), which is related to α by

$$\varepsilon = (\alpha - 1) \times 1000 \tag{3}$$

For systems where the transfer of substrate from the bulk liquid to the location of the enzymes is a rate limiting step for biodegradation, the enzymatic isotope fractionation factor (α_0) determined by the enzyme kinetics differs from the observed isotope fractionation factor (α^*) derived from changes of substrate concentration and isotope ratios detected in the bulk liquid (*37, 38*). When (i) the enzymatic degradation follows Michaelis−Menten kinetics, (ii) the transfer from the bulk liquid to the location of the enzyme can be described by an exchange term ($k_{tr} * \Delta C$) given by the difference between concentration in the bulk and at the location of the enzymes, and a constant rate parameter, k_{tr}, and (iii) the transfer process is nonfractionating, observed and enzymatic fractionation factors are linked by the expression (*1*)

$$\alpha^* = \alpha_0 \cdot \frac{1 + \frac{{}^{l}a}{k_{tr}} \cdot e}{1 + \frac{{}^{h}a}{k_{tr}} \cdot e} \tag{4}$$

where ${}^{h}a$ and ${}^{l}a$ are the specific affinities of the microorganisms toward substrate (defined by the ratio of the maximum biodegradation rate and the Michaelis−Menten constant (*39*)) containing the heavy and the light isotope, respectively. e is the fraction of free enzyme molecules, i.e. not involved in activated substrate complexes. As this fraction varies with the substrate concentration in the system, the observed isotope fractionation factor also depends on the substrate concentration. Using the assumption of $R+1 \approx 1$, eq 4 can be modified to express the dependency of the observed isotope fractionation factor on the bulk substrate concentration explicitly (*1*):

$$\alpha^* = \alpha_0 \cdot \frac{1 + \frac{1}{2}\cdot\left(\frac{a}{k_{tr}} - \frac{c_{bulk}}{K_M} - 1\right) + \sqrt{\frac{a}{k_{tr}} + \frac{1}{4}\cdot\left(\frac{a}{k_{tr}} - \frac{c_{bulk}}{K_M} - 1\right)^2}}{1 + \alpha_0 \cdot \left[\frac{1}{2}\cdot\left(\frac{a}{k_{tr}} - \frac{c_{bulk}}{K_M} - 1\right) + \sqrt{\frac{a}{k_{tr}} + \frac{1}{4}\cdot\left(\frac{a}{k_{tr}} - \frac{c_{bulk}}{K_M} - 1\right)^2}\right]} \tag{5}$$

K_M is the Michaelis−Menten constant of the enzymatic degradation kinetics, and a is the specific affinity, both referring to substrate containing the light isotope.

Results and Discussion

Influence of Toluene Concentration on Observed Fractionation Factors. Experiments were performed to determine the effect of toluene concentration on the enrichment factor by comparing isotopologue-resolved concentration decreases in batch cultures with different initial toluene concentrations. The decrease in toluene concentration during batch biodegradation was accompanied by a decrease in the enrichment factor. Figure 1 shows a typical Rayleigh plot exemplifying the increasing divergence from linearity when the biodegradation of lower substrate concentrations is included. The enrichment factor (ε), as a result of increasingly inadequate linear regression, appears to depend on how much of the toluene has been degraded. The average enrichment factor $\varepsilon = -934‰ \pm 21‰$ obtained after 50% degradation is in agreement with the value determined by Morasch et al. ($\varepsilon = -905‰ \pm 71‰$) for the same degradation range (*17*). When measurements between 50% and 70% degradation are included, an enrichment factor of $\varepsilon = -856‰ \pm 35‰$ is obtained. Theoretically, a flattening of the Rayleigh plot toward the end of a biodegradation experiment may also be explained by changes in cell physiology in different growth phases (*40, 41*). We excluded this possibility by conducting our experiments under nongrowth conditions, where the microbial activity can be assumed to remain constant. Similarly, the addition of chloramphenicol did not

have an effect on the isotope fractionation either, indicating that there was no enzyme synthesis involved in the observed changes of the enrichment factor. The only obvious change in the system was the decrease in the toluene concentration, i.e. toluene bioavailability. The observed flattening of Rayleigh plots is in good qualitative agreement with the theoretical predictions by Thullner et al. (*1*). To confirm the effect of bioavailability on isotope fractionation, and to see if the initial slope of the Rayleigh plot can vary as well, biodegradation experiments with three different initial concentrations were performed. The obtained isotope enrichment factors clearly depended on the initial toluene concentration (Figure 2)—note that the observed changes of the enrichment factors correspond to change of α^* by a factor of approximately 4. This clearly observed dependency on the initial toluene concentration confirmed that enrichment factors based on 50% degradation showed higher absolute values than those based on 70% degradation

Effective Bioavailability. When biodegradation of a pollutant is controlled by its bioavailability, the biodegradation rate is influenced by transfer processes rather than the biochemical capacity of the degrader organisms. As a consequence, the observed isotope fractionation factor in bioavailability-affected systems might differ from values obtained for the nonbioavailability-limited biochemical reaction only. The sensitivity analysis of theoretical predictions at varied bioavailability conditions (i.e., with different ratios of a/k_{tr}; cf. eq 5) in Figure 2 indicates that observed fractionation factors could be used as a diagnostic tool for the assessment of bioavailability at different concentrations in well defined systems. It should be noted that the simplifying assumption of $R+1 \approx 1$ used to derive eq 5 may result in an overestimation of fractionation and thus provides a conservative estimate for the observed changes of the enrichment factor (Figure 2; solid line). This is principally due to the fact that the significant amounts of heavy isotopes at given c_{bulk} lead to a higher concentration of free enzymes because the enzymatic reaction for heavy isotopes proceeds slower than for the light ones. Alternatively, using $(1 - R/(R+1)) * c_{bulk}$ instead of c_{bulk} in eq 5 would lead to an overestimation of free enzymes (as their binding to the heavy isotope is neglected) and thus to an underestimation of the isotope fractionation (Figure 2; dashed line). In the present study, differences between enrichment factors estimated by each of the above approaches are relatively small for all toluene concentrations analyzed. An elaborate discussion on the potential error at different conditions can be found in the Supporting Information of ref *1*, where eq 5 as well as the equation for the upper limit are also explained in detail.

A definition for the effective bioavailability (B_{eff}) as a function of the substrate concentration and the ratio of a/k_{tr} is derived in the following.

If enzymatic degradation is limited by the biochemical capacity, the biodegradation rate (r) is given by Michaelis–Menten kinetics

$$r_{MM} = r_{\max} \cdot \frac{c_{bulk}}{K_M + c_{bulk}} = r_{\max} \cdot \frac{\frac{c_{bulk}}{K_M}}{1 + \frac{c_{bulk}}{K_M}} \quad (6)$$

where r_{max} is the maximum biodegradation rate. In contrast, if the bioavailability of the substrate is controlled by its transfer from the bulk liquid to the location of the enzymes and the substrate bioavailability is limiting the enzymatic degradation, the overall degradation rate is given by the Best equation (for a detailed derivation see refs *33* and *42*):

$$r_{Best} = r_{\max} \cdot \frac{1 + \frac{c_{bulk}}{K_M} + \frac{a}{k_{tr}}}{2 \cdot \frac{a}{k_{tr}}} \cdot \left(1 - \sqrt{1 - \frac{4 \cdot \frac{c_{bulk}}{K_M} \frac{a}{k_{tr}}}{\left(1 + \frac{c_{bulk}}{K_M} + \frac{a}{k_{tr}} \right)^2}} \right) \quad (7)$$

assuming that the substrate transfer process can be described as an exchange between the bulk and at the location of the enzymes (cf. the derivation of eq 4 above). Bosma (*33*) used this ratio to quantify substrate bioavailability by introducing the bioavailability number $Bn = k_{tr}/a$ (*33*). However, as the influence of bioavailability on the overall degradation kinetics also depends on the substrate concentration, we here define the effective bioavailability (B_{eff}) as the ratio of the actual degradation rate affected by substrate bioavailability (eq 7) to the optimal degradation rate to be achieved in the absence of any bioavailability restriction (eq 6):

$$B_{eff} = \frac{r_{Best}}{r_{MM}} = \frac{\left(1 + \frac{c_{bulk}}{K_M}\right) \cdot \left(1 + \frac{c_{bulk}}{K_M} + \frac{a}{k_{tr}}\right) \cdot \left(1 - \sqrt{1 - \frac{4 \cdot \frac{c_{bulk}}{K_M} \cdot \frac{a}{k_{tr}}}{\left(1 + \frac{c_{bulk}}{K_M} + \frac{a}{k_{tr}} \right)^2}} \right)}{2 \cdot \frac{c_{bulk}}{K_M} \cdot \frac{a}{k_{tr}}}$$

$$= \frac{\left(1 + \frac{c_{bulk}}{K_M}\right) \cdot \left(1 + \frac{c_{bulk}}{K_M} + \frac{1}{Bn}\right) \cdot \left(1 - \sqrt{1 - \frac{4 \cdot \frac{c_{bulk}}{K_M} \cdot \frac{1}{Bn}}{\left(1 + \frac{c_{bulk}}{K_M} + \frac{1}{Bn} \right)^2}} \right)}{2 \cdot \frac{c_{bulk}}{K_M} \cdot \frac{1}{Bn}} \quad (8)$$

Please note that for high substrate concentrations, bioavailability restrictions on the substrate degradation rate diminish ($r_{Best} \approx r_{MM}$ or $B_{eff} \approx 1$, respectively) regardless of the value of a/k_{tr} or $1/Bn$ (Figure 3). In contrast, for low substrate concentrations B_{eff} decreases as a function of a/k_{tr} or $1/Bn$.

Influence of Bioavailability on Observed Stable Isotope Fractionation. In Figure 4 observed isotope enrichment factors (ϵ) are plotted against the effective bioavailability (B_{eff}) of the substrate. Our experimental results show a clear dependency of the isotope enrichment factor on substrate bioavailability and hence confirm the hypothesized effect of bioavailability on stable isotope fractionation (*1*). The results are in agreement with previous findings on the effect of substrate availability on fractionation in the context of CO_2 fixation and methane oxidation (*28–30*).

Since it is unlikely that the biochemical mechanism of a bond cleavage (i.e., the isotope sensitive step of the reaction) is changing with substrate concentration, the detected changes in isotope fractionation need to be associated with the extent the transfer of substrate from the bulk solution to the enzymes is limiting the overall reaction rate. These rate limitations associated with substrate bioavailability result in an isotope composition at the enzyme, which is at low substrate concentrations not in equilibrium with the bulk medium. In this case, the unidirectional reaction step is not exclusively related to the isotope sensitive bond cleavage, but it becomes associated with nonisotopically sensitive processes, such as transport of substrate to the cell or uptake by the cell, thus lowering the observed isotope fractionation (*38*). In an extreme case, an observed fractionation factor of 1 might be obtained even for isotopically sensitive reactions, as illustrated by Thullner et al. (*1*). The decrease of B_{eff} with

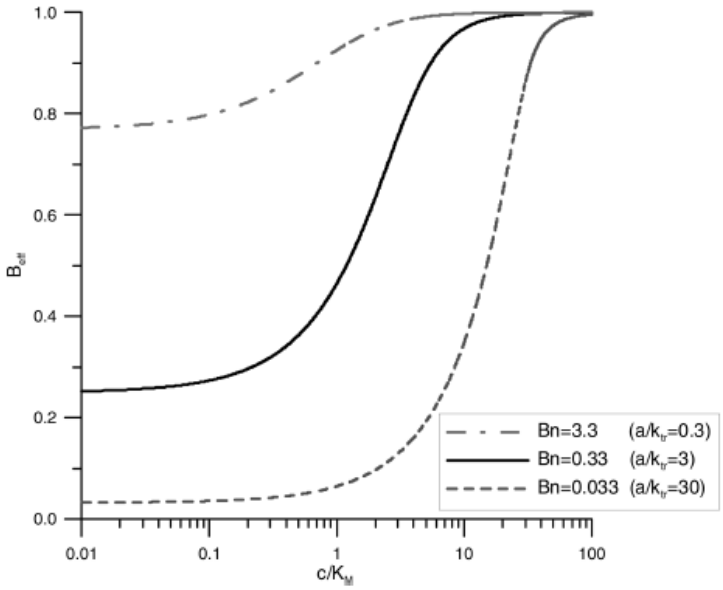

FIGURE 3. Effective bioavailability (eq 8) for different substrate concentration ranges (K_M = 7.7 μM (*43*)) and bioavailability numbers (*Bn*). *Bn* = 0.33 (a/k_{tr} = 3) represents the conditions estimated for the batch experiments (Figure 2), and the other two values are given for comparison. A high effective bioavailability ($B_{eff} \approx 1$) indicates no bioavailability restriction of the degradation rate, a low value ($B_{eff} \ll 1$) indicates degradation rates highly restricted by substrate bioavailability.

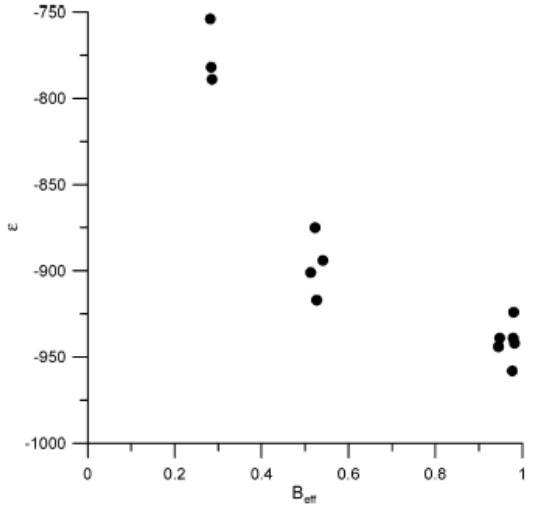

FIGURE 4. Observed isotope enrichment factors for different effective bioavailabilities. B_{eff} for each batch experiment was calculated using initial concentration values and *Bn* = 0.33 (best fit from Figure 2). At $B_{eff} \ll 1$ (i.e., low concentrations, low mass transfer rates, and concomitant low toluene bioavailability) the enrichment factors (ε) are 100−150‰ below the literature value of 905‰ determined at conditions of high bioavailability. (*17*)

substrate concentration also explains the nonlinearity observed for individual Rayleigh plots. A previous study has associated the approximately 2-fold reduction of the observed isotope fractionation to the substrate fluxes over the cell membrane (*19*). The up to 4-fold reduction of the observed isotope fractionation factor observed in this study is in the same order of magnitude and further illustrates that nonisotope-sensitive processes can significantly affect isotope composition of contaminants compared to pure chemical or biochemical reactions. It further corroborates that transport processes to and across the cell membrane may influence the extent of observed isotope fractionation in a given (macroscopic) system. Our results thus suggest that the bioavailability of a substrate should be considered during quantitative analysis of microbial degradation based on SIFA.

Consequences for the Quantification of Contaminant Biodegradation in Natural Systems Using Isotope Fractionation. The importance of the observed deviation from the Rayleigh-relationship at low bioavailability for the practical application of SIFA remains to be investigated. Theoretical predictions for the introduced error are developed in the accompanying paper (*1*). Stable isotope fractionation has been successfully applied to the assessment of biodegradation at several field sites (*11, 44, 45*), and tracer experiments in aquifers have shown that anaerobic biodegradation of toluene could be quantified with laboratory derived isotope fractionation factors (*11*). As it can be seen from the theoretical predictions in Figures 2 and 3 (a/k_{tr} = 1 and a/k_{tr} = 0.1, respectively), the phenomenon described here is important only under bioavailability-restricted conditions. At our experimental setup the rate parameter for the mass transfer of toluene toward a single bacterial cell is roughly estimated to be in the order of $k_{tr} \approx 10^{-14}$ m^3 s^{-1} (assuming the cell radius and the diffusive boundary to be in the μm-range (*33*)). In the field this value is assumed to decrease significantly due to longer diffusion pathways and/or additional processes affecting mass transfer rates. An even more reduced bioavailability with mass transfer coefficients of up to 10^{-22} m^3 s^{-1} is to be expected for hydrophobic compounds in structured soil (*33*). SIFA is also used for hydrophobic contaminants, such as chlorinated hydrocarbons and naphthalene, for which sorption on organic matter may significantly reduce the bioavailability. In such cases, the application of laboratory-derived fractionation factors to field observations should be conducted with great caution. However, it should be kept in mind that in our definition bioavailability is not equivalent with the mass transfer flux but includes the relationship between supply and consumption. In the field, cell densities as well as degradation rates in the subsurface vary greatly, depending on a number of environmental factors. The amount of biomass and its

degradation capacity play an important role for specific affinities to be found in the field. It is therefore possible that for cell activities limited by the lack of other chemical species than the substrate and for lower cell densities, as they are typical for aquifers, only very low substrate concentrations are needed to saturate the enzymatic degradation capacity. For instance, under anoxic conditions, degradation rates are usually very low, and a low mass transfer flux may be sufficient for unlimited substrate availability. A straightforward prediction of effective bioavailability and thus observed fractionation factors in field is therefore not possible. Nevertheless, fractionation factors determined in batch cultures with high contaminant concentration do probably not always represent the bioavailability conditions in the soils and sediments. Therefore physicochemical processes need to be taken into account when stable isotope fractionation analysis is used for the quantification of environmental contaminant degradation. For further research, it would be important to investigate the different processes that restrict bioavailability in the field, such as sorption, partitioning in nonaqueous phase liquid (NAPL), and their effect on the observed isotope fractionation, in order to understand the practical impact of this phenomenon.

Acknowledgments

This study was supported by the European MEST-CT-2004-8332 grant (AXIOM) and the Helmholtz Association grant VG-NG-338 (Great MoDE). Skilled technical help by Birgit Würz, Jana Reichenbach, Rita Remer, Martina Kolbe, and Katrin Lübke is greatly acknowledged.

Literature Cited

(1) Thullner, M.; Kampara, M.; Richnow, H. H.; Harms, H.; Wick, L. Y. Impact of bioavailability restrictions on microbially induced apparent stable isotope fractionation: Theoretical calculations. *Environ. Sci. Technol* **2008**, *42*, 6544–6551.

(2) Meckenstock, R. U.; Morasch, B.; Griebler, C.; Richnow, H. H. Stable isotope fractionation analysis as a tool to monitor biodegradation in contaminated acquifers. *J. Contam. Hydrol.* **2004**, *75*, 215–255.

(3) Kaschl, A.; Vogt, C.; Uhlig, S.; Nijenhuis, I.; Weiss, H.; Kastner, M.; Richnow, H. H. Isotopic fractionation indicates anaerobic monochlorobenzene biodegradation. *Environ. Toxicol. Chem.* **2005**, *24*, 1315–1324.

(4) Griebler, C.; Safinowski, M.; Vieth, A.; Richnow, H. H.; Meckenstock, R. U. Combined application of stable carbon isotope analysis and specific metabolites determination for assessing in situ degradation of aromatic hydrocarbons in a tar oil-contaminated aquifer. *Environ. Sci. Technol.* **2004**, *38*, 617–631.

(5) Dempster, H. S.; Sherwood Lollar, B.; Feenstra, S. Tracing organic contaminants in groundwater: A new methodology using compound-specific isotopic analysis. *Environ. Sci. Technol.* **1997**, *31*, 3193–3197.

(6) Harrington, R. R.; Poulson, S. R.; Drever, J. I.; Colberg, P. J. S.; Kelly, E. F. Carbon isotope systematics of monoaromatic hydrocarbons: vaporization and adsorption experiments. *Org. Geochem.* **1999**, *30*, 765–775.

(7) Schuth, C.; Taubald, H.; Bolano, N.; Maciejczyk, K. Carbon and hydrogen isotope effects during sorption of organic contaminants on carbonaceous materials. *J. Contam. Hydrol.* **2003**, *64*, 269–281.

(8) Slater, G. F.; Ahad, J. M. E.; Sherwood Lollar, B.; Allen-King, R.; Sleep, B. Carbon isotope effects resulting from equilibrium sorption of dissolved VOCs. *Anal. Chem.* **2000**, *72*, 5669–5672.

(9) Richnow, H. H.; Annweiler, E.; Michaelis, W.; Meckenstock, R. U. Microbial in situ degradation of aromatic hydrocarbons in a contaminated aquifer monitored by carbon isotope fractionation. *J. Contam. Hydrol.* **2003**, *65*, 101–120.

(10) Sherwood Lollar, B.; Slater, G. F.; Sleep, B.; Witt, M.; Klecka, G. M.; Harkness, M.; Spivack, J. Stable carbon isotope evidence for intrinsic bioremediation of tetrachloroethene and trichloroethene at area 6, Dover Air Force Base. *Environ. Sci. Technol.* **2001**, *35*, 261–269.

(11) Fischer, A.; Bauer, J.; Meckenstock, R. U.; Stichler, W.; Griebler, C.; Maloszewski, P.; Kastner, M.; Richnow, H. H. A multitracer test proving the reliability of Rayleigh equation-based approach for assessing biodegradation in a BTEX contaminated aquifer. *Environ. Sci. Technol.* **2006**, *40*, 4245–4252.

(12) Fischer, A.; Theuerkorn, K.; Stelzer, N.; Gehre, M.; Thullner, M.; Richnow, H. H. Applicability of stable isotope fractionation analysis for the characterization of benzene biodegradation in a BTEX-contaminated aquifer. *Environ. Sci. Technol.* **2007**, *41*, 3689–3696.

(13) Vieth, A.; Kastner, M.; Schirmer, M.; Weiss, H.; Godeke, S.; Meckenstock, R. U.; Richnow, H. H. Monitoring in situ biodegradation of benzene and toluene by stable carbon isotope fractionation. *Environ. Toxicol. Chem.* **2005**, *24*, 51–60.

(14) Wilson, J. T.; Kaiser, P.; Adair, C. U.S. Environmental Protection Agency, Washington, DC, 2005.

(15) Rayleigh, J. S. W. Theoretical Considerations respecting the separation of gases by diffusion and similar processes. *Philos. Mag.* **1896**, *42*, 493–498.

(16) Hoefs, J. *Stable isotope geochemistry*; Springer-Verlag: Berlin, 1997.

(17) Morasch, B.; Richnow, H. H.; Schink, B.; Meckenstock, R. U. Stable hydrogen and carbon isotope fractionation during microbial toluene degradation: Mechanistic and environmental aspects. *Appl. Environ. Microb.* **2001**, *67*, 4842–4849.

(18) Hunkeler, D.; Anderson, N.; Aravena, R.; Bernasconi, S. M.; Butler, B. J. Hydrogen and carbon isotope fractionation during aerobic biodegradation of benzene. *Environ. Sci. Technol.* **2001**, *35*, 3462–3467.

(19) Nijenhuis, I.; Andert, J.; Beck, K.; Kastner, M.; Diekert, G.; Richnow, H. H. Stable isotope fractionation of tetrachloroethene during reductive dechlorination by *Sulfurospirillum multivorans* and *Desulfitobacterium* sp strain PCE-S and abiotic reactions with cyanocobalamin. *Appl. Environ. Microb.* **2005**, *71*, 3413–3419.

(20) Chartrand, M. M. G.; Waller, A.; Mattes, T. E.; Elsner, M.; Lacrampe-Couloume, G.; Gossett, J. M.; Edwards, E. A.; Sherwood Lollar, B. Carbon isotopic fractionation during aerobic vinyl chloride degradation. *Environ. Sci. Technol.* **2005**, *39*, 1064–1070.

(21) Conrad, M. E.; Templeton, A. S.; Daley, P. F.; Alvarez-Cohen, L. Isotopic evidence for biological controls on migration of petroleum hydrocarbons. *Org. Geochem.* **1999**, *30*, 843–859.

(22) Schmidt, T. C.; Zwank, L.; Elsner, M.; Berg, M.; Meckenstock, R. U.; Haderlein, S. B. Compound-specific stable isotope analysis of organic contaminants in natural environments: a critical review of the state of the art, prospects, and future challenges. *Anal. Bioanal. Chem.* **2004**, *378*, 283–300.

(23) Rosell, M.; Barcelo, D.; Rohwerder, T.; Breuer, U.; Gehre, M.; Richnow, H. H. Variations in C-13/C-12 and D/H enrichment factors of aerobic bacterial fuel oxygenate degradation. *Environ. Sci. Technol.* **2007**, *41*, 2036–2043.

(24) Johnsen, A. R.; de Lipthay, J. R.; Reichenberg, F.; Sorensen, S. J.; Andersen, O.; Christensen, P.; Binderup, M. L.; Jacobsen, C. S. Biodegradation, bioaccessibility, and genotoxicity of diffuse polycyclic aromatic hydrocarbon PAH) pollution at a motorway site. *Environ. Sci. Technol.* **2006**, *40*, 3293–3298.

(25) O'Leary, M. H. Carbon isotope fractionation in plants. *Phytochemistry* **1980**, *20*, 553–567.

(26) Cichocka, D.; Siegert, M.; Imfeld, G.; Andert, J.; Beck, K.; Diekert, G.; Richnow, H. H.; Nijenhuis, I. Factors controlling the carbon isotope fractionation of tetra- and trichloroethene during reductiove dechlorination by Sulfurospirillum ssp. and Desulfitobacterium sp. strain PCE-S. *FEMS Microbiol. Ecol.* **2007**, *62*, 98–107.

(27) Park, R.; Epstein, S. Carbon Isotope Fractionation during Photosynthesis. *Geochim. Cosmochim. Acta* **1960**, *21*, 110–126.

(28) Pardue, J. W.; Scalan, R. S.; Vanbaalen, C.; Parker, P. L. Maximum Carbon Isotope Fractionation in Photosynthesis by Blue-Green-Algae and a Green-Alga. *Geochim. Cosmochim. Acta* **1976**, *40*, 309–312.

(29) Calder, J. A.; Parker, P. L. Geochemical Implications of Induced Changes in C-13 Fractionation by Blue-Green-Algae. *Geochim. Cosmochim. Acta* **1973**, *37*, 133–140.

(30) Staal, M.; Thar, R.; Kuhl, M.; van Loosdrecht, M. C. M.; Wolf, G.; de Brouwer, J. F. C.; Rijstenbil, J. W. Different carbon isotope fractionation patterns during the development of phototrophic freshwater and marine biofilms. *Biogeoscience* **2007**, *4*, 613–626.

(31) Templeton, A. S.; Chu, K. H.; Alvarez-Cohen, L.; Conrad, M. E. Variable carbon isotope fractionation expressed by aerobic CH4-oxidizing bacteria. *Geochim. Cosmochim. Acta* **2006**, *70*, 1739–1752.

(32) Mancini, S. A.; Hirschorn, S. K.; Elsner, M.; Lacrampe-Couloume, G.; Sleep, B. E.; Edwards, E. A.; Sherwood Lollar, B. Effects of trace element concentration on enzyme controlled stable isotope fractionation during aerobic biodegradation of toluene. *Environ. Sci. Technol.* **2006**, *40*, 7675–7681.
(33) Bosma, T. N. P.; Middeldorp, P. J. M.; Schraa, G.; Zehnder, A. J. B. Mass transfer limitation of biotransformation: Quantifying bioavailability. *Environ. Sci. Technol.* **1997**, *31*, 248–252.
(34) Haws, N. W.; Ball, W. P.; Bouwer, E. J. Modeling and interpreting bioavailability of organic contaminant mixtures in subsurface environments. *J. Contam. Hydrol.* **2006**, *82*, 255–292.
(35) Shaw, J. P.; Harayama, S. Purification and characterization of the NADH - acceptor reductase component of xylene monooxygenase encoded by the Tol plasmid PwwO of *Pseudomonas putida* mt-2. *Eur. J. Biochem.* **1992**, *209*, 51–61.
(36) Harms, H.; Zehnder, A. J. B. Influence of substrate diffusion on degradation of dibenzofuran and 3-chlorodibenzofuran by attached and suspended bacteria. *Appl. Environ. Microb.* **1994**, *60*, 2736–2745.
(37) Mariotti, A.; Mariotti, F.; Champigny, M. L.; Amarger, N.; Moyse, A. Nitrogen isotope fractionation associated with nitrate reductase-activity and uptake of NO_3- by pearl-millet. *Plant Physiol.* **1982**, *69*, 880–884.
(38) Northrop, D. B. The expression of isotope effects on enzyme-catalyzed reactions. *Annu. Rev. Biochem.* **1981**, *50*, 103–131.
(39) Button, D. K. Biochemical basis for whole-cell uptake kinetics-Specific affinity, oligotrophic capacity, and the meaning of the Michaelis constant. *Appl. Environ. Microb.* **1991**, *57*, 2033–2038
(40) Penning, H.; Plugge, C. M.; Galand, P. E.; Conrad, R. Variation of carbon isotope fractionation in hydrogenotrophic methanogenic microbial cultures and environmental samples at different energy status. *Glob. Change Biol.* **2005**, *11*, 2103–2113
(41) Valentine, D. L.; Chidthaisong, A.; Rice, A.; Reeburgh, W. S.; Tyler, S. C. Carbon and hydrogen isotope fractionation by moderately thermophilic methanogens. *Geochim. Cosmochim. Acta* **2004**, *68*, 1571–1590.
(42) Best, J. B. The inference of intracellular enzymatic properties from kinetic data obtained on living cells: Some kinetic considerations regarding an enzyme enclosed by a diffusion barrier. *J. Cell. Comp. Physiol.* **1955**, *46*, 1–27.
(43) Duetz, W. A.; Wind, B.; van Andel, J. G.; Barnes, M. R.; Williams, P. A.; Rutgers, M. Biodegradation kinetics of toluene, m-xylene and their intermediates through the upper TOL pathway in*Pseudomonas putida* (pWW0), **1998**, *144*, 1669–1675.
(44) Meckenstock, R. U.; Morasch, B.; Warthmann, R.; Schink, B.; Annweiler, E.; Michaelis, W.; Richnow, H. H. C-13/C-12 isotope fractionation of aromatic hydrocarbons during microbial degradation. *Environ. Microbiol.* **1999**, *1*, 409–414.
(45) Meckenstock, R. U.; Morasch, B.; Kästner, M.; Vieth, A.; Richnow, H. H. Assessment of bacterial degradation of aromatic hydrocarbons in the environment by analysis of stable carbon isotope fractionation. *Water, Air, Soil Pollut.* **2002**, *2*, 141–152.

ES702781X

Chapter 3

Isotope fractionation – a tool for the assessment of bioavailability?

3.1 The impact of cell density on microbially induced stable isotope fractionation[3]

3.2 Correlation between bioavailability and stable isotope fractionation in column and two-liquid-phase systems[4]

[3] *Appl Microbiol Biotechnol*, in press
[4] in preparation

The correlation between bioavailability and observed isotope fractionation, shown in the previous chapter, may be useful for the assessment of bioavailability. Isotope fractionation could give direct information about the bioavailability conditions a cell is experiencing, i.e. whether substrate transformation is dominated by bioavailability and to what extent. In this chapter, experiments for the validation of this potential new application are presented and discussed.

In Chapter 2, substrate concentration was used to vary the bioavailability conditions, in order to demonstrate the effect of bioavailability on the observed fractionation factors [3, 4]. In this chapter, the sensitivity of the observed isotope fractionation factor towards other variables possibly limiting the bioavailability of contaminants in the environment is assessed. A schematic illustration of the experimental concepts is presented in Figure 3.1. The situation described in Figure 3.1A corresponds to the experiments presented in Chapter 2. Even in a well mixed batch system slow diffusion through the diffusive boundary layer (DBL) at low substrate concentrations may lead to bioavailability limitation (Fig. 3.1A). The flux to a single cell is also influenced by the cell density. The higher the cell density, the more probable is the overlap of the DBLs of two or more cells (Fig. 3.1B). In case of an overlap, the apparent bulk concentration may already be reduced by another cell. The effect of cell density on the observed isotope fractionation is investigated in section 3.1. The substrate mass transfer to microorganisms in the subsurface is often additionally reduced by their attached state. In the experiments described in section 3.2, stable isotope fractionation by attached, immobilized bacteria in a model column system was investigated (Fig. 3.1C). In all the studies mentioned above, diffusion of a substrate to the cell (process 2 in Chapter 1) is seen as the rate limiting step for biodegradation. However, in environmental systems, the preceding process of dissolution or desorption (process 1 in Chapter 1) of the contaminant into the aqueous phase, often plays an important role. In section 3.2, the effect of slow dissolution is investigated

using a two-liquid-phase system (Fig. 3.1D). These experiments have shown that the additional mass transfer step from oil to aqueous phase can further reduce the observed isotope fractionation.

Appl Microbiol Biotechnol
DOI 10.1007/s00253-008-1755-0

ENVIRONMENTAL BIOTECHNOLOGY

Impact of cell density on microbially induced stable isotope fractionation

Makeba Kampara · Martin Thullner · Hauke Harms · Lukas Y. Wick

Received: 23 July 2008 / Revised: 13 October 2008 / Accepted: 18 October 2008

Abstract Quantification of microbial contaminant biodegradation based on stable isotope fractionation analysis (SIFA) relies on known, invariable isotope fractionation factors. The microbially induced isotope fractionation is caused by the preferential cleavage of bonds containing light rather than heavy isotopes. However, a number of non-isotopically sensitive steps preceding the isotopically sensitive bond cleavage may affect the reaction kinetics of a degradation process and reduce the observed (i.e., the macroscopically detectable) isotope fractionation. This introduces uncertainty to the use of isotope fractionation for the quantification of microbial degradation processes. Here, we report on the influence of bacterial cell density on observed stable isotope fractionation. Batch biodegradation experiments were performed under non-growth conditions to quantify the toluene hydrogen isotope fractionation by exposing *Pseudomonas putida* mt-2(pWWO) at varying cell densities to different concentrations of toluene. Observed isotope fractionation depended significantly on the cell density. When the cell density rose from 5×10^5 to 5×10^8 cells/mL, the observed isotope fractionation declined by 70% and went along with a 55% decrease of the degradation rates of individual cells. Theoretical estimates showed that uptake-driven diffusion to individual cells depended on cell density via the overlap of the cells' diffusion-controlled boundary layers. Our data suggest that biomass effects on SIFA have to be considered even in well-mixed systems such as the cell suspensions used in this study.

M. Kampara · M. Thullner · H. Harms · L. Y. Wick (✉)
Department of Environmental Microbiology,
UFZ—Helmholtz Centre for Environmental Research,
Permoserstrasse 15,
04318 Leipzig, Germany
e-mail: lukas.wick@ufz.de

Keywords Bioavailability · Cell density · Biodegradation · Fractionation factor · Stable isotope fractionation analysis · Toluene

Introduction

Stable isotopes have become an important tool for a variety of applications such as the assessment of contaminant biodegradation and the elucidation of degradation pathways (Elsner et al. 2005; Griebler et al. 2004; Meckenstock et al. 2004), the analysis of food webs (March and Pringle 2003), and the evaluation of sources and sinks of greenhouse gases (Braunlich et al. 2001; Gupta et al. 1996; Whiticar 1990). For many applications, knowledge of the factors that influence isotope fractionation is needed. Isotope fractionation occurs due the fact that higher activation energy is needed for the cleavage of a chemical bond containing a heavier isotope. Therefore, molecules containing lighter isotopes are preferably degraded, which leads to an enrichment of heavy isotopes in the residual substrate pool (Elsner et al. 2005; Meckenstock et al. 2004; Schmidt et al. 2004). Fractionation factors are commonly determined in controlled laboratory systems and then applied to diverse, complex systems (Chartrand et al. 2005; Griebler et al. 2004; Hunkeler et al. 2001; Morasch et al. 2001; Nijenhuis et al. 2005). But even if the enzymatic fractionation is invariable, the observable fractionation may be influenced by physical processes in the environment (Thullner et al. 2008). It is known that rate-limiting steps prior to the fractionating bond cleavage may have an impact on the fractionation observed (Northrop 1981). Uptake transport within the cytoplasm and binding to the enzyme were shown to influence the observable isotope fractionation (Nijenhuis et al. 2005; Cichocka et al. 2007). Furthermore,

influences of environmental factors on isotope fractionation, such as the availability of substrate or trace elements, have been observed (Kampara et al. 2008; Mancini et al. 2006; O'Leary 1980; Pardue et al. 1976; Park and Epstein 1960; Templeton et al. 2006; Thullner et al. 2008; Tyler et al. 1994). Substrate availability is controlled by the interplay of bulk substrate concentration and mass transfer on one side and the density and activity of the biomass on the other side. As variability of observable fractionation introduces uncertainty to the use of stable isotope fractionation analysis (SIFA), it is important to be aware of the impact of environmental variables. In this study, we investigated the impact of cell density on the observable stable isotope fractionation.

The effect of cell density on substrate availability to attached cells has been shown by Harms and Zehnder (1994). When cells are attached to a surface and to each other, the approach of substrate becomes restricted. During the development of a biofilm, the ratio of biovolume to exposed surface even increases, and substrate mass transfer limitation becomes more influential. Staal et al. observed decreased isotope fractionation with increasing biomass at the later developmental stages of a phototrophic biofilm, which indicates that the diffusive transport of CO_2 became limiting (Staal et al. 2007). But even in suspension, reduced substrate mass transfer to single cells may occur at high cell density. Substrate consumption creates partly substrate depleted zones around cells (Harms and Zehnder 1994). Diffusion calculations by Boone et al. showed that such zones of reduced substrate concentrations extend about 10 μm from the cell surface in unstirred systems (Boone et al. 1989). If suspended cells are so close to each other that their depletion zones overlap, they become more prone to mass transfer limitation. Our hypothesis was that, depending on the bulk substrate concentration, cell density can have an effect on the substrate availability and consequently on stable isotope fractionation. By exposing differently dense suspension of toluene-degrading *Pseudomonas putida* mt-2 (pWW0) cells to varying initial toluene concentrations, we tested our hypothesis. We analyzed the observable hydrogen isotope fractionation and used it as an analytical tool to assess substrate availability to single cells as proposed in an earlier study (Kampara et al. 2008).

Materials and methods

Organism P. putida mt-2 carries the TOL plasmid pWW0, encoding a pathway for the degradation of xylene and toluene. Degradation is initiated by the oxidation of the methyl side chain of these substrates, catalyzed by the membrane bound xylene monooxygenase (Shaw and Harayama 1992). The initial oxidation is known to cause substantial hydrogen isotope fractionation (Morasch et al. 2001).

Batch degradation experiments Strain mt-2 was grown at 30°C in mineral medium (Harms and Zehnder 1994), with toluene (2.8 mM) as the only carbon and energy source, on a rotary shaker at 140 rpm. Cells were harvested in the mid-exponential growth phase by centrifugation (13,000×g, 10 min), washed four times with 0.1 M phosphate-buffered saline (PBS) to remove toluene traces, and suspended in 0.1 M PBS. This suspension was used as inoculum for the experiments. Toluene degradation experiments were performed at room temperature (20°C) in tightly closed, three-neck 1-L glass bottles with 250 mL PBS containing a 1:1 mixture (*v*/*v*) of toluene-h8 (99.9%, Merck KGaA (Germany)) and per-deuterated toluene-*d*8 (99.6at.% D; Sigma-Aldrich Chemie (Germany)) at either 1, 10, or 100 μM total toluene concentration, standing on a magnetic stirrer (300 rpm). At least 12 h after the addition of the toluene, *P. putida* mt-2 was added to give a cell density of either $n_{cell} = 5 \times 10^5$, 5×10^6, 5×10^7, or 5×10^8 cells/mL. Immediately before and after the inoculation and at regular intervals, samples of 2 mL liquid were taken through air-tight Teflon septa using air-tight syringes (Gastight® #1002, Hamilton Co. Reno, NV, USA). The samples were transferred to 10-mL autosampler vials, containing 20 μL of concentrated H_2SO_4 to inhibit further biodegradation. The vials were closed immediately air-tight with Teflon-coated butyl rubber septa. The cell density was controlled by measuring optical density at 578 nm using a UV–visible spectrophotometer (Cary 400 Scan, Varian). The duration of the experiments ranged from 20 min to 10h, depending on the initial toluene concentrations and cell density. In order to exclude bacterial growth and physiological changes during the experiments, some flasks were amended with 100 mg/L of chloramphenicol (Karl Roth GmbH, Germany), an antibiotic inhibiting protein synthesis. As observed fractionation factors remained uninfluenced by chloramphenicol, the antibiotic was not added in all experiments. Iron, which has been shown to influence toluene degradation and isotope fractionation by *P. putida* mt-2 (Mancini et al. 2006), was not added to the PBS in any of the experiments.

Analytical procedures The analysis of D/H isotope fractionation was based on the method described by Morasch et al. (2001). The concentrations of toluene and toluene-*d*8 were analyzed by headspace gas chromatography with a flame ionization detector (GC-FID; Hewlett Packard 6890 Series). The injection was automated using a headspace autosampler (Hewlett Packard 7694) with an oven temperature of 95°C and an injection volume of 1 mL. A fused silica capillary column (Optima δ-3, length 60 m, inside

diameter 0.32 mm, film thickness 0.35 μm; Macherey-Nagel, Düren, Germany) was used to separate the D/H-toluene isotopologues applying the following temperature sequence: 35°C for 2 min, heat to 94°C at a rate of 6°C/min, cool down to 35°C. Separation of the two toluene species was achieved at 105.7 kPa with a N_2 flowrate of 15.0 mL/min and with a split of 5:1. The FID was operated at 280°C, and helium was used as carrier gas.

Determination of the isotope fractionation factor The isotope fractionation factor (α) for microbial degradation reactions is defined as

$$\alpha = \frac{{}^{h}r/{}^{h}c}{{}^{l}r/{}^{l}c} \tag{1}$$

where ${}^{h}r$ and ${}^{l}r$ are the degradation rates of substrate containing the heavy and the light isotope, respectively, and ${}^{h}c$ and ${}^{l}c$ are the respective substrate concentrations. For closed systems such as the batches used in the present study, the relation between changes of total substrate concentration ($c = {}^{h}c + {}^{l}c$) and substrate isotope ratio ($R = {}^{h}c/{}^{l}c$) is given by the Rayleigh equation (Mariotti et al. 1981; Rayleigh 1896; here expressed in its logarithmic form):

$$\ln\left(\frac{R_t}{R_0}\right) = (\alpha - 1) \times \ln\left(\frac{c_{\mathrm{bulk},t}}{c_{\mathrm{bulk},0}}\right)\left(\frac{R_0 + 1}{R_t + 1}\right) \tag{2}$$

R_t and R_0 are the substrate isotope ratios at times t and zero, respectively, and c_t and c_0 are the total substrate concentrations at these times. Eq. 2 was used for the experimental determination of hydrogen isotope fractionation factors in the batch toluene degradation experiments. α was derived by plotting measured values of ln (R_t/R_0) vs. $\ln\left(\left[c_{\mathrm{bulk},t}/c_{\mathrm{bulk},0}\right]/\left[(R_t+1)/(R_0+1)\right]\right)$ in a Rayleigh plot and obtaining the slope of the linear regression using Eq. 2. In order to avoid increasingly inadequate linear regression, α was calculated based on 50% degradation of the initial toluene concentration only as described earlier (Kampara et al. 2008).

Theory

Substrate consumption by metabolically active bacteria creates a diffusive depletion layer around individual cells. In the following section, we describe two scenarios, how overlapping diffusive depletion layers of cells at high cell densities may limit substrate mass transfer to individual cells and consequently the observed stable isotope fractionation.

Estimation of cell density effects on mass transfer to a single cell

Overlapping boundary layers (scenario 1)

Assuming that for bacterial cells dispersed in a mixed aqueous substrate solution, the mass transfer of substrate to/into a cell is controlled by diffusion across a boundary layer of thickness δ around the cell, and the mass flux, J, toward a single, radial-shaped cell is given by (Bosma et al. 1997) Eq. 3,

$$J = D \times \frac{4\pi \times r \times L}{L - r} \times (c_{\mathrm{bulk}} - c_{\mathrm{bioav}}) \tag{3}$$

where D is the molecular diffusion coefficient, r is the radius of the cell, and L is the distance between cell center and the outer edge of the diffusive boundary layer, i.e., also $\delta = L - r$ (Fig. 1a). The substrate concentration in the bulk liquid of the batch is given by c_{bulk}, whereas c_{bioav} denotes the concentration at or in the cell, i.e., the directly available concentration controlling the kinetics of the enzymatic degradation. The resulting change of bioavailable concentration due to this mass transfer is then given by Eq. 4,

$$\begin{aligned}\frac{\partial c_{\mathrm{bioav,tr}}}{\partial t} &= \frac{J}{V_{\mathrm{cell}}} = D \times \frac{3L}{r^2 \times (L - r)} \times (c_{\mathrm{bulk}} - c_{\mathrm{bioav}}) \\ &= k_{\mathrm{tr}} \times (c_{\mathrm{bulk}} - c_{\mathrm{bioav}})\end{aligned} \tag{4}$$

with k_{tr} as first order rate coefficient of the mass transfer (expressed in per second). The above expressions are valid if the entire surface of the cell is approached by the diffusive flux, i.e., the entire cell is symmetrically surrounded by the diffusive boundary layer. This is the case if this boundary layer is not compromised by other cells and their boundary layers, i.e., when the distance x between two cells is larger than $2L$ (Fig. 1a). When the distance between two cells is smaller than $2L$, the boundary layers overlap (Fig. 1b) and the mass flux toward each of these cells are reduced depending on the degree of overlap. It can consequently be assumed that the flux is decreased proportionally to the reduction of the outer surface of the boundary layer caused by the overlap. This surface reduction, S_x, and the resulting mass flux, J_x, are expressed by Eqs. 5 and 6

$$S_x = 2\pi \times L \times \left(L - {}^{x}/_{2}\right) \tag{5}$$

$$J_x = J_0 \times \left(1 - {}^{S_x}/_{S_0}\right) = J_0 \times \left(1 - \frac{1 - {}^{x}/_{2} \times L}{2}\right) \tag{6}$$

with $S_0 = 4\pi L^2$ as the surface of the entire (non-overlapping) boundary layer and J_0 the flux toward a cell in the absence of any boundary layer overlap (Eq. 3).

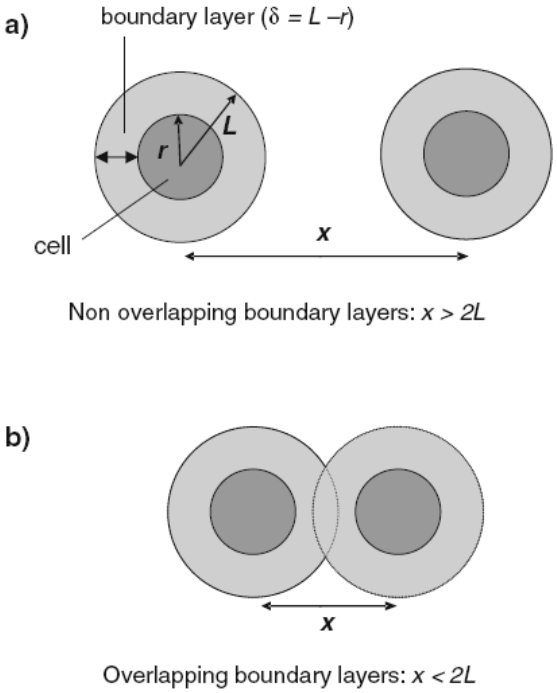

Fig. 1 Conceptualized representation of the role of boundary layers on effective toluene mass fluxes to cells: **a** representation of boundary layers of two non-overlapping bacterial cells, **b** depiction of overlapping boundary layers

In order to calculate the reduction of mass flux toward an individual cell at cell density n_{cell}, the probability of overlapping boundary layers needs to be estimated. For an individual cell, the number of neighboring cells, $N_L(x)$ within a given distance x, $x + dx$ is (Eq. 7)

$$N_L(x) = 4\pi \times x^2 \times dx \times n_{cell} \tag{7}$$

Using this expression, the effective flux J_{eff} toward a single cell reduced by the presence of other substrate-consuming cells can be expressed by Eq. 8,

$$\begin{aligned} J_{eff} &= J_0 - \int_{2r}^{2L} J_0 \times \frac{1 - x/2L}{2} \times N_L(x) \\ &= J_0 \times \left[1 - 2\pi \times n_{cell} \int_{2r}^{2L} \left(1 - x/2L\right) \times x^2 dx\right] \\ &= J_0 \times \left(1 - 4/3\pi \times \left[L^3 - r^3 \times \left(4 - 3r/L\right)\right] \times n_{cell}\right) \end{aligned} \tag{8}$$

which, if $r^3 \ll L^3$ reduces to Eq. 9

$$J_{eff} \approx J_0 \times \left[1 - 4/3\pi \times L^3 \times n_{cell}\right] \tag{9}$$

It should be noted that this approach simply sums up the individual effects of all neighboring cells without accounting for probable influences of higher orders, such as a general reduction of the bulk concentration at very high cells densities. Accounting for this would require additional terms. Hence, Eqs. 8 and 9 are not applicable to cell densities leading to $4/3\pi \times L^3 \times n_{cell} \approx 1$ and higher.

Reversible formation of cell clusters (scenario 2)

Assuming that suspended cells transiently form cell clusters or aggregates of two or more cells, the flux toward such a cluster is shared by all cells within the cluster. For simplicity, we define here a cell as being part of a cluster if there are other (one or more) cells within its range of influence. In analogy to the descriptions above and assuming that the total cell volume is negligible compared to the total volume of the system, this range of influence is given by $\delta = L - r$, and for a single cell, the average number N_L of other cells in a distance closer than δ is given by

$$N_L = 4/3\pi \times \left(L^3 - r^3\right) \times n_{cell} \tag{10}$$

Assuming that the flux, J_0, toward a cluster is given by Eq. 3 (which neglects that such a cluster may have an increased outer surface of the boundary layer allowing for a larger J_0 than given for a single cell), the flux per cell, J_{eff}, is

$$J_{eff} = J_0 \times \frac{1}{N_L + 1} = J_0 \times \frac{1}{4/3\pi \times (L^3 - r^3) \times n_{cell} + 1} \tag{11}$$

Equation 11 can again be simplified assuming that $r^3 \ll L^3$ (Eq. 12)

$$J_{eff} \approx J_0 \times \frac{1}{4/3\pi \times L^3 \times n_{cell} + 1} \tag{12}$$

Estimation of cell density effects on observed stable isotope fractionation

In order to include the influence of cell density on substrate bioavailability and on observed stable isotope fractionation, respectively, Eq. 8 (scenario 1) or Eq. 11 (scenario 2), needs to be coupled with Eq. 13. This equation was derived earlier by Thullner et al. (2008) and successfully relates the

observable stable isotope fractionation factor α^* to the substrate flux to a cell:

$$\alpha^* = \alpha_0 \times \frac{1 + \frac{1}{2} \times \left(\frac{a}{k_{tr}} - \frac{c_{bulk}}{K_M} - 1\right) + \sqrt{\frac{a}{k_{tr}} + \frac{1}{4} \times \left(\frac{a}{k_{tr}} - \frac{c_{bulk}}{K_M} - 1\right)^2}}{1 + \alpha_0 \times \left[\frac{1}{2} \times \left(\frac{a}{k_{tr}} - \frac{c_{bulk}}{K_M} - 1\right) + \sqrt{\frac{a}{k_{tr}} + \frac{1}{4} \times \left(\frac{a}{k_{tr}} - \frac{c_{bulk}}{K_M} - 1\right)^2}\right]} \quad (13)$$

where α_0 is the fractionation factor derived from whole cell degradation experiments in the absence of mass transfer limitations, here referred to as the "enzymatic fractionation factor", a is the specific affinity, K_M is the Michaelis–Menten constant of the enzymatic reaction, c_{bulk} is the bulk substrate concentration, and k_{tr} is the rate constant of the mass transfer flux from the bulk liquid to a single cell. The effective mass transfer flux (J_{eff}; Eq. 3) relates to k_{tr} by Eq. 14,

$$\frac{k_{tr}(n_{cell})}{k_{tr,0}} = \frac{J_{eff}}{J_0} = f(n_{cell}) \quad (14)$$

with $k_{tr}(n_{cell})$ and k_{tr0} being the respective mass transfer coefficients in presence and absence of neighboring cells, and $f(n_{cell})$ is their ratio at n_{cell}.

If a/k_{tr} is known for a given system (e.g., $a/k_{tr}(n_{cell,y}) = 3$ as described for a known cell density ($n_{cell,y} = 5 \times 10^8$cells/mL) by Kampara et al. (2008)), the ratio of a/k_{tr} at any other cell density can be expressed as

$$\frac{a}{k_{tr}(n_{cell})} = \frac{a}{k_{tr}(n_{cell,y}) \times {f(n_{cell})}/{f(n_{cell,y})}} = \frac{a}{k_{tr}(n_{cell,y})} \times \frac{f(n_{cell,y})}{f(n_{cell})} \quad (15)$$

with

$$f(n_{cell}) = 1 - {4}/{3}\pi \times \left(L^3 - r^3 \times \left[4 - 3 \times {r}/{L}\right]\right) \times n_{cell} \quad \text{for scenario1} \quad (16)$$

or

$$f(n_{cell}) = \frac{1}{{4}/{3}\pi \times (L^3 - r^3) \times n_{cell} + 1} \quad \text{for scenario 2} \quad (17)$$

Inserting Eq. 15 into Eq. 13, hence, allows expressing the change of the observable isotope fractionation factor with cell density.

Results

Effect of toluene concentration and cell density on observable isotope fractionation

The effect of cell density (5×10^5 to 5×10^8cells/mL) on D/H-toluene isotope fractionation by strain mt-2(pWWO) at non-growth conditions was studied using initial toluene concentrations of 1, 10, and 100 μM. Observed fractionation factors (α^*) depended both significantly on the cell density and initial toluene concentration (Fig. 2) and were consistently higher than the enzymatic fractionation factors to be observed without any bioavailability restrictions ($\alpha_o = 0.05$ (Kampara et al. 2008)). In general, fractionation decreased with decreasing toluene concentration and/or increasing cell density. At a cell density of 5×10^8 cells/mL, α^* increased from 0.067 ± 0.009 at 100 μM toluene to 0.108 ± 0.007 at 10 μM and 0.178 ± 0.008 at 1 μM. This confirmed earlier observations on the dependency of α^* on substrate concentrations (Kampara et al. 2008). Observed fractionation factors, however, additionally depended on the density of toluene-degrading cells in suspension. At toluene concentrations of 1 μM, the observed fractionation factors increased significantly from $\alpha^* = 0.104 \pm 0.027$ in presence of 5×10^5cells/mL to $\alpha^* = 0.178 \pm 0.008$ ($P < 0.05$) with 5×10^8cells/mL. At 10 μM, the changes in the observed isotope fractionation were less pronounced and varied from $\alpha^* = 0.069 \pm 0.012$ to $\alpha^* = 0.108 \pm 0.007$ ($P < 0.05$) with 5×10^6 and 5×10^8cells/mL, respectively (Fig. 2). At 100 μM toluene, by contrast, no statistically significant influence of the cell density on α^* was found. Figure 3 shows that observed fractionation correlated positively to specific toluene degradation rates as calculated from the initial slopes of degradation curves recorded from the individual experiments at different cell densities. This suggests that observable isotope fractionation is controlled by the substrate flux to a single cell as has been described earlier (Kampara et al. 2008; Thullner et al. 2008).

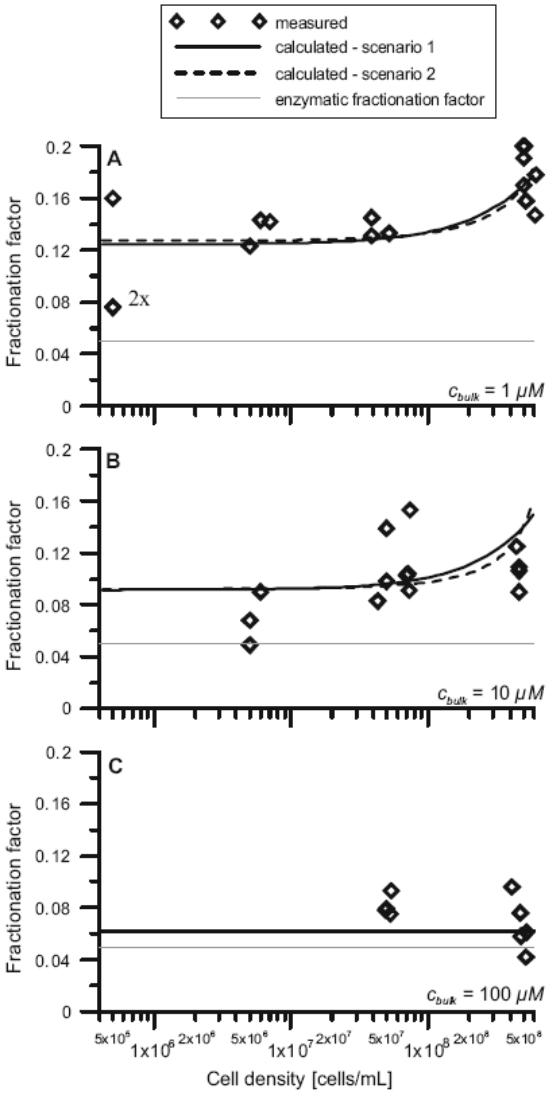

Fig. 2 Impact of cell density of *P. putida* mt-2(pWW0) on observed fractionation (α*) during degradation of toluene at initial bulk concentrations c_{bulk} of approx. 1 µM (**a**), 10 µM (**b**), and 100 µM (**c**). Measured fractionation factors (*symbols*) are compared with estimates calculated using scenario 1 (overlapping boundary layers) and scenario 2 (transient formation of cell clusters). The enzymatic fractionation factor (α_0=0.05; to be observed without any bioavailability restrictions) is shown for comparison as a *grey solid line*

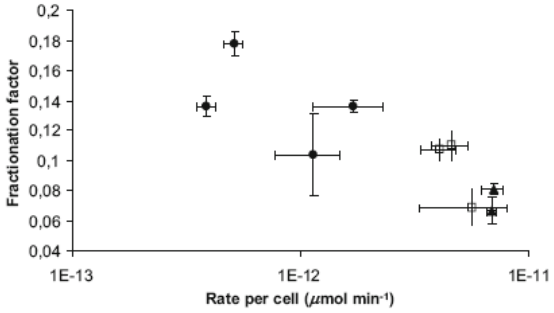

Fig. 3 Influence of calculated single-cell toluene degradation rates of *P. putida* mt-2(pWW0) on observed isotope fractionation factors (α*) at initial bulk concentrations c_{bulk} of 1 µM (*filled circles*), 10 µM (*open squares*), and 100 µM (*filled triangles*). The degradation rates and cell densities are expressed as the arithmetic mean of at least three replicates with error bars showing the 95% confidence interval as derived by the Kruskal–Wallis one–way analysis of variance

Discussion

Effect of cell density on effective toluene fluxes to individual cells

Isotope fractionation factors depended on initial toluene concentration, cell density, and resulting single-cell toluene degradation rates (Figs. 2 and 3). This all suggests that the mass transfer flux to a single cell determines the discrepancy between observable and enzymatic isotope fractionation (Thullner et al. 2008). Figure 4 illustrates the expected effect (based on Eqs. 9 and 11) of cell density on effective toluene mass flux per cell when a cell radius of r = 1 µm and a boundary layer of L = 5 µm are assumed. From Fig. 4, it becomes clear that the increasing presence of neighboring cells affects the mass flux toward individual cells, whereas at a cell density of n_{cell} = 5 × 10^6cells/mL,

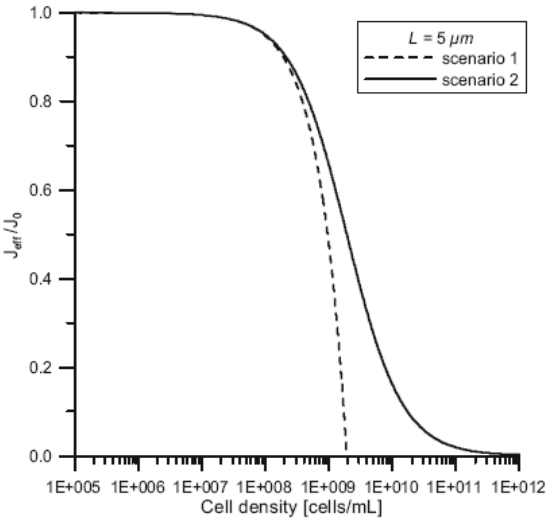

Fig. 4 Calculated effect of cell density on effective substrate mass fluxes towards individual cells assuming a cell radius of r=1 µm and a typical boundary layer of L=5 µm. *Dashed and solid lines* represent effects derived according to scenario 1 (Eq. 9) and 2 (Eq. 11), respectively

J_{eff} is basically equal to J_0; the scenario 1 calculation (Eq. 9) predicts a drop of J_{eff} by about 25% at $n_{cell} = 5 \times 10^8$cells/mL. Please note that estimates based on scenario 1 consider the bacterial cells to be fully dispersed in the medium and thus exclude aggregate and biofilm formation. Interestingly, no major differences to scenario 1 are seen when J_{eff} is calculated based on the assumption of transient formation of cell clusters (option 2; Eq. 11). Here, J_{eff} is again basically unchanged at $n_{cell} = 5 \times 10^6$cells/mL and drops by 21% at $n_{cell} = 5 \times 10^8$cells/mL. It thus supports the assumption that at such cell densities, the close vicinity of the other cells reduces the flux toward a single cell. Note, however, that the scenario 1 calculation does not realistically account for very high cell densities, where it predicts that J_{eff} approaches zero already when $^4/_3\pi \times L^3 \times n_{cell} \rightarrow 1$ (Fig. 4).

Comparison between measured and calculated stable isotope fractionation factors

The clear relationship between fractionation and per cell degradation rate (Fig. 3) suggests that limited mass transfer flux introduces a bias to enzymatic fractionation factors. Since there is no evidence in literature that the biochemical mechanism of bond cleavage (i.e., the isotope sensitive enzymatic step of the reaction) is changing with substrate concentration or cell density, it appears that the slow substrate transfer through the individual cells' diffusion-controlled boundary layers results in an isotopic disequilibrium between the bulk and the immediate vicinity of the intracellular enzyme. The isotope composition of the substrate at the enzyme thus differs from that of the bulk medium. The highest concentration 100 μM is clearly above K_M of strain mt-2 (=7.7 μM) and hence in a range where the degradation rate is not controlled by substrate availability (Kampara et al. 2008). Isotope fractionation at 100 μM consequently was, as expected, also independent of cell density. Figure 2 relates initial toluene concentrations to experimentally determined and predicted fractionation factors (α*) at three cell densities. Predictions of α* using Eq. 13 were based on known K_M = 7.7 μm (Duetz et al. 1998), α_0 = 0.05 (Kampara et al. 2008), r = 1 μm, and a/k_{tr} (5×10^8cells/mL) = 3 as given by Kampara et al. (2008) for a similar system. As a plausibility check, the thickness of the boundary layer was estimated from its influence on α*. δ was fitted separately for the experimental α* results obtained for each of the initial bulk toluene concentrations (Fig. 2) and led to estimates of $\delta = 5.7 - 7.7\ \mu m$ with negligible differences between the two model scenarios only. These values are in accordance with reported thicknesses of the steady state diffusion layers around bacteria in gently stirred systems of ca. 10 μm (van Leeuwen and Köster 2004) and of substrate depleted zones of metabolically active cells (5–10 μm; Boone et al. 1989; Harms and Zehnder 1994).

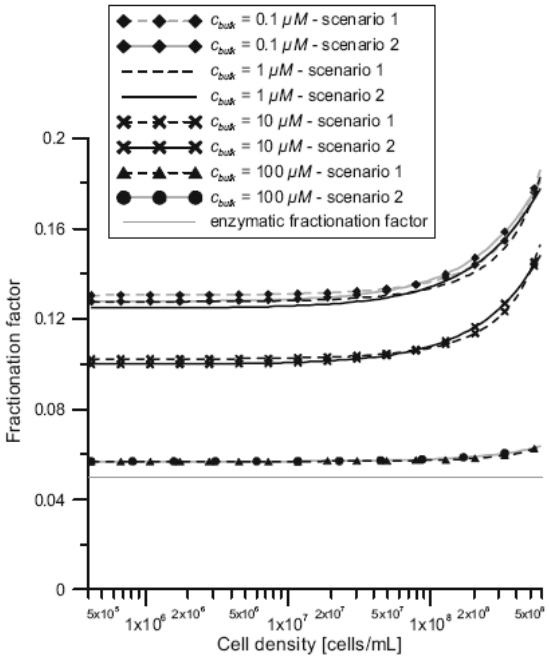

Fig. 5 Predicted changes of the observed stable isotope fractionation factor (α*) at varying bacterial cells densities and initial toluene concentrations c_{bulk} and varying cell densities using values of δ= 5.7 μm (scenario 1) and 6.9 μm (scenario 2) determined at c_{bulk}=1 μM

Implications

Recapitulating Fig. 2, it can be concluded that observed stable isotope fractionation depends not only on the bulk substrate concentration but also on the density of the suspended biomass. In combination, these two factors control the mass transfer of substrate toward a single cell and ultimately the bioavailability of the substrate. Figure 5 relates predicted changes of α* to both bioavailability controlling factors: different bulk concentration of toluene ($c_{bulk} = 0.1 - 100\ \mu M$) and different bacterial cell densities ($n_{cell} = 5 \times 10^5 - 5 \times 10^8$ cells/mL). In addition to the experimental data, these predictions hence underpin the role of mass transfer to a single cell (i.e., the bioavailability of the substrate) to the stable isotope fractionation observed in a system. From Fig. 5, it becomes evident that cell-density-based bioavailability changes should be considered during SIFA-based quantitative analysis of microbial degradation when the bulk concentration is in the range of K_M or below. Our prediction for the influence of biomass on observed stable isotope fractionation is consistent with earlier studies reporting on microbially induced carbon

isotope fractionation shifts during the growth of methane-oxidizing populations (Templeton et al. 2006) and variable isotope fractionation during CO_2 uptake by cyanobacteria (Born et al. 1988; Calder and Parker 1973; Pardue et al. 1976; Staal et al. 2007).

As α^* varies when mass transfer to single cells is restricted, biomass effects need to be accounted for when using SIFA to quantify the extent of in situ biodegradation in complex systems such as subsurface environments. Fast microbial substrate turnover, low substrate bulk concentrations of, e.g., hydrophobic contaminants, and slow substrate diffusion from sorbed or non-aqueous phase-bound chemicals to the water phase or biomass hotspots may govern substrate bioavailability and hence influence observed isotope fractionation. Our findings further suggest that initial conditions of $c_{bulk} >> K_M$ and moderately dense cell suspension should be used when estimating enzymatic fractionation factors (α_o) in the laboratory. Due to its analytical simplicity and its relative sensitivity, our results further suggest that, for well-characterized systems, deviations of observed from known laboratory derived fractionation factors can be used to determine the bioavailability of a compound to single catabolically active microorganisms. This may open new avenues for SIFA applications in environmental diagnostics and biotechnology, where it, e.g., may allow for a quantitative consideration of the role of the bioavailability for the uptake and transformation of hydrophobic substrates at the single-cell level in two-phase partitioning bioreactors.

Acknowledgments This study was supported by the European MEST-CT-2004-8332 grant (AXIOM) and the Helmholtz Association grant VG-NG-338 (Great MoDE). Skilled technical help by Birgit Würz, Jana Reichenbach and Rita Remer is greatly acknowledged. This work contributed to the SAFIRA II Research Programme.

References

Boone DR, Johnson RL, Liu Y (1989) Diffusion of the interspecies electron carriers H2 and formate in methanogenic ecosystems and its implications in the measurement of Km for H2 or formate uptake. Appl Environ Microbiol 55:1735–1741

Born M, Dorr H, Levin I, Munnich KO (1988) Methane concentration in aerated soils in West-Germany. Chem Geol 70:101–101

Bosma TNP, Middeldorp PJM, Schraa G, Zehnder AJB (1997) Mass transfer limitation of biotransformation: quantifying bioavailability. Environ Sci Technol 31:248–252

Braunlich M, Aballanin O, Marik T, Jockel P, Brenninkmeijer CAM, Chappellaz J, Barnola JM, Mulvaney R, Sturges WT (2001) Changes in the global atmospheric methane budget over the last decades inferred from 13C and D isotopic analysis of Antarctic firn air. J Geophys Res Atmos 106:20465–20481

Calder JA, Parker PL (1973) Geochemical implications of induced changes in C-13 Fractionation by blue-green algae. Geochim Cosmochim Acta 37:133–140

Chartrand MMG, Waller A, Mattes TE, Elsner M, Lacrampe-Couloume G, Gossett JM, Edwards EA, Sherwood Lollar B (2005) Carbon isotopic fractionation during aerobic vinyl chloride degradation. Environ Sci Technol 39:1064–1070

Cichocka D, Siegert M, Imfeld G, Andert J, Beck K, Diekert G, Richnow HH, Nijenhuis I (2007) Factors controlling the carbon isotope fractionation of tetra- and trichloroethene during reductiove dechlorination by Sulfurospirillum ssp. and Desulfitobacterium sp. strain PCE-S. FEMS Microbiol Ecol 62:98–107

Duetz WA, Wind B, van Andel JG, Barnes MR, Williams PA, Rutgers M (1998) Biodegradation kinetics of toluene, m-xylene, p-xylene and their intermediates through the upper TOL pathway in Pseudomonas putida (pWW0). Microbiol SGM 144:1669–1675

Elsner M, Zwank L, Hunkeler D, Schwarzenbach RP (2005) A new concept linking observable stable isotope fractionation to transformation pathways of organic pollutants. Environ Sci Technol 39:6896–6916

Griebler C, Safinowski M, Vieth A, Richnow HH, Meckenstock RU (2004) Combined application of stable carbon isotope analysis and specific metabolites determination for assessing in situ degradation of aromatic hydrocarbons in a tar oil-contaminated aquifer. Environ Sci Technol 38:617–631

Gupta M, Tyler S, Cicerone R (1996) Modeling atmospheric delta (CH4)-13C and the causes of recent changes in atmospheric CH4 amounts. J Geophys Res-Atmos 101:22923–22932

Harms H, Zehnder AJB (1994) Influence of substrate diffusion on degradation of dibenzofuran and 3-chlorodibenzofuran by attached and suspended bacteria. Appl Environ Microbiol 60:2736–2745

Hunkeler D, Anderson N, Aravena R, Bernasconi SM, Butler BJ (2001) Hydrogen and carbon isotope fractionation during aerobic biodegradation of benzene. Environ Sci Technol 35:3462–3467

Kampara M, Thullner M, Harms H, Wick LY (2008) Impact of bioavailability restrictions on microbially induced stable isotope fractionation: 2. Experimental evidence. Environ Sci Technol 42:6552–6558

Mancini SA, Hirschorn SK, Elsner M, Lacrampe-Couloume G, Sleep BE, Edwards EA, Sherwood Lollar B (2006) Effects of trace element concentration on enzyme controlled stable isotope fractionation during aerobic biodegradation of toluene. Environ Sci Technol 40:7675–7681

March JG, Pringle CM (2003) Food web structure and basal resource utilization along a tropical island stream continuum, Puerto Rico. Biotropica 35:84–93

Mariotti A, Germon JC, Hubert P, Kaiser P, Letolle R, Tardieux A, Tardieux P (1981) Experimental determination of nitrogen kinetic isotope fractionation—some principles—illustration for the denitrification and nitrification processes. Plant Soil 62:413–430

Meckenstock RU, Morasch B, Griebler C, Richnow HH (2004) Stable isotope fractionation analysis as a tool to monitor biodegradation in contaminated acquifers. J Contam Hydrol 75:215–255

Morasch B, Richnow HH, Schink B, Meckenstock RU (2001) Stable hydrogen and carbon isotope fractionation during microbial toluene degradation: mechanistic and environmental aspects. Appl Environ Microbiol 67:4842–4849

Nijenhuis I, Andert J, Beck K, Kastner M, Diekert G, Richnow HH (2005) Stable isotope fractionation of tetrachloroethene during reductive dechlorination by Sulfurospirillum multivorans and Desulfitobacterium sp strain PCE-S and abiotic reactions with cyanocobalamin. Appl Environ Microbiol 71:3413–3419

Northrop DB (1981) The Expression of isotope effects on enzyme-catalyzed reactions. Annu Rev Biochem 50:103–131

O'Leary MH (1980) Carbon isotope fractionation in plants. Phytochem 20:553–567

Pardue JW, Scalan RS, Vanbaalen C, Parker PL (1976) Maximum carbon isotope fractionation in photosynthesis by blue-green algae and a green algae. Geochim Cosmochim Acta 40:309–312

Park R, Epstein S (1960) Carbon isotope fractionation during photosynthesis. Geochim Cosmochim Ac 21:110–126

Rayleigh JSW (1896) Theoretical considerations respecting the separation of gases by diffusion and similar processes. Philos Mag 42:493–498

Schmidt TC, Zwank L, Elsner M, Berg M, Meckenstock RU, Haderlein SB (2004) Compound-specific stable isotope analysis of organic contaminants in natural environments: a critical review of the state of the art, prospects, and future challenges. Anal Bioanal Chem 378:283–300

Shaw JP, Harayama S (1992) Purification and characterization of the NADH-acceptor reductase component of xylene monooxygenase encoded by the TOL plasmid pWW0 of Pseudomonas putida mt2. Eur J Biochem 209:51–61

Staal M, Thar R, Kuhl M, van Loosdrecht MCM, Wolf G, de Brouwer JFC, Rijstenbil JW (2007) Different carbon isotope fractionation patterns during the development of phototrophic freshwater and marine biofilms. Biogeosci 4:613–626

Templeton AS, Chu KH, Alvarez-Cohen L, Conrad ME (2006) Variable carbon isotope fractionation expressed by aerobic CH4-oxidizing bacteria. Geochim Cosmochim Acta 70:1739–1752

Thullner M, Kampara M, Harms H, Wick LY (2008) Impact of bioavailability restrictions on microbially induced stable isotope fractionation: 1. Theoretical calculations. Environ Sci Technol 42:6544–6551

Tyler SC, Crill PM, Brailsford GW (1994) 13C/12C fractionation of methane during oxidation in a temperate forested soil. Geochim Cosmochim Acta 58:1625–1633

van Leeuwen HP, Köster W (2004) Physicochemical kinetics and transport at biointerfaces: setting the stage. In: van Leeuwen HP, Koester W (eds) Physicochemical kinetics and transport at chemical-biological interphases. IUPAC series in analytical and physical chemistry of environmental systems. Wiley, Chichester, pp 401–444

Whiticar MJ (1990) A geochemical perspective of natural gas and atmospheric methane. Org Geochem 16:531–547

Correlation between bioavailability and stable isotope fractionation in column and two-liquid-phase systems

Abstract

In the context of contaminant biodegradation, isotope fractionation is often implicitly assumed to be independent of the availability of the contaminant. It is known, however, that slow mass transfer processes preceding the fractionating bond cleavage may decrease the observed isotope fractionation. Biodegradation of hydrophobic organic contaminants in the environment is often controlled by the availability of the contaminant rather than the maximal capacity of the biochemical degradation process. Earlier studies in laboratory batch systems have shown that the observed fractionation is determined by the substrate flux to a single cell. In a contaminated aquifer, additional factors contribute to the restricted bioavailability of contaminants for degrading cells. First, cells in the aquifer tend to stay attached on solid surfaces, which reduces the substrate uptake. Second, contaminants may be partitioned in a non-aqueous phase liquid (NAPL) phase from which they need to dissolve to the aqueous phase in order to be degraded. Here, the effect of these two phenomena on the observed isotope fractionation was studied separately in well defined laboratory systems. Isotope fractionation by attached cells was studied in a column system with *Pseudomonas putida* mt-2(pWW0) immobilized on sea sand. A toluene solution was pumped through and isotope fractionation factors were derived from the inflow and outflow concentrations. Both bioavailability and stable isotope fractionation seemed to increase with flow rate. In a two-liquid-phase system consisting of an aqueous phase containing toluene degrader *P. putida* mt-2(pWW0) and a NAPL phase spiked with toluene, isotope fractionation was determined at different cell densities and NAPL-water contact surfaces. The reduction of the observed fractionation at high cell densities was clearly stronger than in previous experiments without a

NAPL phase. The results presented here underline the importance of mass transfer restrictions when using stable isotope fractionation analysis and support the possible use of stable isotope fractionation for the assessment of bioavailability.

Introduction

Quantification of pollutant biodegradation in groundwater by stable isotope fractionation relies on constant fractionation factors that do not depend on physical and/or chemical changes in the heterogeneous aquifer. It is known, however, that the enzymatic fractionation that is indeed constant can only be observed when the fractionating bond cleavage is the rate limiting step of the overall degradation process. When a mass transfer process prior to the fractionating reaction step is rate limiting, a reduced fractionation is observed [2]. In the subsurface, degradation of hydrophobic organic contaminants is mostly controlled by the availability of the contaminant rather than the degradation capacity of the microorganisms [8]. Previous studies have shown that bioavailability restrictions due to low substrate concentrations and/or high cell densities in well mixed homogeneous batch systems may lead to reduced observed fractionation [3, 4, 57]. An additional factor decreasing the contaminant bioavailability for cells in an aquifer as opposed to a mixed batch system is their tendency to stay attached to surfaces. The advective groundwater flow provides the immobilized cells with nutrients. Previous studies have shown that attached cells in a flow through system are more likely subject to bioavailability limitations than suspended cells due to the more likely interference with neighboring cells and the smaller shell plane of the diffusive boundary layer (see below) [73]. As discussed in Chapter 2 and section 3.1, suspended cells in a mixed batch system are surrounded by a diffusive boundary layer (DBL), created by viscous forces, which cause the water film to stick to the solid surface [9]. In systems with laminar flow, the "diffusive boundary layer" concept may also be used to describe the diffusive transport of solutes. The thickness of the diffusive boundary layer depends on the geometry and the flow

velocity in the system. A fast flow reduces the thickness of the layer and as a consequence steepens the concentration gradient and increases the diffusive substrate flux to the cells [73].

In the subsurface, the availability of contaminants may also be restricted by the partitioning of the contaminant in a non-aqueous phase liquid (NAPL) phase, the reduction of the observed isotope fractionation may be even more pronounced. Many contaminated soils and groundwater sites contain NAPLs originating from e.g. dry cleaning fluids, fuel oil and gasoline. NAPLs are particularly hard to remove from the water, and besides their own hazardousness, complex NAPLs also serve as a reservoir for poorly water soluble organic contaminants. Since bacteria are believed to exclusively take up molecules dissolved in water, contaminants partitioned in the NAPL phase are not directly available for degradation by microorganisms. If the transfer from NAPL phase to water is slow, it may constitute the rate limiting step for degradation.

The aim of the experiments presented here was to separately investigate the effects of bacterial attachment and the presence of a NAPL phase on the observed isotope fractionation under well defined laboratory conditions and, furthermore, to see if stable isotope fractionation could be used to assess the bioavailability conditions in different systems. The column experiments were performed in a model laboratory column system with *Pseudomonas putida* mt-2(pWW0) immobilized on either sand or glass bead packing. A toluene solution was pumped through the column, and hydrogen isotope fractionation factors were derived from the inflow and outflow concentrations. Bioavailability was varied by changing either the inflow concentration or the flow rate. Columns with killed cells were used as controls for toluene losses not due to degradation.

The model laboratory two-liquid-phase system consisted of 2,2,4,4,6,8,8-heptamethylnonane (HMN) as NAPL phase spiked with toluene and an aqueous phase, where the toluene degrading strain *Pseudomonas putida* mt-2 p(WW0) was present. Different mass transfer fluxes were obtained by using two different NAPL-water contact areas. Experiments with each contact area were also performed at different cell densities.

Material and methods

Organism and culture conditions

The organism *Pseudomonas putida* mt-2(pWW0) and the culture conditions, as well as harvesting and washing of the cells, are described in sections 2.2 and 3.1.

Column experiments

The transformation of toluene by strain mt-2 was studied in glass columns (length=10 cm, radius=0.5 cm) equipped with porous glass frits at the lower ends. The experiments were performed at room temperature (20°C). The setup is shown in Figure 3.2. Columns were wet-packed with sea sand (0.1-0.3 mm) or glass beads (0.25-0.50 mm), washed with phosphate buffered saline (PBS) and baked at 450˚C for five hours, prior to use. Four columns were operated in parallel in a down flow mode with a peristaltic pump and Tygon® tubings. The buffer saturated columns were percolated with PBS for at least 15 h, before cells were loaded by replacing the influent with cell suspensions in PBS (OD 0.1 – 0.4). The columns were loaded to saturation, two with living cells and two with cells killed with 20 mM $HgCl_2$. After loading to the desired density of attached cells had been achieved, the columns were rinsed with PBS to wash out planktonic and loosely attached cells. The optical densities at the inflow and the outflow were measured over time, during both loading and rinsing, so that the number of cells attached to the column could be calculated. A typical loading curve can be seen in Figure 3.3. The number of cells attached varied between approximately 1×10^8 and 2×10^9

cells. There was assumed to be no cell growth in the columns, since the PBS buffer lacked essential nutrients. In order to minimize substrate losses due to sorption or degradation in the tubing, the tubings were replaced by Teflon® tubings for pumping the toluene solution, except for approximately 20 cm Tygon tubing, necessary for peristaltic pumping. The Teflon® tubings were presaturated by flushing with 1 L of the same toluene solution used in the experiment. A 1:1 mixture (v/v) of toluene-h8 (99.9%, Merck KGaA (Germany)) and per-deuterated toluene-d8 (99.6 atom % D; Sigma-Aldrich Chemie (Germany)) was pumped through the columns. In different experiments, flow rates were varied between 0.3 and 8 mL min^{-1}. The toluene solution reservoir was closed tight with a screw cap with septum. The presaturated Teflon tubing was stuck through the septum and attached to the column inlet using a piece of silicon tubing. At the outlet, each column was connected to a ca. 4 cm long piece of Teflon tubing, which was stuck through the septum into a closed 10 mL GC vial. From this vial, samples of 2 mL liquid were taken through the air-tight septa using air-tight syringes (Gastight® model 1002, Hamilton Co. Reno, Nevada). Through a separate tubing, the toluene solution from the reservoir was pumped directly to a vial. Samples taken from this vial represented the inflow concentration for the columns. The samples were transferred to 10-mL autosampler vials, containing 20 µl of concentrated H_2SO_4 to inhibit further biodegradation. The vials were closed immediately air-tight with Teflon-coated butyl rubber septa. The duration of the experiments ranged from 5 to 30 min, depending on the flow rate. The concentrations of the two toluene species were analyzed using headspace gas chromatography, as described in sections 2.2 and 3.1.

Determination of fractionation factors. Fractionation factors were determined using the Rayleigh equation (see Chapter 2)

$$\alpha = 1 + \frac{\ln\left(R_t / R_0\right)}{\ln\left[\left(c_t / c_0\right) \times \left((R_0 + 1) / (R_t + 1)\right)\right]}$$

α is the fractionation factor, R_t and R_0 are the substrate isotope ratios at the outflow during steady state and at the inflow, respectively, and c_t and c_0 are the total substrate concentrations in these samples.

Experiments in the two-liquid-phase system

Abiotic mass transfer experiments. Experiments were performed at room temperature (20°C) in tightly closed, three necked, 1-L glass bottles equipped with a vertical glass tube inside (Fig. 3.4). The bottles were filled with 500 mL PBS buffer. The HMN, spiked with a 1:1 mixture (v/v) of toluene and per-deuterated toluene-d8 to a total concentration of 1 mM, was added to cover the surface of the PBS, either inside the glass tube to a surface area of 3.8 cm^2 or outside it to a surface area of 59.8 cm^2. A larger contact surface area enables a faster toluene mass transfer from the HMN to the PBS. The HMN did not mix with the aqueous phase, and only a minor fraction of the toluene partitioned in the air phase. The system was kept on a magnetic stirrer at 300 rpm throughout the experiment. Toluene concentrations from the aqueous phase were analyzed, as described in sections 2.2 and 3.1. The equilibrium concentrations (c_{eq}) for toluene with the two different contact areas were graphically estimated from the plateaus reached. The HMN to water mass transfer coefficients (k) were determined graphically by plotting time (t) vs. the initial concentration change ln ((c_{eq} - $c(t)$) / c_{eq}). k was obtained from the slope.

Biodegradation experiments. The setup was prepared as described above for abiotic experiments. The washed cell suspension (see section 3.1) was added after the system had

reached equilibrium, and the concentrations of the two toluene species were analyzed in the aqueous phase during degradation.

Determination of fractionation factors. The isotope fractionation factor (α) for microbial degradation reactions is generally defined as

$$\alpha = \frac{{}^{D}r / {}^{D}c}{{}^{H}r / {}^{H}c} \tag{2}$$

where r denotes degradation rates and c aqueous concentration of non-deuterated toluene and toluene-d8, indicated by superscripts H and D, respectively. At steady state conditions, r is equal to the transfer flux of toluene from oil to water (q), thus ${}^{D}q = {}^{D}r$ and ${}^{H}q = {}^{H}r$. Equation (2) becomes:

$$\alpha = \frac{{}^{D}q / {}^{D}c}{{}^{H}q / {}^{H}c} \tag{3}$$

q for deuterated and nondeuterated toluene can be defined as

$${}^{D}q = k({}^{D}c_{eq} - {}^{D}c) \tag{4}$$

$${}^{H}q = k({}^{H}c_{eq} - {}^{H}c) \tag{5}$$

where k is the mass transfer coefficient for the transfer from NAPL to water (assumed to be the same for both isotope fractions as no fractionation was observed in the abiotic experiments), c_{eq} is the equilibrium concentration in the aqueous phase before the addition of bacteria and c is the steady state aqueous concentration during degradation. Inserting expressions (4) and (5) into equation (3) gives the expression for α used in this study:

$$\alpha = \frac{{}^{H}c}{{}^{D}c} \times \frac{{}^{D}c_{eq} - {}^{D}c}{{}^{H}c_{eq} - {}^{H}c} \tag{6}$$

Errors of the different parameters were combined to a total error of α, using common rules of error propagation.

Calculation of the toluene mass transfer to the cells. The flux of toluene from NAPL to aqueous phase (q) is driven by the concentration difference between the aqueous steady state concentration (c_{ss}) and the equilibrium concentration (c_{eq}) (from abiotic experiments). This concentration difference together with the NAPL to water mass transfer coefficient (k) (from abiotic experiments) determines the flux.

$$q = k(c_{eq} - c_{ss}) \quad (7)$$

The obtained flux (q) for the system was divided by the number of cells for each experiment, in order to infer the degradation rate for a single cell.

Results and discussion

Toluene mass transfer and isotope fractionation in the column system

Firgure 3.5 shows a typical result of the column degradation experiments. Toluene is known to accumulate in biological membranes [74], which is probably the reason for the retarded toluene breakthrough in the columns with killed cells. After 18 minutes the system was apparently saturated with toluene and a steady state was reached. Only the steady state data was used for the calculation of fractionation factors. Preliminary experiments at slow flow rates (0.3 to 1 mL min^{-1}) with glass bead packing did not show any clear effect of inflow concentration or flow rate on the degradation rate or the isotope fractionation. Large variations in the fractionation factors and small number of replicates make interpretation of the data uncertain. At flow rates above 2 mL min^{-1}, bacteria did not attach well to glass beads, and sea sand was used instead. Between 2 and 8 mL min^{-1} the fractionation factor seemed to decrease (i.e. observed fractionation increased) at high flow rates, but the quality of the data does not allow conclusive interpretation (Fig. 3.6). At flow rates as high as 6 and 8 mL min^{-1}, the calculated fractionation factors became lower than in the nonlimited batch systems, in

some cases even indicating inverse fractionation. This is probably due to too little change in the toluene concentration leading to $c_t/c_0 \approx 1$ and a negative fractionation factor. The supposed increase in fractionation seemed to be accompanied by increasing degradation rates for a single cell, as would be expected (Fig. 3.6). Increased biodegradation rate at higher flow rates have also been observed in previous studies with saturated columns [75]. Single cell degradation rates in the columns (25 μM toluene) were approximately ten times smaller than in batch experiments (10 μM toluene). The bioavailability in the columns thus seems to be more limited than in a batch system, as expected. Fractionation factors determined in the column experiments were, however, relatively low at all flow rates and did not significantly differ from the ones determined in batch systems. The column system may not be directly comparable with the batch due to the different physical conditions. The toluene concentration in the columns was clearly above K_M, and although the amount of cells was high, only a limited number of cells is competing for the substrate at each location. The reduced degradation rates would, nevertheless, indicate a bioavailability limitation. Reduced degradation rates without reduction in observed isotope fractionation could be observed if only part of the cells would contribute to the degradation. However, further studies are needed to investigate the possible reasons for this, before final conclusions can be drawn. Running more parallel experiments could improve the quality of the data, since it is impossible to exactly reproduce a single column experiment. Possible experimental problems include differences in the amount and distribution of biomass and its imprecise quantification, physiological changes of the cells and clogging of pores. Some of these factors may also change, when varying the flow rate. These changes are difficult to detect and complicate the interpretation of observed effects. For mimicking aquifer systems, flow rates should anyhow be kept below 0.5 mL min^{-1}, which might also facilitate the practical execution of the experiments. Also, an improved method for the determination of fractionation factors should be developed. Finally, the results of the column experiments do not contradict the hypothesis

of higher flow rates leading to higher observed fractionation due to increased bioavailability. The discrepancy between the observed fractionation in column and batch experiments may be due to the different physical conditions in the column system, leading to heterogeneities in the distribution and degradation activity of the attached bacteria. Further studies are needed to clarify this and to confirm the correlation between bioavailability and observed isotope fractionation in column systems.

Toluene mass transfer and isotope fractionation in the two-liquid-phase system

Equilibrium concentrations and mass transfer coefficients for toluene were first determined in the two-liquid-phase system without bacteria. With the larger contact area (59.8 cm^2) the system reached its equilibrium concentration of 2.1 μM of total toluene within six hours, whereas with the smaller contact area (3.8 cm^2) the equilibrium concentration of 1.4 μM was reached within 30 hours. The approach to equilibrium for the larger area is shown in Figure 3.7. The difference in equilibrium concentrations is due to different volumes of the HMN toluene mixture. The mass transfer coefficients for the small and large area respectively were 0.321 L h^{-1} and 0.107 L h^{-1}. No significant fractionation during phase transfer was observed in these abiotic systems.

A typical result obtained from degradation experiments is shown in Figure 3.8. The aqueous toluene concentration first decreased until a steady state was reached. A substantial isotope fractionation was observed during degradation. As shown in section 3.1., the restricted bioavailability at high cell densities was accompanied by decreased observed fractionation, i.e. higher fractionation factors (Fig. 3.9). The fractionation factor obtained from the two-liquid-phase experiments increased from 0.060 in presence of 1×10^7 cells mL^{-1} to 0.114 in presence of 6×10^7 cells mL^{-1} and to 0.263 with 5×10^8 cells mL^{-1}. The effect was more pronounced than in the batch experiments without NAPL phase, where an increase of 20%

was found between 5×10^7 and 5×10^8 cells mL^{-1} (section 3.1). There was no difference in fractionation between the two different mass transfer areas at cell densities of 1×10^7 mL^{-1} and 6×10^7 mL^{-1}. With 1×10^8 cells mL^{-1} observed fractionation was lower for the small area. Even higher cell densities should be tested to confirm the trend. However, at cell densities above 1×10^8 cells mL^{-1}, an increase in the aqueous toluene concentration was observed before a clear steady state could be defined, and no fractionation factors could be calculated. This increase is probably due to a reduction of degradation activity, the cause of which still remains unclear. The substrate flux to a single cell was, however, lower with the small area, at all cell densities (Fig. 3.10). Possibly the difference in substrate flux was not large enough to have an effect on the isotope fractionation at low cell densities. Nevertheless, a clear correlation, between fractionation factors and mass transfer fluxes to a single cell, was obtained, independent of the different mass transfer areas (Fig. 3.11). These results confirm the effect of cell density shown in section 3.1 and demonstrate the additional impact of the mass transfer from NAPL to the aqueous phase (cf. Fig. 2 in section 3.1 and Fig. 3.10). The observed additional mass transfer limitation could also be seen by comparing the calculated mass transfer rate with maximal Michaelis-Menten degradation rate at steady state concentrations. Consequently, the experiments in the two-liquid-phase system again support the use of isotope fractionation for the assessment of bioavailability.

The overall mass transfer limitation affecting the toluene degradation and the observed isotope fractionation in the two-liquid-phase system is a combination of the mass transfer from NAPL to aqueous phase and the mass transfer to the cell within the aqueous phase. The bioavailability limitation caused by the NAPL to aqueous phase transfer could be estimated from the relation between the potential Michaelis-Menten degradation rates at equilibrium and at the actual steady state concentrations. The limitation within the water phase is given by the potential steady state Michaelis-Menten degradation rate relative to the actual mass transfer

flux (Eq. 7), i.e. the effective bioavailability as described in Chapter 2 [4]. Note that at steady state this mass transfer flux equals the actual degradation rate. Calculations of these two ratios showed that the limitation due to the mass transfer from NAPL to aqueous phase was dominating in most cases. At high cell density and larger contact area, the mass transfer in the aqueous phase became more important, as would be expected. In the environment, where cell densities are generally lower, the mass transfer from a NAPL phase to the water would most likely be dominating.

FIGURES

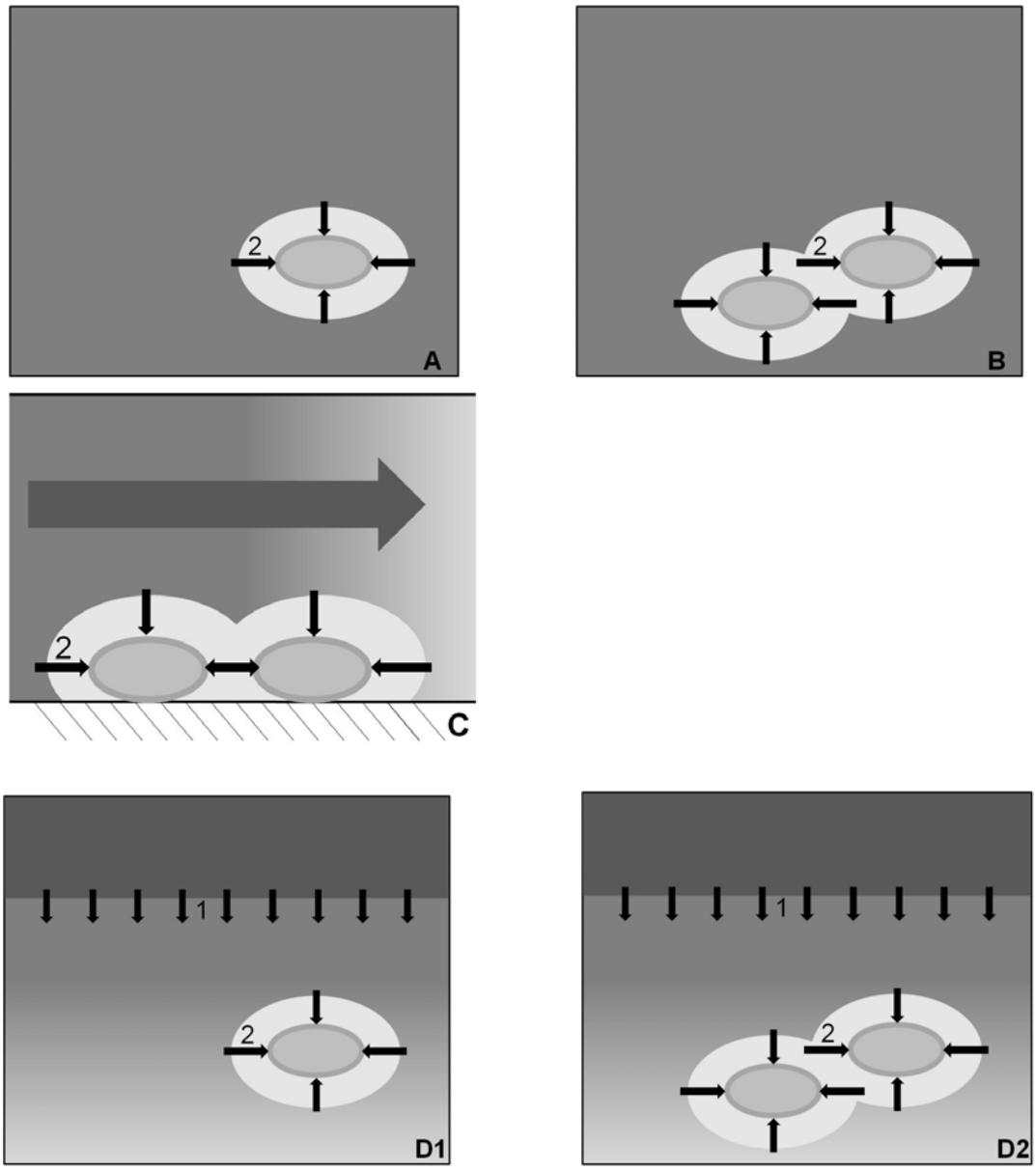

Figure 3.1. Schematic representation of the experiments. Fluxes 1 and 2 refer to the mass transfer processes listed in chapter one, i.e. 1 is the dissolution of the substrate into the water phase and 2 is the mass transfer from the bulk to the cell surface. In experiments A-C the diffusion from the bulk liquid to the cell, through the unstirred boundary layer (2) was varied by changing the substrate concentration (A), the cell density (B) or the flow rate (C). In experiment D the transfer from another phase to water (1) was included and combined with the effect of cell density (D2).

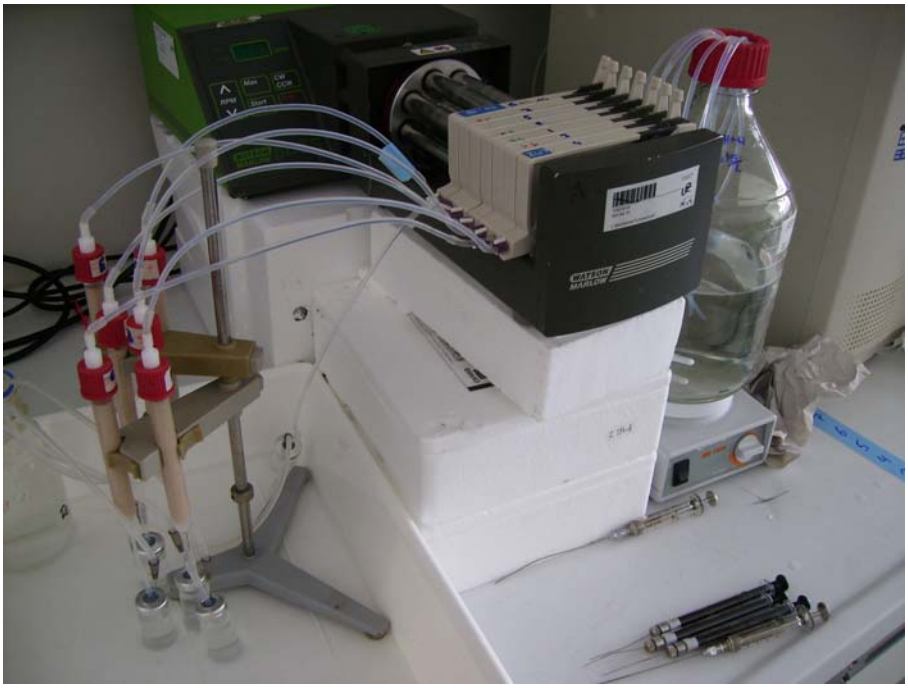

Figure 3.2. Setup for column experiments. The toluene solution was pumped from the reservoir (right) to the columns (left) connected to collector vials (lower left corner) from which samples were taken.

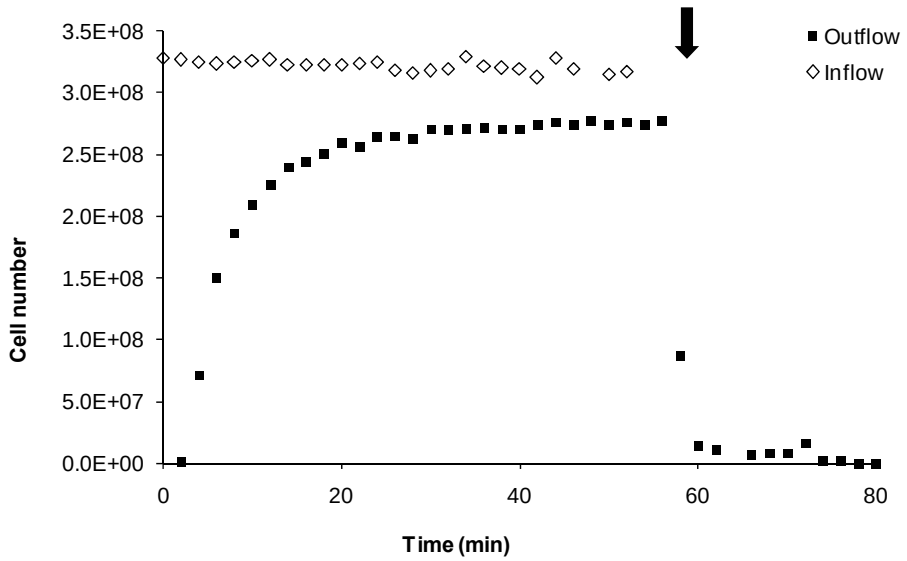

Figure 3.3. Typical breakthrough of bacteria in the column, showing cell numbers at the inflow and at the outflow. At 54 min (arrow) the cell suspension at the inflow was replaced by PBS buffer in order to flush out loosely attached cells.

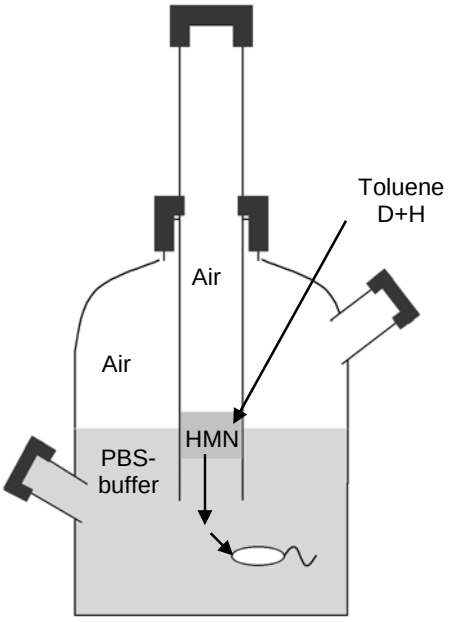

Figure 3.4. Setup for two-liquid-phase experiments.

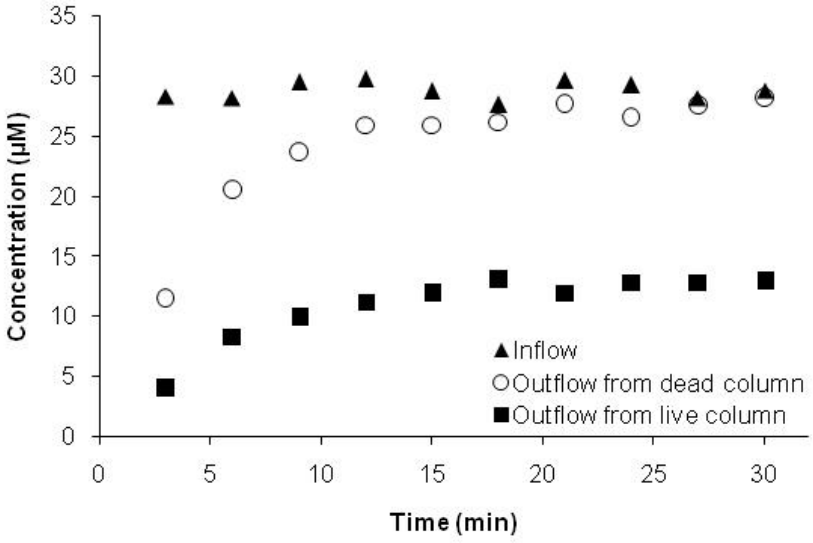

Figure 3.5. Typical result of column degradation experiments (flow rate 2 mL min^{-1}, retention time 1.6 min), representing the toluene concentrations at the inflow and at the outflow of columns with killed cells and live cells. For this experiment the concentration data from 18 min on was used for calculating the fractionation factor.

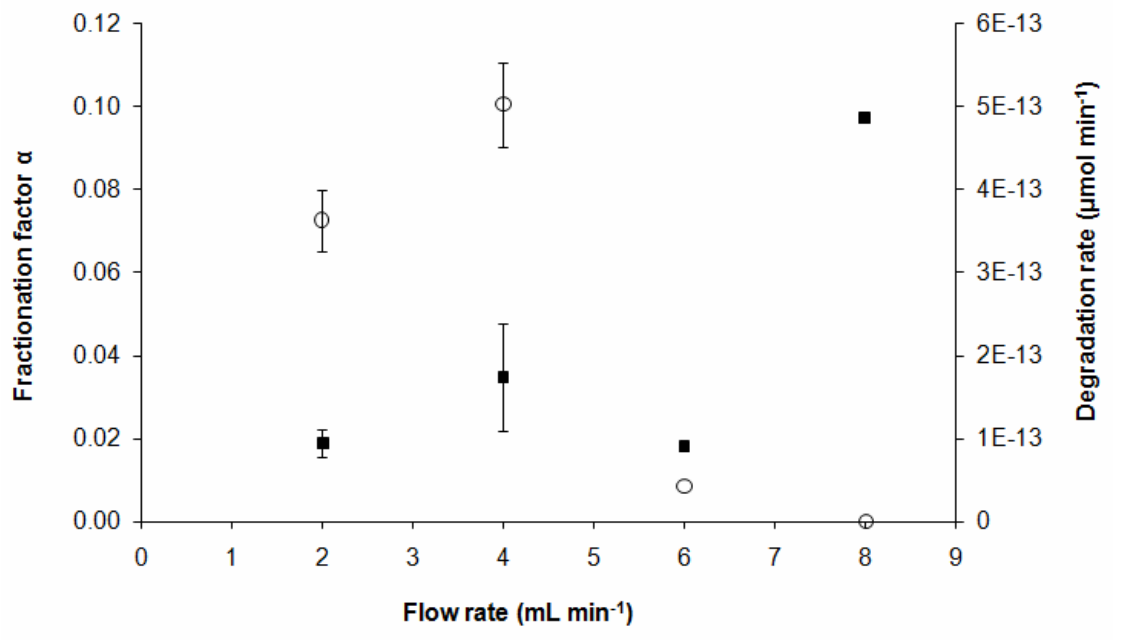

Figure 3.6. Fractionation factors (circles) and degradation rates for a single cell (squares) in function of flow rate. Error bars represent the 95% confidence interval for three or more experiments. No error bars are shown for experiments with less than three replicates.

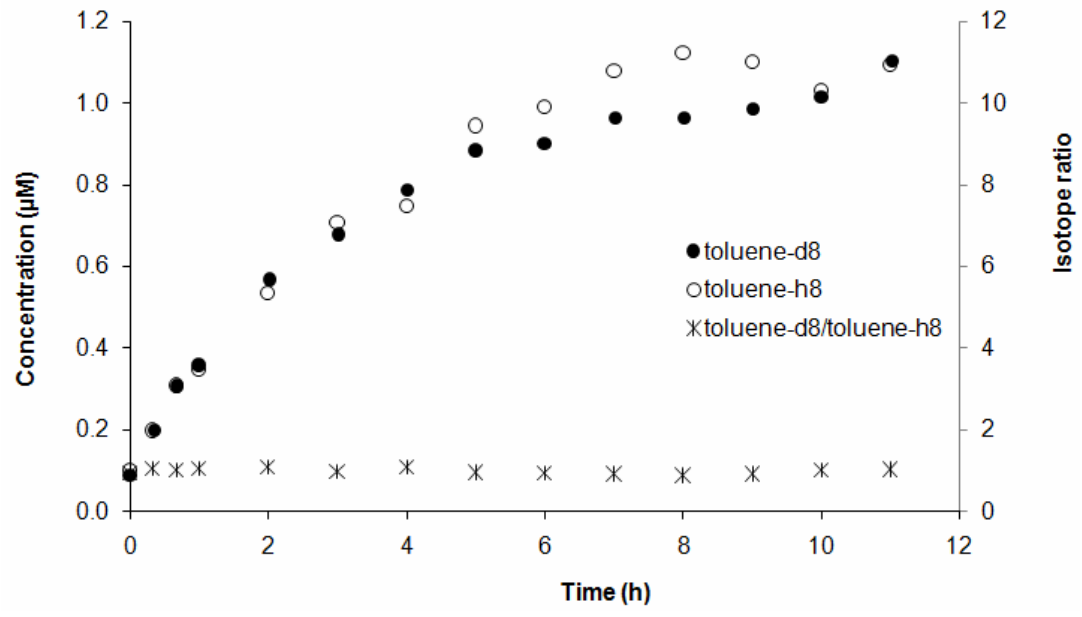

Figure 3.7. Equilibrium curve from the abiotic experiment in the two-liquid-phase system, with the large contact area. The phase transfer did not cause significant fractionation.

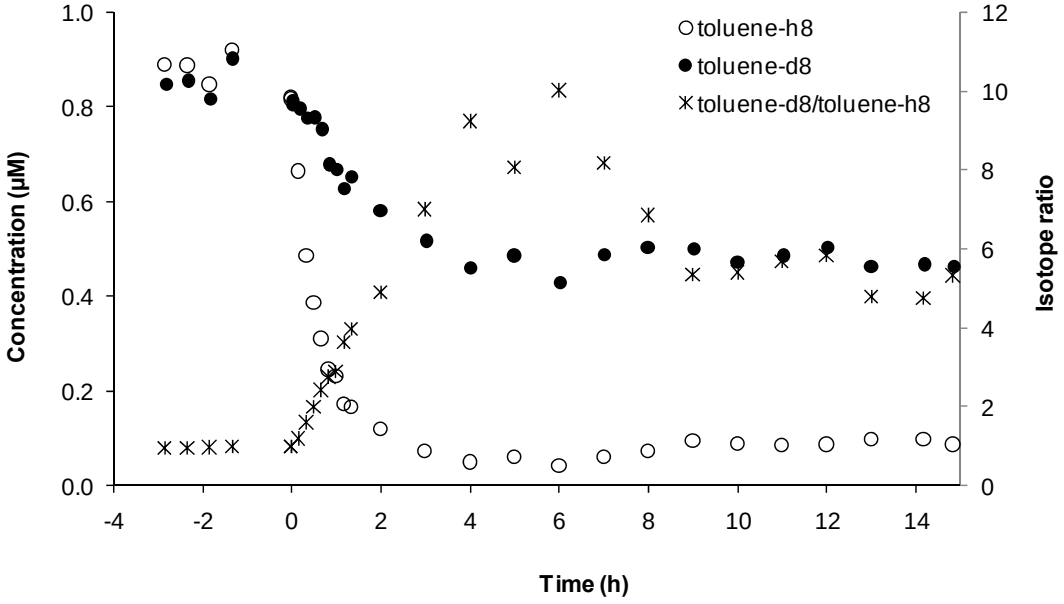

Figure 3.8. Typical degradation experiment in the multiphase system with 10^7 cells per mL^{-1}. The cell suspension was added at time zero.

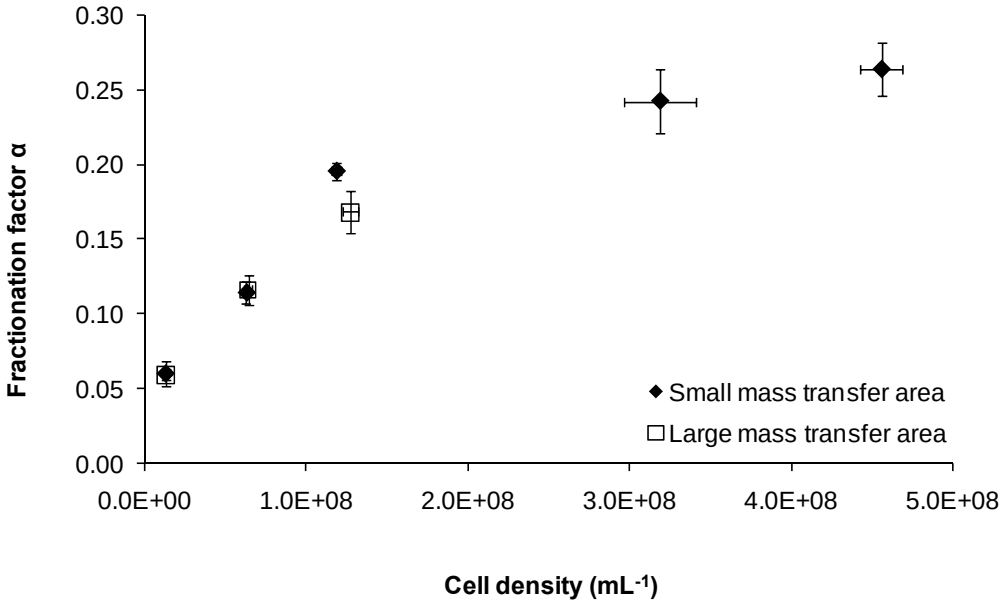

Figure 3.9. Correlation between cell density and fractionation factors. A difference between the two areas was only seen at the higher cell density. Error bars represent the 95% confidence interval for three or more experiments.

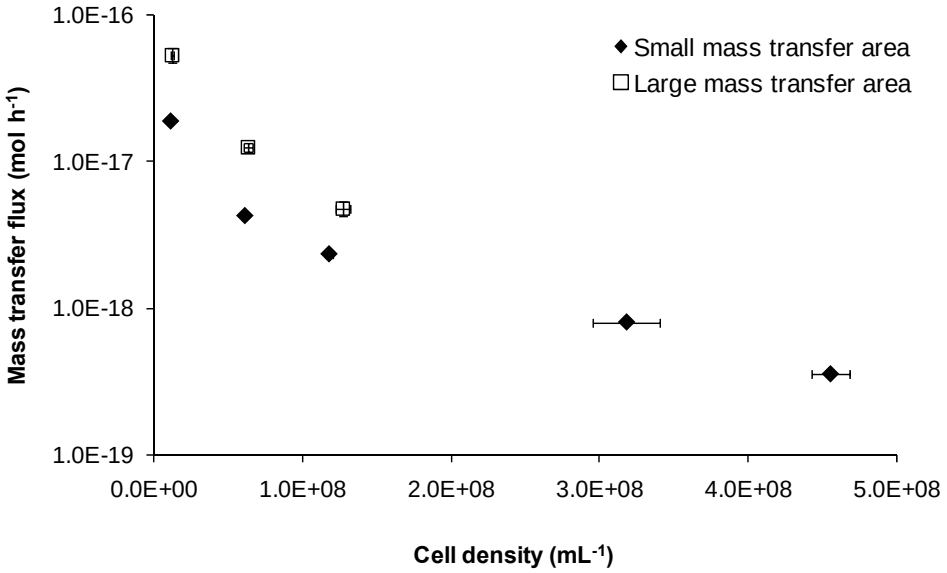

Figure 3.10. The substrate flux to a single cell decreases with increasing cell density. The flux is higher with the larger NAPL water contact area at all cell densities. Error bars represent the 95% confidence interval for three or more experiments.

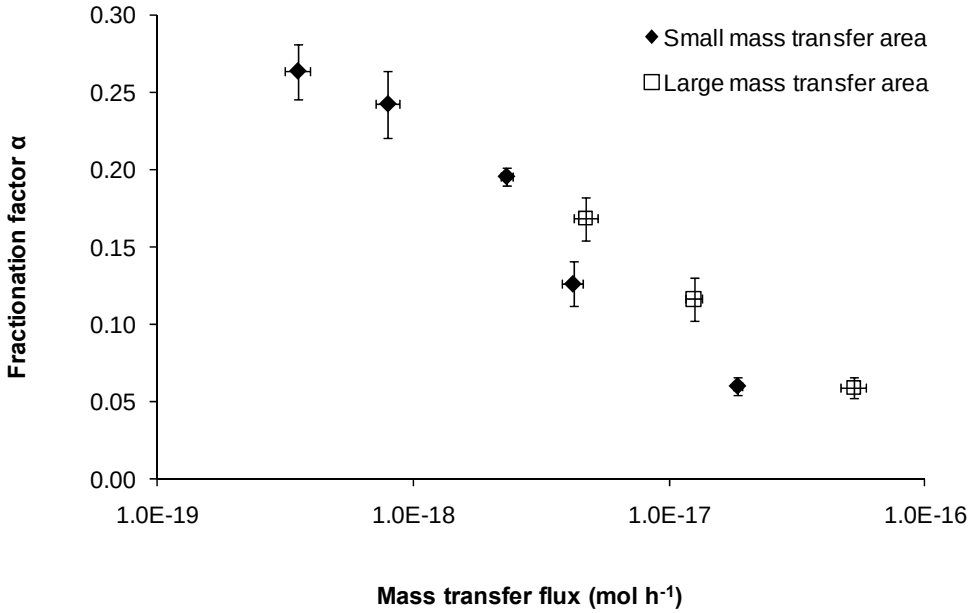

Figure 3.11. Isotope fractionation in function of substrate flux to a single cell. The fractionation factor decreases with the substrate flux, independently of the area. Error bars represent the 95% confidence interval for three or more experiments.

Chapter 4

Practical implications and further research needs

4.1 Implications for the quantification of biodegradation

4.2 Stable isotope fractionation – a tool for the assessment of bioavailability

In this thesis, laboratory model systems were used to demonstrate and explain the effect of bioavailability on stable isotope fractionation. The observed fractionation factor was found to significantly depend on both substrate concentration and cell density. These results, together with our theoretical calculations, support the hypothesis that in mass transfer limited systems, the observed isotope fractionation is determined by the substrate flux to the single cells that contribute to the degradation. Also the previous mass transfer step taking the substrate from a NAPL phase to water, may limit biodegradation and was shown to influence isotope fractionation. This explains effects of further mass transfer steps in the membrane and inside the cell as observed by Nijenhuis et al. [40]. This variability of the observed isotope fractionation factors might, on the one hand, lead to uncertainties in the assessment of biodegradation by SIFA in some cases. On the other hand, the correlation between substrate flux and isotope fractionation might be useful for the assessment of bioavailability for biodegradation. Both implications are discussed in this final chapter and recommendations for further research are given.

4.1 Implications for the quantification of biodegradation

The variability of the observed fractionation factors obtained in our experiments is due to the physical process of mass transfer. The effect can therefore be assumed to exist in any system, also in the environment, where it would lead to an underestimation of biodegradation (see section 2.1) [3]. Stable isotope fractionation analysis has, however, been used frequently for the assessment of biodegradation [25, 37, 76-78]. In a few studies, quantification of biodegradation by isotope fractionation could indeed be validated by other independent quantitative methods [78, 79]. The significance of the effect described in this work, under field conditions, depends on a variety of parameters. First, this effect is of importance only in cases where substrate bioavailability is restricted, and secondly, even in such cases the effect of bioavailability may be covered by larger variability of the isotope data caused by sampling,

sample treatment or data analysis [80, 81]. If degradation is limited by the availability of electron acceptors, as is often the case in aquifers, no reduction of isotope fractionation would be expected. Mass transfer fluxes in the aquifer depend on the physico-chemical properties of the contaminant (aqueous solubility, partitioning coefficients, density, etc.) and on soil properties, e.g. soil organic matter. It is therefore especially a problem for hydrophobic organic contaminants (HOC), such as polycyclic aromatic hydrocarbons (PAH), characterized by low aqueous solubility and high affinity to organic and solid phases. Until now, only a few attempts have been made in using stable isotope fractionation to assess the microbial degradation of naphthalene, the smallest PAH [37, 82]. Low aqueous concentrations and the large number of non reacting atoms in larger PAHs complicate the analysis of isotope fractionation induced by biodegradation. For PAHs the isotope composition is commonly used for source identification, since the isotope composition has been shown to remain constant despite biodegradation (Mazeas, 2002). With new techniques enhancing the detection limit of the isotope-ratio-mass-spectrometer (IRMS), there is, however, an increasing interest for using SIFA to analyze PAH biodegradation. Also, other hydrophobic compounds, such as hexachlorocyclohexanes (HCH) and n-alkanes, have shown to exhibit strong isotope fractionation that might be used to assess their biodegradation [47, 83, 84]. When attempting to analyze the biodegradation of hydrophobic organic contaminants, the possible effect of bioavailability should be taken into account.

So far, the use of isotope fractionation for the assessment of biodegradation has mainly focused on monoaromatic hydrocarbons, chlorinated solvents (PCE and TCE) and methyl tert-butyl ether (MTBE). BTEX compounds, i.e. benzene, toluene, ethylbenzene and xylenes are relatively water soluble and should therefore be readily accessible for microorganisms. Isotope fractionation with the Rayleigh approach has indeed been used to calculate the extent of biodegradation of these compounds under anaerobic conditions [37, 76-78, 85]. Despite

high solubility, mass transfer limitations could be an issue at low contaminant concentrations, as described in Chapter 2. Isotope fractionation of tetrachloroethene (PCE) and trichloroethene (TCE) during dehalogenation reactions has been observed under laboratory and field conditions and has been used for the assessment of biodegradation in the field [25, 86, 87]. In case of quantitative analysis of biodegradation, using isotope fractionation factors, care should be taken for the possible effects of mass transfer limitations, especially for PCE. In fact, mass transfer of PCE through the cell membrane has been shown to reduce the observed isotope fractionation in laboratory batch cultures [40]. In the presence of a NAPL phase, the transfer from NAPL to aqueous phase might become rate limiting and decrease the observed isotope fractionation. Yet, it must be noted that in the case of chlorinated ethenes, a high variability of isotope fractionation factors is also caused by a variety of different degradation pathways, leading to different enzymatic isotope fractionation [88]. This limits the quantification of the biodegradation of chlorinated ethenes to situations where the degrading population is known to exhibit a uniform isotope fractionation and adequate fractionation factors are known. In such cases the possible effect of mass transfer limitation should be taken into account.

The mass transfer flux of a contaminant to a single cell also depends on the cell density in the system, as demonstrated in section 3.1. For the purpose of this study, high cell densities were used in order to demonstrate the effect of strong mass transfer limitations. In the subsurface, however, cell densities are usually much lower, and a lower total substrate availability may thus be sufficient for the small number of degraders. Nevertheless, cells in the aquifer are not equally distributed, and an important part of biodegradation takes place in biofilms and microbial hot spots, where cell densities can be relatively high [89]. Since bioavailability is here defined as the interplay between supply and consumption, the microbial degradation rates also play a role. Most of the degradation taking place in contaminated aquifers is,

anaerobic and much slower than the degradation by aerobic toluene degrader *P. putida* mt-2 used in this study. Such slow degradation is saturated with slower mass transfer fluxes, and there is less risk for bioavailability limitations.

How well the Rayleigh model can quantify biodegradation, depends on the accuracy of the parameters included in it. Thus errors in concentration measurements or an incorrect isotope fractionation factor are important sources of uncertainty. Since, the isotope fractionation factor depends primarily on the biochemical isotope effect, it should be determined in cultures corresponding to the degraders in the aquifer. Additionally, the physicochemical conditions should be similar to the aquifer. It should also be kept in mind that the Rayleigh model rests on several assumptions that may not be true in all systems. The Rayleigh equation assumes that the fractionation factor is constant and does not change during the course of degradation. It has, however, been shown that the fractionation factor can vary with substrate concentration [3, 4, 52] or even with temperature in some cases [39]. It is also assumed that the contaminant pool is homogeneous, which does not apply to all heterogeneous aquifers [90]. Contaminants in groundwater flow may take different paths and arrive to a monitoring point after different degrees of degradation and isotope fractionation. The violation of these assumptions would lead to an underestimation of biodegradation. Changes in contaminant concentration by nonfractionating physical processes may, in contrast, result in an overestimation of biodegradation [81, 91].

An additional factor possibly influencing biodegradation in the field is the presence of compounds toxic for the microorganisms. In preliminary experiments, membrane disruption by 4-chlorophenol was shown to have an effect on the toluene hydrogen isotope fractionation by *P. putida* mt-2 (Fig. 4.1). An increase in membrane permeability could be expected to decrease mass transfer limitations, resulting in higher fractionation [40]. Interestingly, isotope

fractionation decreased with increasing chlorophenol concentrations. This could possibly be explained by changes in the binding efficiency of the enzyme to the substrate, leading to a higher commitment to catalysis (see section 1.3.1). Alternatively, the increased mobility of the reaction components within the membrane would allow faster potential degradation rates, resulting in bioavailability restrictions and thereby reduced isotope fractionation. Further studies are, however, needed for the confirmation and mechanistic understanding of this effect.

The results of this study show that substrate bioavailability may be a factor influencing the fractionation factor. The bioavailability conditions in the system should thus be taken into account, when the applicability of laboratory derived fractionation factors for a field site is considered. Care should be taken especially with aged contaminations and hydrophobic compounds, such as PAHs or alkanes, and when bulk concentrations are in the range of K_M or below. In order to determine enzymatic fractionation factors, substrate concentrations clearly above K_M should be used to exclude mass transfer limitation effects. The use of such "maximum fractionation" factors would also allow getting a conservative estimate for the extent of biodegradation. Another approach would be to try to tailor laboratory microcosms to simulate field conditions. The subsurface is, however, a heterogeneous matrix, where mass transfer conditions vary. The equations derived in chapters two and three allow a quantitative prediction for the magnitude of this effect if the bulk concentration and bioavailability conditions can be estimated. Simulations may be used to evaluate the usability of SIFA for a particular case. However, in order to get a concrete idea about the effect of bioavailability on isotope fractionation in the field, systematic investigations in a field system, including different contaminants and degraders, are still needed. It would be for instance interesting to compare isotope fractionation for fresh and aged contaminations of the same compound. Also the presence and concentration of dissolved organic matter may influence the bioavailability

and could thereby have an effect on isotope fractionation. The column system described in section 3.2 could be developed to a more aquifer like system, using a longer column with several sampling points and slower flow rates. Also a column with immobilized pollutant, similar to the one used by Zyakun et al. could be used [62]. Bacteria would be pumped through the column, and variations of contaminant release from the packing could be related to the observed isotope fractionation. In field experiments care should, however, be taken to exclude other factors possibly influencing the isotope fractionation, e.g. different degradation pathways with different enzymatic fractionation, heterogeneity of the matrix, preferential flow paths or the presence of toxic compounds.

Finally, this thesis is a fundamental study showing and explaining the influence of substrate bioavailability on stable isotope fractionation in different well defined laboratory systems. It emphasizes the need to investigate the impact of this effect on the *in situ* quantification of contaminant biodegradation in soils and aquifers.

4.2 Stable isotope fractionation – a tool for the assessment of bioavailability

An interesting outcome of this work is the potential use of stable isotope fractionation for the assessment of bioavailability, discussed in Chapter 3. Already in 1973 Calder et al. proposed that the isotope composition of fossil cyanobacteria, corresponding to strong fractionation, could possibly be taken as an indication of high CO_2 content in the air of the early Earth [54]. Later Lehmann *et al*. suggested that variations in stable isotope fractionation could be used to get information about denitrification rates, since a correlation had been observed in several cases [44, 68]. However, no practical method has yet been reported, probably due to the lack of systematic quantitative studies. In the context of contaminant biodegradation, the measurement of bioavailability is becoming increasingly important, and tools for a straight forward analysis, providing a clear quantitative result are still needed. Stable isotope

fractionation would be especially suitable for well defined model systems, where different new approaches to enhance bioavailability are evaluated. The use of stable isotope fractionation to assess the availability of contaminants under field conditions would require a good knowledge about the site, in order to exclude other parameters possibly influencing isotope fractionation. Since our bioavailability concept is based on fluxes, the assessment of bioavailability may also give information about diffusive fluxes and degradation rates in the system. A new biotechnological application could be the optimization of the efficiency of biocatalysts in bioreactors. Biosynthesis rate limitations due to substrate availability could be evaluated by determining the isotope fractionation.

Our experiments in batch and two-liquid-phase systems clearly demonstrate the sensitivity of the fractionation factor to parameters influencing the substrate flux to a single cell. They provide a fundamental basis for further investigations needed to validate stable isotope fractionation as a tool for the assessment of bioavailability, e.g. using different organisms with different substrates in different matrices similar to environmental conditions.

The variability of isotope fractionation in function of environmental conditions may also be used to assess other variables in specific cases. As discussed in the previous section, the presence of a membrane disrupting solvent also affects the observed isotope fractionation. Morasch et al. observed different fractionation factors for *P. putida* mt-2 at different temperatures. In any case, a better understanding of the factors influencing isotope fractionation may extend the application potential of SIFA to new fields.

FIGURES

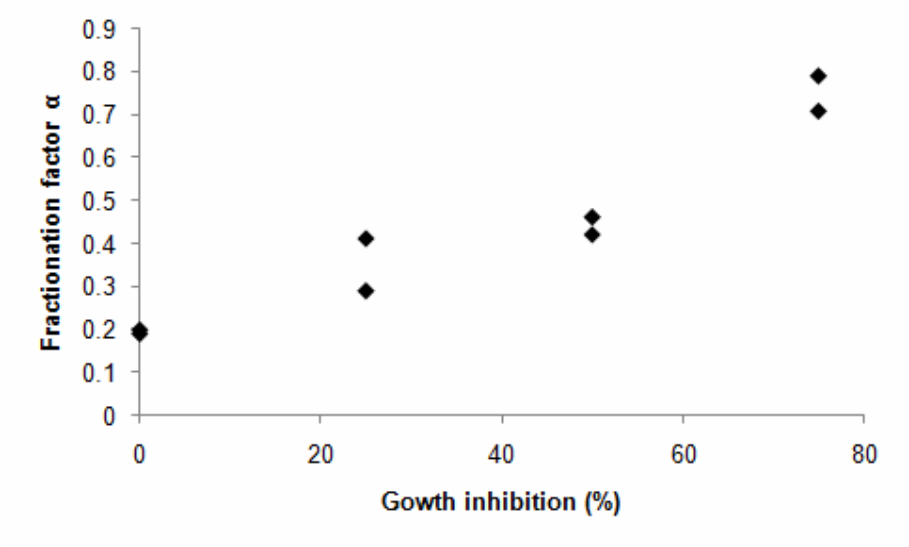

Figure 4.1. Toluene hydrogen isotope fractionation factors for *P. putida* mt-2 at different 4-chlorophenol concentrations. The amount of 4-chlorophenol is given in percentage of growth inhibition, determined in a previous study. These experiments were performed under non growth conditions.

REFERENCES

[1] Elsner, M., Zwank, L., Hunkeler, D. and Schwarzenbach, R.P. (2005) A new concept linking observable stable isotope fractionation to transformation pathways of organic pollutants. Environmental Science & Technology 39, 6896-6916.

[2] Northrop, D.B. (1981) The expression of isotope effects on enzyme-catalyzed reactions. Annual Review of Biochemistry 50, 103-131.

[3] Thullner, M., Kampara, M., Richnow, H.H., Harms, H. and Wick, L.Y. (2008) Impact of bioavailability restrictions on microbially induced apparent stable isotope fractionation: Theoretical calculations. Environmental Science & Technology 42, 6544-6551.

[4] Kampara, M., Thullner, M., Richnow, H.H., Harms, H. and Wick, L.Y. (2008) Impact of bioavailability restrictions on microbially induced apparent stable isotope fractionation: 2. Experimental evidence. Environmental Science & Technology 42, 6552-6558.

[5] Ehlers, L.J. and Luthy, R.G. (2003) Contaminant bioavailability in soil and sediment. Environmental Science & Technology 37, 295A-302A.

[6] Harmsen, J. (2007) Measuring bioavailability: From a scientific approach to standard methods. Journal of Environmental Quality 36, 1420-1428.

[7] Bosma, T.N.P., Middeldorp, P.J.M., Schraa, G. and Zehnder, A.J.B. (1997) Mass transfer limitation of biotransformation: Quantifying bioavailability. Environmental Science & Technology 31, 248-252.

[8] Harms, H. and Bosma, T.N.P. (1997) Mass transfer limitation of microbial growth and pollutant degradation. Journal of Industrial Microbiology & Biotechnology 18, 97-105.

[9] Jorgensen, B.B. and Revsbech, N.P. (1983) Colorless sulfur bacteria, *Beggiatoa* Spp and *Thiovulum* Spp in O_2 and H_2S microgradients. Applied and Environmental Microbiology 45, 1261-1270.

[10] Haws, N.W., Ball, W.P. and Bouwer, E.J. (2006) Modeling and interpreting bioavailability of organic contaminant mixtures in subsurface environments. Journal of Contaminant Hydrology 82, 255-292.

[11] Liste, H.H. and Alexander, M. (2002) Butanol extraction to predict bioavailability of PAHs in soil. Chemosphere 46, 1011-1017.

[12] Rhodes, A.H., Dew, N.M. and Semple, K.T. (2008) Relationship between cyclodextrin extraction and biodegradation of phenanthrene in soil. Environmental Toxicology and Chemistry 27, 1488-1495.

[13] Semple, K.T., Doick, K.J., Wick, L.Y. and Harms, H. (2007) Microbial interactions with organic contaminants in soil: Definitions, processes and measurement. Environmental Pollution 150, 166-176.

[14] Semple, K.T., Doick, K.J., Jones, K.C., Burauel, P., Craven, A. and Harms, H. (2004) Defining bioavailability and bioaccessibility of contaminated soil and sediment is complicated. Environmental Science & Technology 38, 228A-231A.

[15] Tecon, R., Wells, M. and van der Meer, J.R. (2006) A new green fluorescent protein-based bacterial biosensor for analysing phenanthrene fluxes. Environmental Microbiology 8, 697-708.

[16] Hoefs, J. (1997) Stable isotope geochemistry, pp. Springer-Verlag, Berlin.

[17] Schmidt, T.C., Zwank, L., Elsner, M., Berg, M., Meckenstock, R.U. and Haderlein, S.B. (2004) Compound-specific stable isotope analysis of organic contaminants in natural environments: a critical review of the state of the art, prospects, and future challenges. Analytical and Bioanalytical Chemistry 378, 283-300.

[18] Meckenstock, R.U., Morasch, B., Griebler, C. and Richnow, H.H. (2004) Stable isotope fractionation analysis as a tool to monitor biodegradation in contaminated acquifers. Journal of Contaminant Hydrology 75, 215-255.

[19] Mariotti, A., Germon, J.C., Hubert, P., Kaiser, P., Letolle, R., Tardieux, A. and Tardieux, P. (1981) Experimental-determination of nitrogen kinetic isotope fractionation - Some Principles - Illustration for the denitrification and nitrification processes. Plant and Soil 62, 413-430.

[20] Rayleigh, J.S.W. (1896) Theoretical Considerations respecting the separation of gases by diffusion and similar processes. Philos. Mag. 42, 493-498.

[21] Gonfiantini, R., Stichler, W. and Rozanski, K. Standards and intercomparison materials distributed by the international atomic energy agency for stable isotope measurements. In: Vol. Isotope hydrology section, International Atomic Energy Agency, Vienna.

[22] Cleland, W.W. (2005) The use of isotope effects to determine enzyme mechanisms. Archives Of Biochemistry And Biophysics 433, 2-12.

[23] Parmentier, L.E., Weiss, P.M., Oleary, M.H., Schachman, H.K. and Cleland, W.W. (1992) C-13 And N-15 isotope effects as a probe of the chemical mechanism of Escherichia-Coli Aspartate-Transcarbamylase. Biochemistry 31, 6577-6584.

[24] Rawlings, J., Cleland, W.W. and Hengge, A.C. (2006) Metal-catalyzed phosphodiester cleavage: Secondary O-18 isotope effects as an indicator of mechanism. Journal Of The American Chemical Society 128, 17120-17125.

[25] Sherwood Lollar, B., Slater, G.F., Sleep, B., Witt, M., Klecka, G.M., Harkness, M. and Spivack, J. (2001) Stable carbon isotope evidence for intrinsic bioremediation of tetrachloroethene and trichloroethene at area 6, Dover Air Force Base. Environmental Science & Technology 35, 261-269.

[26] McKelvie, J.R., Mackay, D.M., de Sieyes, N.R., Lacrampe-Couloume, G. and Lollar, B.S. (2007) Quantifying MTBE biodegradation in the Vandenberg Air Force Base ethanol release study using stable carbon isotopes. Journal Of Contaminant Hydrology 94, 157-165.

[27] Nijenhuis, I., Nikolausz, M., Koth, A., Felfolfi, T., Weiss, H., Drangmeister, J., Grossmann, J., Kastner, M. and Richnow, H.H. (2007) Assessment of the natural attenuation of chlorinated ethenes in an anaerobic contaminated aquifer in the Bitterfeld/Wolfen area using stable isotope techniques, microcosm studies and molecular biomarkers. Chemosphere 67, 300-311.

[28] Rugner, H., Finkel, M., Kaschl, A. and Bittens, M. (2006) Application of monitored natural attenuation in contaminated land management - A review and recommended approach for Europe. Environmental Science & Policy 9, 568-576.

[29] Dempster, H.S., Sherwood Lollar, B. and Feenstra, S. (1997) Tracing organic contaminants in groundwater: A new methodology using compound-specific isotopic analysis. Environmental Science & Technology 31, 3193-3197.

[30] Harrington, R.R., Poulson, S.R., Drever, J.I., Colberg, P.J.S. and Kelly, E.F. (1999) Carbon isotope systematics of monoaromatic hydrocarbons: vaporization and adsorption experiments. Organic Geochemistry 30, 765-775.

[31] Schuth, C., Taubald, H., Bolano, N. and Maciejczyk, K. (2003) Carbon and hydrogen isotope effects during sorption of organic contaminants on carbonaceous materials. Journal of Contaminant Hydrology 64, 269-281.

[32] Slater, G.F., Ahad, J.M.E., Sherwood Lollar, B., Allen-King, R. and Sleep, B. (2000) Carbon isotope effects resulting from equilibrium sorption of dissolved VOCs. Analytical Chemistry 72, 5669-5672.

[33] Zwank, L., Elsner, M., Aeberhard, A., Schwarzenbach, R. and Haderlein, S. (2005) Carbon isotope fractionation in the reductive dehalogenation of carbon tetrachloride at iron (hydr)oxide and iron sulfide minerals. Environmental Science & Technology 39, 5634-5641.

[34] Hartenbach, A., Hofstetter, T., Berg, M., Bolotin, J. and Schwarzenbach, R. (2006) Using nitrogen isotope fractionation to assess abiotic reduction of nitroaromatic compounds. Environmental Science and Technology 40, 7710-7716.

[35] Oba, Y. and Naraoka, H. (2008) Carbon and hydrogen isotopic fractionation of low molecular weight organic compounds during ultraviolet degradation. Organic Geochemistry 39, 501-509.

[36] Chartrand, M.M.G., Waller, A., Mattes, T.E., Elsner, M., Lacrampe-Couloume, G., Gossett, J.M., Edwards, E.A. and Sherwood Lollar, B. (2005) Carbon isotopic fractionation during aerobic vinyl chloride degradation. Environmental Science & Technology 39, 1064-1070.

[37] Griebler, C., Safinowski, M., Vieth, A., Richnow, H.H. and Meckenstock, R.U. (2004) Combined application of stable carbon isotope analysis and specific metabolites determination for assessing in situ degradation of aromatic hydrocarbons in a tar oil-contaminated aquifer. Environmental Science & Technology 38, 617-631.

[38] Hunkeler, D., Anderson, N., Aravena, R., Bernasconi, S.M. and Butler, B.J. (2001) Hydrogen and carbon isotope fractionation during aerobic biodegradation of benzene. Environmental Science & Technology 35, 3462-3467.

[39] Morasch, B., Richnow, H.H., Schink, B. and Meckenstock, R.U. (2001) Stable hydrogen and carbon isotope fractionation during microbial toluene degradation: Mechanistic and environmental aspects. Applied and Environmental Microbiology 67, 4842-4849.

[40] Nijenhuis, I., Andert, J., Beck, K., Kastner, M., Diekert, G. and Richnow, H.H. (2005) Stable isotope fractionation of tetrachloroethene during reductive dechlorination by *Sulfurospirillum multivorans* and *Desulfitobacterium* sp strain PCE-S and abiotic reactions

with cyanocobalamin. Applied and Environmental Microbiology 71, 3413-3419.

[41] O'Leary, M.H. (1980) Carbon isotope fractionation in plants. Phytochemistry 20, 553-567.

[42] Park, R. and Epstein, S. (1960) Carbon isotope fractionation during photosynthesis. Geochimica Et Cosmochimica Acta 21, 110-126.

[43] Zyakun, A.M., Bondar, V.A. and Namsaraev, B.B. (1979) Fractionation of stable carbon isotopes of methane in process of microbiological oxidation. Geokhimiya 291-297.

[44] Lehmann, M.F., Reichert, P., Bernasconi, S.M., Barbieri, A. and McKenzie, J.A. (2003) Modelling nitrogen and oxygen isotope fractionation during denitrification in a lacustrine redox-transition zone. Geochimica Et Cosmochimica Acta 67, 2529-2542.

[45] Sebilo, M., Billen, G., Grably, M. and Mariotti, A. (2003) Isotopic composition of nitrate-nitrogen as a marker of riparian and benthic denitrification at the scale of the whole Seine River system. Biogeochemistry 63, 35-51.

[46] Tyler, S.C., Crill, P.M. and Brailsford, G.W. (1994) C-13/C-12 fractionation of methane during oxidation in a temperate forested soil. Geochimica Et Cosmochimica Acta 58, 1625-1633.

[47] Bouchard, D., Hunkeler, D. and Hohener, P. (2008) Carbon isotope fractionation during aerobic biodegradation of n-alkanes and aromatic compounds in unsaturated sand. Organic Geochemistry 39, 23-33.

[48] Kinnaman, F.S., Valentine, D.L. and Tyler, S.C. (2007) Carbon and hydrogen isotope fractionation associated with the aerobic microbial oxidation of methane, ethane, propane and butane. Geochimica Et Cosmochimica Acta 71, 271-283.

[49] Pond, K.L., Huang, Y.S., Wang, Y. and Kulpa, C.F. (2002) Hydrogen isotopic composition of individual n-alkanes as an intrinsic tracer for bioremediation and source identification of petroleum contamination. Environmental Science & Technology 36, 724-728.

[50] Dinkla, I.J.T., Gabor, E.M. and Janssen, D.B. (2001) Effects of iron limitation on the degradation of toluene by *Pseudomonas* strains carrying the TOL (pWWO) plasmid. Applied and Environmental Microbiology 67, 3406-3412.

[51] Mancini, S.A., Hirschorn, S.K., Elsner, M., Lacrampe-Couloume, G., Sleep, B.E., Edwards, E.A. and Sherwood Lollar, B. (2006) Effects of trace element concentration on enzyme controlled stable isotope fractionation during aerobic biodegradation of toluene. Environmental Science & Technology 40, 7675-7681.

[52] Slater, G.F., Sherwood Lollar, B., Sleep, B.E. and Edwards, E.A. (2001) Variability in carbon isotopic fractionation during biodegradation of chlorinated ethenes: Implications for field applications. Environmental Science & Technology 35, 901-907.

[53] Pardue, J.W., Scalan, R.S., Vanbaalen, C. and Parker, P.L. (1976) Maximum carbon isotope fractionation in photosynthesis by blue-green-algae and a green-alga. Geochimica Et Cosmochimica Acta 40, 309-312.

[54] Calder, J.A. and Parker, P.L. (1973) Geochemical implications of induced changes in C-13 fractionation by blue-green-algae. Geochimica Et Cosmochimica Acta 37, 133-140.

[55] Bouchard, D., Hunkeler, D., Gaganis, P., Aravena, R., Hohener, P., Broholm, M.M. and Kjeldsen, P. (2008) Carbon isotope fractionation during diffusion and biodegradation of petroleum hydrocarbons in the unsaturated zone: Field experiment at Vaerlose airbase, Denmark, and modeling. Environmental Science & Technology 42, 596-601.

[56] Anderson, R.S., Huang, L., Iannone, R., Thompson, A.E. and Rudolph, J. (2004) Carbon kinetic isotope effects in the gas phase reactions of light alkanes and ethene with the OH radical at 296 +/- 4 K. Journal Of Physical Chemistry A 108, 11537-11544.

[57] Kampara, M., Thullner, M., Harms, H. and Wick, L.Y. (2008) Impact of cell density on microbially induced stable isotope fractionation. Applied Microbiology and Biotechnology *submitted*.

[58] Templeton, A.S., Chu, K.H., Alvarez-Cohen, L. and Conrad, M.E. (2006) Variable carbon isotope fractionation expressed by aerobic CH4-oxidizing bacteria. Geochimica Et Cosmochimica Acta 70, 1739-1752.

[59] Madigan, M.T., Martinko, J.M. and Parker, J. (2000) Brock Biology of Microorganisms, pp. Prentice Hall, London.

[60] Berg, J.M., Tymoczko, J.L. and Stryer, L. (2001) Biochemistry, pp. W.H. Freeman, New York.

[61] Staal, M., Thar, R., Kuhl, M., van Loosdrecht, M.C.M., Wolf, G., de Brouwer, J.F.C. and Rijstenbil, J.W. (2007) Different carbon isotope fractionation patterns during the development of phototrophic freshwater and marine biofilms. Biogeosciences 4, 613-626.

[62] Zyakun, A.M., Bondar, V.A., Namsaraev, B.B. and Nesterov, A.I. (1983) Use of carbon isotopic analysis to determine the intensity of methane microbiologic oxidation in natural ecosystems. Geokhimiya 759-765.

[63] Zyakun, A.M. and Zakharchenko, V.N. (1998) Carbon isotope discrimination by methanotrophic bacteria: Practical use in biotechnological research (review). Applied Biochemistry and Microbiology 34, 207-219.

[64] Zyakun, A.M., Bondar, V.A., Mshensky, Y.N., Zakharchenko, V.N., Bayazov, R.R. and Shishkina, V.N. (1987) Fractionation of carbon isotopes by methane-oxidizing bacteria *Methylomonas Methanica* in the process of their continuous growth. Geokhimiya 1007-1013.

[65] Valentine, D.L., Chidthaisong, A., Rice, A., Reeburgh, W.S. and Tyler, S.C. (2004) Carbon and hydrogen isotope fractionation by moderately thermophilic methanogens. Geochimica Et Cosmochimica Acta 68, 1571-1590.

[66] Penning, H., Plugge, C.M., Galand, P.E. and Conrad, R. (2005) Variation of carbon isotope fractionation in hydrogenotrophic methanogenic microbial cultures and environmental samples at different energy status. Global Change Biology 11, 2103-2113.

[67] Mariotti, A., Mariotti, F., Champigny, M.L., Amarger, N. and Moyse, A. (1982) Nitrogen isotope fractionation associated with nitrate reductase-activity and uptake of NO_3 by pearl-millet. Plant Physiology 69, 880-884.

[68] Mariotti, A., Landreau, A. and Simon, B. (1988) N-15 Isotope biogeochemistry and natural denitrification process in groundwater - Application to the chalk aquifer of northern France. Geochimica Et Cosmochimica Acta 52, 1869-1878.

[69] Hoch, M.P., Fogel, M.L. and Kirchman, D.L. (1992) Isotope fractionation associated with ammonium uptake by a marine bacterium. Limnology and Oceanography 37, 1447-1459.

[70] Hoch, M.P., Fogel, M.L. and Kirchman, D.L. (1994) Isotope fractionation during ammonium uptake by marine microbial assemblages. Geomicrobiology Journal 12, 113-127.

[71] Pennock, J.R., Sharp, J.H., Ludlam, J.M., Velinsky, D.J. and Fogel, M.L. (1988) Isotopic fractionation of nitrogen during the uptake NH_4^+ and NO_3^- by *Skeletonema costatum*. Eos 69, 1098.

[72] Pennock, J.R., Velinsky, D.J., Ludlam, J.M., Sharp, J.H. and Fogel, M.L. (1996) Isotopic fractionation of ammonium and nitrate during uptake by Skeletonema costatum: Implications for delta N-15 dynamics under bloom conditions. Limnology And Oceanography 41, 451-459.

[73] Harms, H. and Zehnder, A.J.B. (1994) Influence of substrate diffusion on degradation of dibenzofuran and 3-chlorodibenzofuran by attached and suspended bacteria. Applied and Environmental Microbiology 60, 2736-2745.

[74] Sikkema, J., Debont, J. and Poolman, B. (1994) Interactions of cyclic hydrocarbons with biological membranes. Journal of Biological Chemistry 269, 8022-8028.

[75] Aksu, Z. and Bulbul, G. (1998) Investigation of the combined effects of external mass transfer and biodegradation rates on phenol removal using immobilized P-putida in a packed-bed column reactor. Enzyme and Microbial Technology 22, 397-403.

[76] Richnow, H.H., Annweiler, E., Michaelis, W. and Meckenstock, R.U. (2003) Microbial in situ degradation of aromatic hydrocarbons in a contaminated aquifer monitored by carbon isotope fractionation. Journal of Contaminant Hydrology 65, 101-120.

[77] Meckenstock, R.U., Morasch, B., Kästner, M., Vieth, A. and Richnow, H.H. (2002) Assessment of bacterial degradation of aromatic hydrocarbons in the environment by analysis of stable carbon isotope fractionation. Water, Air, & Soil Pollution: Focus 2, 141-152.

[78] Fischer, A., Bauer, J., Meckenstock, R.U., Stichler, W., Griebler, C., Maloszewski, P., Kastner, M. and Richnow, H.H. (2006) A multitracer test proving the reliability of Rayleigh equation-based approach for assessing biodegradation in a BTEX contaminated aquifer. Environmental Science & Technology 40, 4245-4252.

[79] Peter, A., Steinbach, A., Liedl, R., Ptak, T., Michaelis, W. and Teutsch, G. (2004) Assessing microbial degradation of o-xylene at field-scale from the reduction in mass flow rate combined with compound-specific isotope analyses. Journal of Contaminant Hydrology 71, 127-154.

[80] Blessing, M., Jochmann, M.A. and Schmidt, T.C. (2008) Pitfalls in compound-specific isotope analysis of environmental samples. Analytical and Bioanalytical Chemistry 390, 591-603.

[81] Kopinke, F., Georgi, A., Voskamp, M. and Richnow, H. (2005) Carbon isotope

fractionation of organic contaminants due to retardation on humic substances: Implications for natural attenuation studies in aquifers. Environmental Science and Technology 39, 6052-6062.

[82] Meckenstock, R.U., Safinowski, M. and Griebler, C. (2004) Anaerobic degradation of polycyclic aromatic hydrocarbons. Fems Microbiology Ecology 49, 27-36.

[83] Pond, K., Huang, Y.S., Wang, Y. and Kulpa, C. (2001) Hydrogen isotope fractionation during aerobic biodegradation of crude oil. Abstracts of Papers of the American Chemical Society 222, U485-U485.

[84] Badea, S.L., Vogt, C., Danet, A.F. and Richnow, H.H. (2008) Stable isotope fractionation of hexachlorocyclohexanes during reductive dehalogenation. Organohalogen Compounds 70, 1097-1100.

[85] Mancini, S.A., Lacrampe-Couloume, G., Jonker, H., Van Breukelen, B.M., Groen, J., Volkering, F. and Sherwood Lollar, B. (2002) Hydrogen isotopic enrichment: An indicator of biodegradation at a petroleum hydrocarbon contaminated field site. Environmental Science & Technology 36, 2464-2470.

[86] Imfeld, G., Nijenhuis, I., Nikolausz, M., Zeiger, S., Paschke, H., Drangmeister, J., Grossmann, J., Richnow, H.H. and Weber, S. (2008) Assessment of in situ degradation of chlorinated ethenes and bacterial community structure in a complex contaminated groundwater system. Water Research 42, 871-882.

[87] Morrill, P.L., Lacrampe-Couloume, G., Slater, G.F., Sleep, B.E., Edwards, E.A., McMaster, M.L., Major, D.W. and Sherwood Lollar, B. (2005) Quantifying chlorinated ethene degradation during reductive dechlorination at Kelly AFB using stable carbon isotopes. Journal Of Contaminant Hydrology 76, 279-293.

[88] Cichocka, D., Imfeld, G., Richnow, H.H. and Nijenhuis, I. (2008) Variability in microbial carbon isotope fractionation of tetra- and trichloroethene upon reductive dechlorination. Chemosphere 71, 639-648.

[89] Knoller, K., Vogt, C., Richnow, H. and Weise, S. (2006) Sulfur and oxygen isotope fractionation during benzene, toluene, ethyl benzene, and xylene degradation by sulfate-reducing bacteria. Environmental Science and Technology 40, 3879-3885.

[90] Abe, Y. and Hunkeler, D. (2006) Does the Rayleigh equation apply to evaluate field isotope data in contaminant hydrogeology? Environmental Science & Technology 40, 1588-1596.

[91] Fischer, A., Theuerkorn, K., Stelzer, N., Gehre, M., Thullner, M. and Richnow, H.H. (2007) Applicability of stable isotope fractionation analysis for the characterization of benzene biodegradation in a BTEX-contaminated aquifer. Environmental Science & Technology 41, 3689-3696.

Acknowledgements

First, I want to thank Lukas Wick and Hauke Harms for the opportunity to do my PhD thesis at the UFZ and for good supervision of the thesis. Martin Thullner deserves special thanks for his invaluable input in the theoretical and modeling part. I am especially grateful for Martin's always patient clarifications and helpful discussions throughout my PhD work. Members of the EU project AXIOM are acknowledged for scientific exchange and nice social events, and Ivonne Nijenhuis and Hans Richnow also for helpful comments during the writing of the thesis. Help with the german summary by Anko Fischer and Ingo Fetzer was much appreciated.

Very deep thanks go to all students who contributed to my work (in chronological order): Philipp Fuchs, Maren Ziegler, Aaron Lee, Hilde Koch, Annele Kaski, Ankit Singh and Sebastian Schieferdecker.

I appreciated the nice work atmosphere created by all members of the bioavailability group. The assistance in the lab by Jana Reichenbach, Rita Remer and Birgit Würz was priceless. I also want to thank all my office mates (from all my offices) for help and advice in everyday matters as well as for nice company.

Last but not least, my deepest thanks go to all the people at UFZ who contributed to making my PhD time enriching and enjoyable. Also the hospitality during my later stays in Leipzig was much appreciated. I always felt like coming home. Friendships outside the UFZ were greatly appreciated and helped to keep things in perspective. I also thank all my friends and family around the world for keeping contact despite long distances. Special thanks go to Curzio Scheurer for years of patient travelling, which now should come to an end.

Publication list

Publications

1. M. Thullner, **M. Kampara**, H.H. Richnow, H. Harms, L.Y. Wick. (2008) Impact of bioavailability restrictions on microbially induced apparent stable isotope fractionation: Theoretical calculations. *Environ. Sci. Technol.* 2008, **42**, 6544-6551
2. **M. Kampara**, M. Thullner, H.H. Richnow, H. Harms, L.Y. Wick. (2008) Impact of bioavailability restrictions on microbially induced apparent stable isotope fractionation: Experimental evidence. *Environ. Sci. Technol.* 2008, **42**, 6552-6558
3. **M. Kampara**, M. Thullner, H. Harms, L.Y. Wick. (2008) Impact of cell density on microbially induced stable isotope fractionation. *Appl. Microb. Biotechnol.* in press

Oral presentations

1. Jahrestagung der Vereinigung für Allgemeine und Angewandte Mikrobiologie (VAAM), Jena, Germany, 1 – 4 April 2007
   Influence of bioavailability on the apparent stable isotope fractionation
   M. KAMPARA, M. THULLNER, H. HARMS, L.Y. WICK

2. European Geosciences Union General Assembly 2007, Vienna, Austria, 15 – 20 April 2007
   Influence of bioavailability on the apparent stable isotope fractionation
   M. KAMPARA, M. THULLNER, H. HARMS, L.Y. WICK

3. Stable Isotope Conference "Stable Isotope Tools for the Assessment of Chemical and Microbial Transformation Reactions in Complex Natural and Contaminated Environments", Monte Verità, Switzerland, 18 – 23 November 2007,
   Influence of bioavailability on the apparent stable isotope fractionation
   M. KAMPARA, M. THULLNER, H.H. RICHNOW, H. HARMS, L.Y. WICK

4. AXIOM-VIBE-eTRAP-HIGRADE Workshop "Electron transfer processes at biogeochemical gradients", Leipzig, Germany, 4 – 7 March 2008
   Impact of bioavailability restrictions on microbially induced stable isotope fractionation
   M. KAMPARA, M. THULLNER, H. HARMS, L.Y. WICK

Posters

1. AXIOM-Virtual Institute Spring School, "Microbial Activity at Biochemical Gradients". Leipzig, Germany, 3 – 6 April 2006
   The influence of bioavailability on isotope fractionation
   M. KAMPARA, M. THULLNER, H. HARMS, L.Y. WICK

2. International Symposium on Environmental Biotechnology, Leipzig, Germany, 3 – 6 April 2006
   The influence of bioavailability on stable isotope fractionation
   M. KAMPARA, M. THULLNER, H. HARMS, L.Y. WICK

3. 4th International Workshop "Bioavailability of Pollutants and Soil Remediation", Seville, Spain, 10 – 13 September 2006
   Influence of bioavailability on isotope fractionation
   M. KAMPARA, M. THULLNER, H. HARMS, L.Y. WICK

4. RAISEBIO – AXIOM – NOMIRACLE Summer School "Chemicals in Soil: Interactions, Availability and Residue Formation", Leipzig, Germany, 24 – 27 September 2007
   Influence of substrate bioavailability on the apparent stable isotope fractionation
   M. KAMPARA, M. THULLNER, H. HARMS, L.Y. WICK

5. SoilCritZone Workshop 3, Chania, Greece, 5 – 9 September 2008
   Influence of substrate bioavailability on the apparent stable isotope fractionation
   M. KAMPARA, M. THULLNER, H. HARMS, L.Y. WICK

Curriculum Vitae

CONTACT

Makeba Kampara
c/o C. Scheurer
Gassa Suto 20
7013 Domat/Ems
Schweiz

E-mail: makeba@hush.com
Phone: +41(0)81 6303194
Cell phone: +49(0)176 24823323

PERSONAL DATA

Nationality:	Finnish
Date of birth:	20 May 1978
Place of birth:	Helsinki, Finland

EDUCATION

Oct 2005 – Mar 2008 (expected)	PhD in Biochemistry at the Faculty of Biology, Pharmacy and Psychology, Leipzig University, Germany Topic of PhD thesis: *The impact of substrate bioavailability on the microbially induced stable isotope fractionation during contaminant biodegradation*
Sep 2000 – Jun 2005	Master of Science in Engineering, Degree programme in Biotechnology at the Department of Biotechnology, Royal Institute of Technology (KTH), Sweden Topic of MSc thesis: *Solar water treatment in an African context: A study on the evolution of biodegradability and the bacterial charge of the water during the treatment*. in collaboration with the Federal Institute of Technology Lausanne (EPFL), Switzerland, performed at the Ecole d'Ingenieurs de l'Equipement Rural (EIER), Ouagadougou, Burkina Faso Oct 2003 – Jun 2004 Attended two semesters as an exchange student (ERASMUS) at the Federal Institute of Technology Zürich (ETHZ), Switzerland
Sep 1999 – Jun 2000	Student at the Department of Biology, Stockholm University, Sweden
Aug 1994 – May 1997	High school diploma at the French-Finnish School of Helsinki (Lycée Franco-Finlandais d'Helsinki), Finland

WORK EXPERIENCE

Oct 2005 – Oct 2008	Helmholtz Centre for Environmental Research – UFZ Leipzig-Halle GmbH, Germany Position: PhD candidate
Oct 2003 – Jun 2004	Institute of Cell Biology, ETHZ, Switzerland Position: Auxiliary laboratory assistant, 10h /week (February full time) within a brain research project; molecular biological techniques, statistical analysis of behaviour experiments
Jun 2003 – Jul 2003	Laboratory of Environmental Microbiology, Department of Biotechnology, KTH Stockholm, Sweden Position: Auxiliary laboratory assistant, full time, at a pilot plant combining hydrobotanic wastewater treatment with microbiological processes; Chemical and microbiological analyses of wastewater during treatment
Jun 2002 – Aug 2002	Swedish Pulp and Paper Research Institute (Present STFI-Packforsk AB), Sweden Position: Auxiliary laboratory assistant, full time; participated in the development of a composite material reinforced with wood fibres

INTERNSHIPS

Mar 2004 – Jun 2004	Department of Environmental Toxicology, Swiss Federal Institute of Aquatic Science and Technology (EAWAG), Switzerland, 1 day /week Project: Attempts for cloning of the estrogen receptor alpha of rainbow trout in E. coli
Aug 2003 – Sep 2003	Institute of Cell Biology, ETHZ, Switzerland, full time Project: Localization of corticotrophin-releasing factor (CRF) receptors in mouse brain, using molecular biological and histological techniques

FURTHER TRAINING

Presentation technique and Rethorics (in german), 20. – 21.07.2007, UFZ Leipzig

Leadership, Time Management and Career Coaching, 11. – 13.02.2008, UFZ Leipzig

Selbstständigkeitserklärung

Ich erkläre dass ich die vorliegende Doktorarbeit selbstständig und nur unter Verwendung der angegebenen Quellen und Hilfsmittel angefertigt habe.

Leipzig, den 05.12.2008

Makeba Kampara